Antiviral Mechanisms of Small Molecules Targeting the Endoplasmic Reticulum and Golgi Apparatus

A Thesis Submitted to the Board of Faculty of Biological Sciences, University of Oxford, in Partial Fulfillment of the Requirements for Degree of Doctor of Philosophy

Jonathon D. Howe

Linacre College

University of Oxford, Trinity Term 2014

Antiviral Mechanisms of Small Molecules Targeting the Endoplasmic Reticulum and Golgi Apparatus

Jonathon D. Howe, Linacre College, DPhil Thesis, Trinity Term 2014

Abstract

N-linked glycosylation is the most common form of post-translational modification in nature and is essential to almost all enveloped viruses, including members of the Flaviviridae family. The host cell N-linked glycoprotein processing pathway is utilised by these viruses and as such has long been identified as a potential target for the development of antiviral drugs. Here, the antiviral mechanisms of three classes of small molecules targeting the secretory pathway and altering viral envelope glycosylation are investigated, using the HCV surrogate model, BVDV. The antiviral activity of imino sugars, principally through α-glucosidase inhibition, is well-characterised and here, a group of novel adamantyl-coupled imino sugars are investigated and demonstrated to inhibit ER α-glucosidases, which correlates with their antiviral activity against BVDV. Additionally, BVDV is used to study the antiviral mechanism of action of nitazoxanide. Nitazoxanide, the parent compound of the thiazolide class of structures, is a broadly antimicrobial compound with antiviral activity against HBV, HCV, influenza, JEV and others. Here, nitazoxanide is shown to be antiviral against BVDV by inducing Ca^{2+} release from ATP-sensitive intracellular calcium stores, disrupting ER-Golgi trafficking and inhibiting complex glycan formation. Finally, the potential of Golgi endo-α-mannosidase as an antiviral target is explored, using the endomannosidase inhibitor glucose-isofagomine in conjunction with the imino sugar α-glucosidase inhibitor NAP-DNJ. Endomannosidase is shown to be a valid antiviral target for BVDV, both alone and in combination with α-glucosidase inhibition, and is utilised by viral glycoproteins to acquire complex glycan structure, even in the absence of α-glucosidase inhibition. Altogether, this work furthers our understanding of the varied antiviral mechanisms of small molecules targeting the secretory pathway, enhancing the search for novel antiviral drugs directed against host cell machinery.

Acknowledgements

Firstly, I would like to thank my supervisor, Dr. Terry Butters, who has offered constant support, help, advice and friendship to me throughout my DPhil. His enthusiasm and passion for science, together with the care and support offered to all his students, have made him an ideal supervisor.

Alongside Terry, I would also like to thank Dr. Dominic Alonzi, who has provided help, advice, entertainment and distraction, all in equal measure, over the past few years, making my time in the Butters' group an enjoyable one.

I would also like to thank Dr. Omodele Ashiru. Dele's infectious enthusiasm for science, neverending ideas and thought-provoking discussions have been truly appreciated. The work on nitazoxanide has been a collaborative effort towards which her expertise has greatly contributed.

In addition, I'd like to thank all other members of the Butters' group for their support and friendship. A lot has changed over the last four years but the lab will always be fondly remembered.

I would like to thank Professor Raymond Dwek, Dr. Mark Wormald and Professor Nicole Zitzmann for their advice and support throughout my DPhil, and for making the Oxford Glycobiology Institute a rewarding and enjoyable working environment.

And finally, special thanks to my parents and family for all their support, and of course to Hayley, who has put up with me admirably over the last few years.

Contents

Abstract ii

Acknowledgements iii

Contents iv

List of abbreviations ix

1 General Introduction 1

1.1 N-linked glycosylation 1

1.1.1 N-linked glycosylation occurs in the endoplasmic reticulum 1

1.1.2 ER-associated degradation of glycoproteins 5

1.1.3 Cytosolic generation and fate of free oligosaccharides 8

1.1.4 Glycoprocessing in the Golgi apparatus 8

1.1.5 Glycoprocessing enzymes as antiviral targets 11

1.2 Bovine viral diarrhea virus 13

1.2.1 BVDV encodes a single ORF that is processed into structural and non-structural proteins 14

1.2.2 BVDV virions contain three envelope glycoproteins 17

1.3 Antiviral compounds 19

1.3.1 Thiazolides 19

1.3.2 Imino sugars 22

1.4 Project aims 29

1.5 References 31

2 Novel imino sugar α-glucosidase inhibitors as antiviral compounds 50
2.1 Introduction 50
2.2 Materials and methods 54
2.2.1 Materials 54
2.2.2 Cell culture 54
2.2.3 Cell proliferation assays 54
2.2.4 Carbohydrate analysis 55
2.2.5 Fluorescence focus assay 56
2.2.6 Real-time RT-PCR analysis 57
2.2.7 Immunoblotting 57
2.3 Results 59
2.3.1 Effect on cell proliferation increases with N-alkyl chain length 59
2.3.2 ER α-glucosidase inhibition correlates with N-alkyl chain length 61
2.3.3 Antiviral activity correlates with ER α-glucosidase inhibition 66
2.3.4 ER α-glucosidase inhibition increases glucosylation of intracellular BVDV E2 protein 68
2.4 Discussion 69
2.5 References 72
3 Nitazoxanide 75
3.1 Introduction 75
3.2 Materials and methods 79
3.2.1 Materials 79

3.2.2 Cell culture 79
3.2.3 Cell proliferation assays 80
3.2.4 Translation reporter assay 81
3.2.5 Focus-forming assay 81
3.2.6 Endo H digests of BVDV E2 glycoprotein 82
3.2.7 Western blot analysis 82
3.2.8 Carbohydrate analysis 83
3.2.9 Measurement of cytosolic Ca^{2+} 83
3.3 Results 85
3.3.1 NTZ inhibits BVDV replication 85
3.3.2 NTZ reduces cell proliferation 87
3.3.3 NTZ increases PKR and eIF2α phosphorylation 88
3.3.4 NTZ depletes intracellular ATP-sensitive Ca^{2+} stores 90
3.3.5 NTZ disrupts glycoprocessing and viral glycosylation 94
3.4 Discussion 98
3.4.1 Antiviral properties of NTZ 98
3.4.2 Effect of NTZ on cell survival and proliferation 98
3.4.3 NTZ-mediated mobilisation of intracellular Ca^{2+} 99
3.4.4 NTZ-mediated PKR phosphorylation 100
3.4.5 NTZ and the UPR 101
3.4.6 Effect of NTZ on BVDV glycosylation 102

3.5 References 104

4 Host cell glycoprocessing enzymes as antiviral targets 108

4.1 Introduction 108

4.2 Material and Methods 111

4.2.1 Materials 111

4.2.2 Cell culture 111

4.2.3 Cell proliferation assay 111

4.2.4 Carbohydrate analysis 111

4.2.5 BVDV infection 112

4.2.6 Endoglycosidase treatments 113

4.2.7 Western blot analysis 113

4.2.8 Viral titre determination by RT-PCR 114

4.2.9 Fluorescence focus-forming assay 114

4.3 Results 116

4.3.1 NAP-DNJ inhibits ER α-glucosidases in MDBK cells 116

4.3.2 Inhibition of α-glucosidases by NAP-DNJ results in specific degradation of BVDV glycoproteins 119

4.3.3 NAP-DNJ prevents complex glycan formation in secreted virions 121

4.3.4 GlcIFG inhibits endomannosidase in MDBK cells 123

4.3.5 Inhibition of endomannosidase prevents complex glycan formation 128

4.3.6 Antiviral activity of GlcIFG 130

4.3.7 Kifunensine treatment reduces BVDV infectivity 132

4.4 Discussion 135
4.4.1 ER α-glucosidases as antiviral targets 135
4.4.2 Golgi endomannosidase as an antiviral target 137
4.4.3 Antiviral activity of kifunensine against BVDV 138
4.5 References 141
5 General Discussion 143
5.1 Discussion 143
5.2 References 149

List of abbreviations

2-AA – 2-anthranilic acid

AIDS – acquired immunodefiency syndrome

ATF4 – activating transcription factor 4

BAPTA-AM – 1,2-bis(2-aminophenoxy)ethane-N,N,N’,N’-tetraacetic acid tetrakis (acetoxymethyl ester)

BSA – bovine serum albumin

Bu-CAST – 6-O-butyl-castanospermine

BVDV – bovine viral diarrhea virus

C protein – core protein

CAST – castanospermine

CC_{50} – concentration at which cell proliferation is reduced to 50% relative to control

CCCP – carbonyl cyanide 3-chlorophenylhydrazone

CFSE – carboxyfluorescein succinimidyl ester

CHO – Chinese hamster ovary

CGT – ceramide glucosyl transferase

ConA – Concanavalin A

COPII – coat protein complex II

cp – cytopathic

CSFV – classical swine fever virus

DAAs – direct acting antivirals

DAPI – 4’,6-diamidino-2-phenylindole

DGJ – deoxygalactonojirimycin

DMSO – dimethyl sulfoxide

DMJ – 1-deoxymannojirimycin

DNJ – 1-deoxynojirimycin

eIF2α – eukaryotic initiation factor 2α

EndoH – endoglycosidase H

ENGase – endo-β-α-N-acetylglucosaminidase

ER – endoplasmic reticulum

E^{rns} – envelope protein, RNase, secreted

ERAD – endoplasmic reticulum-associated degradation

FCS – fetal calf serum

FFA – focus-forming assay

FFU – focus-forming unit

FITC – fluorescein isothiocyanate

FLuc – firefly luciferase

FOS – free oligosaccharide

Glc – glucose

GlcIFG – glucose-isofagomine

GlcNAc – N-acetylglucosamine

HA – hemagglutinin

HBSS – Hank's Balanced Salt Solution

HBV – hepatitis B virus

HCV – hepatitis C virus

HIV – human immundeficiency virus

HPLC – high performance liquid chromatography

IC_{50} – concentration at which infectivity is reduced to 50% relative to control

IFN – interferon

IRES – internal ribosome entry site

IRF-3 – interferon regulatory factor 3

ISG – interferon-stimulated gene

JEV – Japanese encephalitis virus

Man – mannose

MDBK – Mardin-Darby bovine kidney

MFI – geometric mean of fluorescent intensity

MOI – multiplicity of infection

MON-DNJ – *N*-9-methoxynonyl-deoxynojimycin

MTS – 3-(4,5-dimethylthiazol-2-yl)-5-(3-carboxymethoxyphenyl)-2-(4-sulfophenyl-2H tetrazolium)

NADL – National Animal Disease Laboratory

NAP-DNJ – *N*-*N*-4'-azido-2'-nitrophenyl-6-aminohexyl-deoxynojimycin

*N*B-DNJ – *N*-butyl-deoxynojirimycin

ncp – non-cytopathic

*N*N-DNJ – *N*-nonyl-deoxynojirimycin

NP-HPLC – normal phase high performance liquid chromatography

NTZ – nitazoxanide

ORF – open reading frame

OST – oligosaccharyltransferase

PACT – PKR activating protein

PBS – phosphate-buffered saline

PERK – PKR-like ER kinase

PNGase – peptide:N-glycanase

PKR – protein kinase activated by double-stranded RNA

PMS – phenazine methosulfate

SDS-PAGE – sodium dodecyl sulfate-polyacrylamide gel electrophoresis

SERCA – sarcoplasmic/endoplasmic reticulum calcium ATPase

SIV – simian immunodeficiency virus

SOC – standard of care

SVR – sustained virological response

TCTP – translationally controlled tumour protein

TIZ – tizoxanide

UGGT – UDP-glucose:glycoprotein glucosyltransferase

UTR – untranslated region

VSV – vesicular stomatitis virus

1 General Introduction

1.1 N-linked glycosylation

Glycosylation is the most common type of post-translational modification of proteins (Varki *et al*, 2009), and is found throughout nature, from eubacteria and archea (Lechner & Wieland, 1989; Messner, 1997) to eukaryotes, with more than half of all eukaryotic proteins predicted to be glycosylated (Apweiler *et al*, 1999). The roles of glycosylation are extensive and varied, ranging from aiding glycoprotein folding and stabilising protein structure, to mediating cell-cell interactions and contributing to pathogen immune evasion. In eukaryotes, the two major types of protein glycosylation are N-linked and O-linked. O-linked glycosylation occurs by the sequential addition of monosaccharides to hydroxyl groups of serine and threonine side chains. N-linked glycosylation involves the *en bloc* transfer of an oligosaccharide to the amino group of asparagine side chains, and of the known, well-characterised glycoproteins, N-linked glycosylation accounts for approximately 90% (Apweiler *et al*, 1999).

1.1.1 N-linked glycosylation occurs in the endoplasmic reticulum

Prior to N-linked glycosylation of proteins, a dolichol phosphate-linked precursor is synthesised. This begins on the cytosolic surface of the endoplasmic reticulum (ER) with sequential addition of two N-acetylglucosamine (GlcNAc) and five mannose (Man) residues to dolichol phosphate (Huffaker & Robbins, 1983). The dolichol phosphate-heptasaccharide is then flipped by an ATP-dependent flippase to the luminal side of the ER membrane (Helenius *et al*, 2002), where a further four Man and three glucose (Glc) residues are added (Huffaker & Robbins, 1983). This tetradecaoligosaccharide ($Glc_3Man_9GlcNAc_2$) precursor is then transferred *en bloc*

from dolichol phosphate to the carboxyamido group of asparagine side chains on nascent polypeptides (Figure 1.1), cotranslationally as they enter the ER (Kornfeld & Kornfeld, 1985), with the sequence motif Asn-X-Ser/Thr (where X is any amino acid except proline) essential for glycosylation (Marshall, 1972; Hart *et al*, 1979). This transfer is catalysed by oligosaccharyltransferase (OST), which associates with Sec61 translocase on the luminal face of the ER (Wang & Dobberstein, 1999; Yan & Lennarz, 1999).

Following the *en bloc* transfer, processing of the glycan begins with immediate cleavage of the terminal α-1,2-linked glucosyl residue by α-glucosidase I (Shailubhai *et al*, 1987; Shailubhai *et al*, 1991).

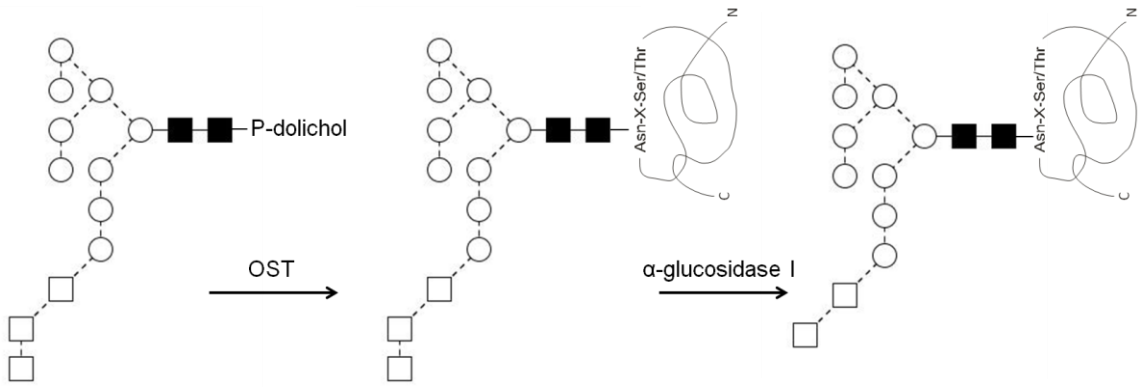

Figure 1.1 - N-linked glycosylation of proteins. The tetradecasaccharide is transferred *en bloc* by OST from dolichol to the nascent polypeptide as it enters the ER lumen, before the terminal glucose residue is removed by ER α-glucosidase I. Glycan structures in accordance with (Harvey *et al*, 2009).

The middle α-1,3-linked glucosyl residue is then rapidly removed by α-glucosidase II (Figure 1.2) (Grinna & Robbins, 1980; Trombetta *et al*, 1996). Removal of this glucose produces the monoglucosylated species $Glc_1Man_9GlcNAc_2$, allowing the glycosylated polypeptide to be recognised and bound by calnexin, a membrane-bound folding chaperone (Ware *et al*, 1995), and/or calreticulin, its soluble homologue found in the ER lumen. Calnexin and calreticulin are lectins that specifically bind monoglucosylated glycans, and are central to the quality control system of the ER (Ellgaard & Helenius, 2003), ensuring that glycoproteins are correctly folded before exit from the ER is allowed.

Calnexin assists folding of nascent glycoproteins by preventing aggregation in the protein-concentrated environment of the ER and recruiting the oxidoreductase ERp57, a homologue of protein disulphide isomerase (Leach *et al*, 2002; Frickel *et al*, 2004). ERp57 aids folding by forming disulphide-bonded intermediates with the glycoprotein (Lindquist *et al*, 2001), allowing for the correct formation of disulphide bonds in the glycoprotein to form. Retention of monoglucosylated glycoproteins by membrane-bound calnexin also prevents premature exit of folding intermediates to the Golgi apparatus.

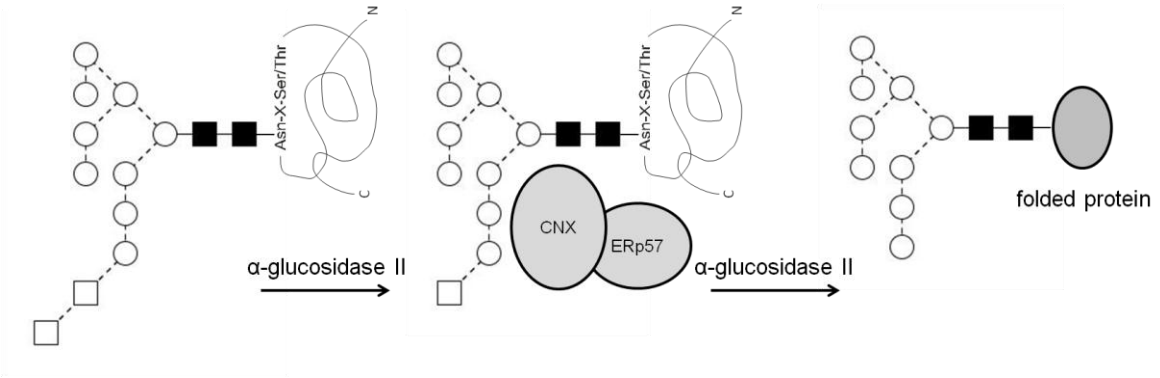

Figure 1.2 – Calnexin-mediated glycoprotein folding. α-Glucosidase II removes the second glucose residue from the glycan structure, allowing association with the ER chaperone calnexin (CNX). Further processing by α-glucosidase II removes the final glucose residue, allowing the now folded protein to dissociate from calnexin.

In a step that occurs at a much slower rate than the initial deglucosylations, α-glucosidase II acts again to remove the final α-1,3-linked glucosyl residue, producing the de-glucosylated glycan $Man_9GlcNAc_2$ (Figure 1.2). This slow removal of the final glucose from the glycan allows a time window for calnexin and calreticulin to interact with and attempt to fold the monoglucosylated polypeptide (Grinna & Robbins, 1980; Daniels *et al*, 2003; Deprez *et al*, 2005). In its de-glucosylated form, the glycoprotein is released by calnexin and is then subjected to quality control checking by UDP-glucose:glycoprotein glucosyltransferase (UGGT). UGGT acts as a folding sensor, reglucosylating misfolded glycoproteins, so that they become substrates once again for calnexin and folding can be reattempted (Parodi, 2000). UGGT distinguishes between misfolded and native proteins by, in part, recognising hydrophobic clusters of amino acids on the surface of the protein, which are assumed to indicate misfolding (Sousa & Parodi, 1995; Caramelo *et al*, 2003; Totani *et al*, 2009). Whilst for the majority of proteins, one phase of interaction with calnexin or calreticulin is sufficient for correct folding, reglucosylation has been found to be necessary for some slow-folding proteins (Pearse *et al*, 2008). Correctly-folded

glycoproteins are not recognised by UGGT and are therefore not reglucosylated, and are able to proceed to the Golgi apparatus, where further glycan processing can occur. UGGT, together with α-glucosidase II and calnexin/calreticulin, completes the calnexin cycle (Figure 1.3), in which proteins can, if necessary, undergo several rounds of folding in order to achieve their native state (Ellgaard & Helenius, 2003; Helenius & Aebi, 2004).

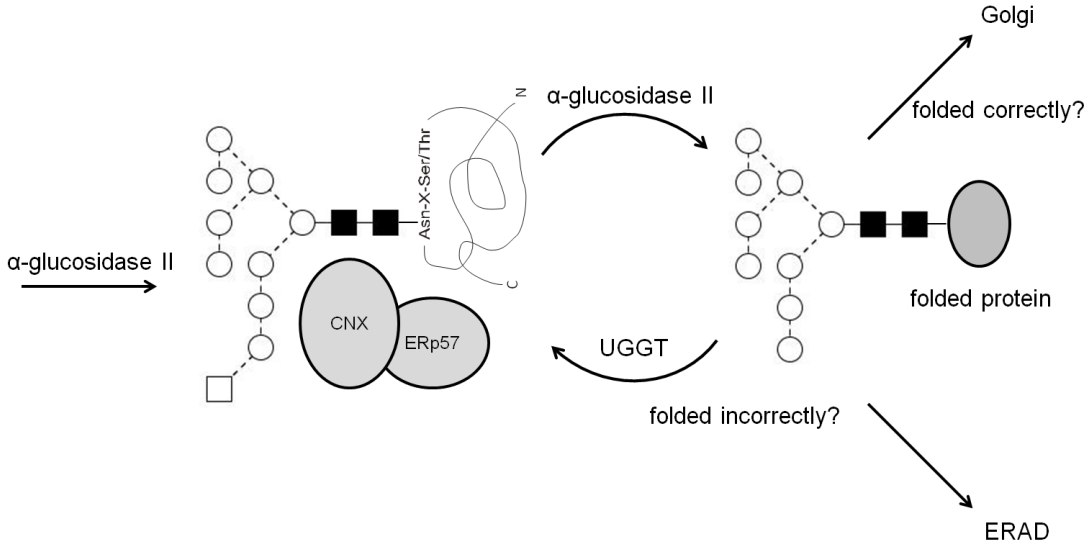

Figure 1.3 – Calnexin quality control cycle. Following processing by α-glucosidase II, the nascent polypeptide, displaying a monoglucosylated glycan, is bound by the ER folding chaperone calnexin (CNX). α-Glucosidase II deglucosylates the glycan, allowing release from calnexin and folding checks are performed by UGGT, which reglucosylates the protein if it is incorrectly or incompletely folded, allowing for reassociation with calnexin.

1.1.2 ER-associated degradation of glycoproteins

Glycoproteins in the calnexin cycle can have one of three fates. If they are folded correctly, they will not be reglucosylated by UGGT, and can be trafficked to the Golgi apparatus for further processing and maturation. This will be discussed in more detail in section 1.1.4 below. If they are incorrectly folded, they will be reglucosylated by UGGT to re-associate with calnexin and attempt folding again. In some cases,

nascent glycoproteins are terminally misfolded by the calnexin cycle, and must be removed from the ER to maintain homeostasis. This process is termed ER-associated protein degradation (ERAD, Figure 1.4), where such proteins are polyubiquitinated and dislocated from the ER (Jarosch *et al*, 2002), and targetted for proteolytic degradation by the 26S proteasome.

Two ER proteins, XTP3-B and, in particular, OS-9, are thought to be involved in the recognition of terminally-misfolded glycoproteins (Christianson *et al*, 2008; Tamura *et al*, 2008). The yeast homologue of OS-9, Yos9p, has been shown to be essential for ERAD (Buschhorn *et al*, 2004), acting as part of a complex with Hrd3p and Kar2p to traffick misfolded proteins to the ER membrane through association with the transmembrane ubiquitin ligase Hrd1p (Denic *et al*, 2006). The exact mechanism of how misfolded proteins are recognised as substrates for ERAD remains unclear, although further trimming of glycans by ER mannosidases appears to be essential (Weng & Spiro, 1993; Jakob *et al*, 1998; Frenkel *et al*, 2003). OS-9 and XTP3-B, like Yos9p, both contain lectin-like domains, but recent studies have shown that these are not required for recognition and binding of misfolded proteins (Christianson *et al*, 2008), but instead, are essential for binding to the membrane adaptor protein SEL1L, the human homologue of Hrd3p. The same study has also identified the ER chaperone GRP94 as a component of ERAD. It is thought that GRP94 associates with OS9, and helps to transfer the misfolded protein onto the membrane bound Sel1L/Hrd1 complex for ubiquitination and dislocation (Tamura *et al*, 2008).

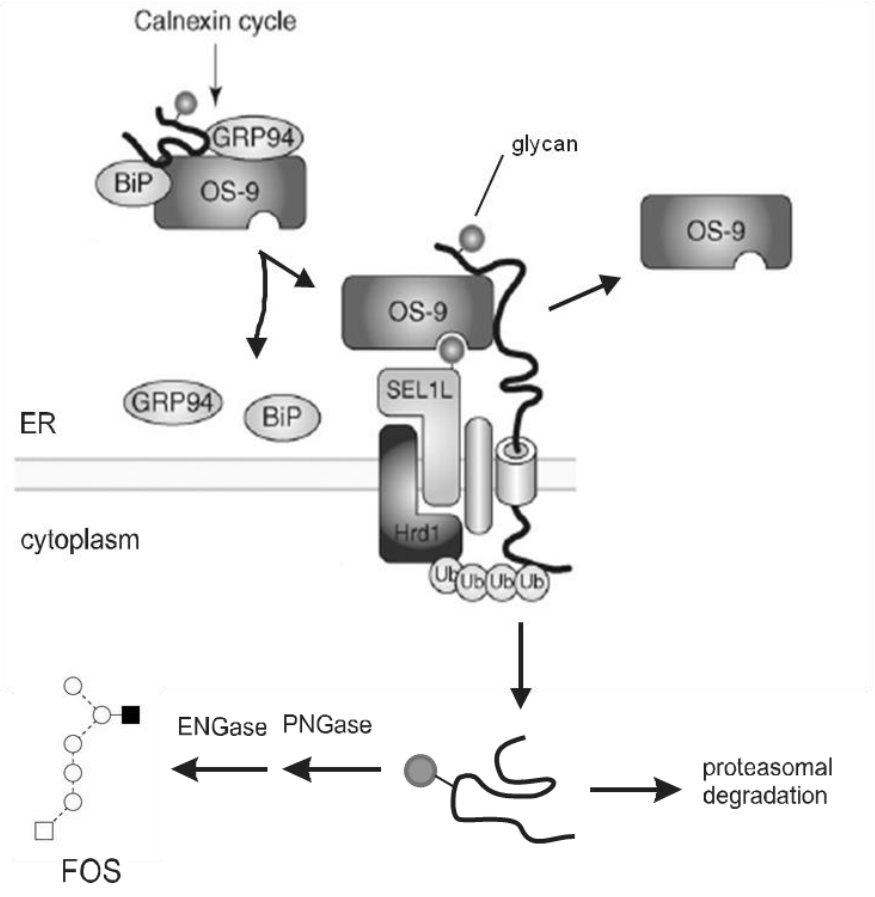

Figure 1.4 – Retrotranslocation of misfolded glycoproteins from the ER into the cytoplasm. The polypeptide chain is polyubiquitinated upon translocation into the cytoplasm and targeted to the proteasome for degradation, whilst the glycan is released as a free oligosaccharide (FOS) by PNGase. Figure adapted from (Tamura *et al*, 2008).

Hrd1 has been identified as the ubiquitin ligase component of the membrane complex involved in the dislocation of luminal ER proteins (Bays *et al*, 2001). Sec61 and Derlin-1 have both been suggested as protein-conducting channels for retrotranslocation (Wiertz *et al*, 1996; Lilley & Ploegh, 2004), as well as Hrd1 itself (Gauss *et al*, 2006) but the identity of such a channel remains uncertain.

1.1.3 Cytosolic generation and fate of free oligosaccharides

Misfolded proteins in the ER lumen are identified by ERAD proteins, dislocated from the ER and polyubiquitinated. Once in the cytoplasm, peptide:N-glycanase (PNGase) deglycosylates N-linked glycoproteins, cleaving the bond between the asparagine residue and the proximal GlcNAc (Suzuki *et al*, 2002a), producing a free oligosaccharide (FOS) with a chitobiose core of two GlcNAc residues at the reducing end (FOS-$GlcNAc_2$) and a deglycosylated, polyubiquitinated polypeptide which is subsequently degraded by the proteasome. PNGase activity has also been detected in the ER (Weng & Spiro, 1997), but deglycosylation has been shown to be unnecessary for retrotranslocation to occur (Wiertz *et al*, 1996). Following cytosolic PNGase action, the terminal GlcNAc residue is quickly removed by either endo-β-α-N-acetylglucosaminidase (ENGase) (Pierce *et al*, 1979; Suzuki *et al*, 2002b) or a neutral chitobiase enzyme (Cacan *et al*, 1996) to produce oligosaccharides with a single GlcNAc residue at the reducing end (FOS-$GlcNAc_1$).

FOS-$GlcNAc_1$ species are further degraded by cytosolic α-mannosidase (Moore & Spiro, 1994), from high-mannose species to $Man_5GlcNAc_1$, which accumulates in the cytosol (Saint-Pol *et al*, 1997; Yanagida *et al*, 2006). Accumulation of the monoglucosylated FOS species $Glc_1Man_5GlcNAc_1$ is also observed (Cacan *et al*, 2001; Yanagida *et al*, 2006). These oligosaccharides can then be translocated into the lysosome for recycling into monosaccharides (Saint-Pol *et al*, 1997; Saint-Pol *et al*, 1999).

1.1.4 Glycoprocessing in the Golgi apparatus

Following successful folding in the ER, glycoproteins can proceed to the Golgi apparatus for further processing and secretion. Trafficking to the Golgi occurs via the

budding of coat protein complex II (COPII)-coated vesicles (Orci *et al*, 1991; Bannykh *et al*, 1996; Rossanese *et al*, 1999), initiated by a Sar1p GTPase (Matsuoka *et al*, 1998). Trafficking of proteins can either be passive (where soluble proteins simply pass to the Golgi through diffusion into COPII vesicles) or active, where proteins are sequestered in COPII vesicles, either by binding directly to COPII components including Sec24p (Miller *et al*, 2003) or through adaptor proteins.

Throughout the ER and Golgi, further processing of N-linked glycans by mannosidases and glycosyltransferases occurs (Kornfeld & Kornfeld, 1985). Processing can be limited to simply leave a 'high-mannose' structure ($Man_{5-9}GlcNAc_2$), or removal of mannose residues down to a core $Man_3GlcNAc_2$ species can allow complex glycan formation, where additional monosaccharides including GlcNAc, galactose and N-acetylneuraminic acid are then transferred to the glycan in the Golgi. Alternatively, partial mannosidase processing can result in the formation of hybrid glycan structures. The resultant glycan structures depend on both the target protein sequence and on the cell or tissue involved.

In addition to the glycan processing discussed above, an alternative processing pathway exists that can circumvent ER α-glucosidase action and calnexin-mediated folding. Golgi endo-α-mannosidase can process glucosylated glycans that have escaped α-glucosidase digestion, cleaving the internal α-1,2 link between the glucose-substituted mannose residue and the remainder of the oligosaccharide, to produce a non-glucosylated glycan ($Man_{5-8}GlcNac_2$) and $Glc_{1-3}Man$ (Figure 1.5) (Anumula & Spiro, 1983; Lubas & Spiro, 1987; Lubas & Spiro, 1988; Moore & Spiro, 1990). Thus, it is thought to provide a backup processing pathway for glycoproteins that have escaped the ER prior to complete glucosidase processing (Weng & Spiro,

1996). Removal of the glucose cap allows further processing of glycans, and is essential to allow complex glycan formation (Gross *et al*, 1986).

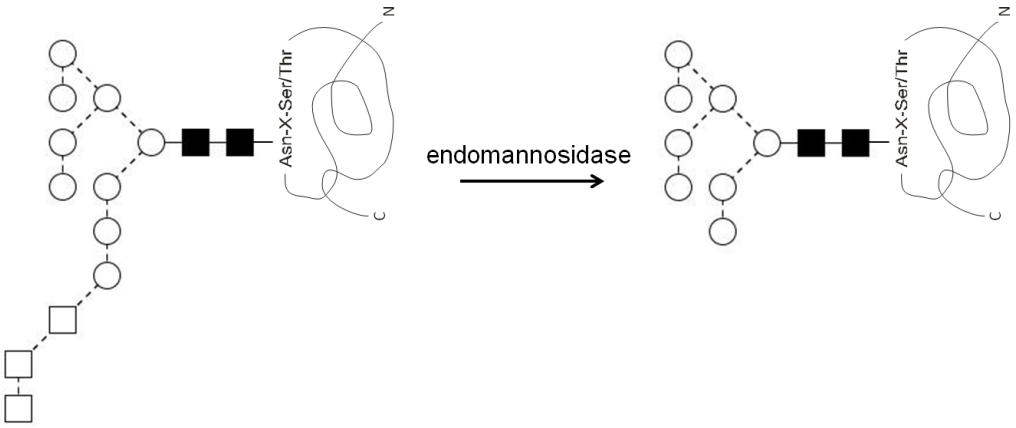

Figure 1.5 – Endomannosidase processing of glucosylated proteins. Endomannosidase cleaves the terminal mannose residue from the glucosylated branch on N-linked glycans, bypassing the ER quality control cycle and allowing further processing for complex glycan production.

The activity and substrate specificity of endomannosidase varies greatly across mammalian cell lines (Karaivanova *et al*, 1998). Chinese hamster ovary (CHO) cells express a defunct endomannosidase that mislocalises to the ER instead of the Golgi, due to a mutation to a highly conserved tryptophan residue (Torossi *et al*, 2007). In Madin-Darby bovine kidney (MDBK) cells, commonly used for studies of bovine viral diarrhea virus (BVDV), endomannosidase shows restricted substrate processing. In a study using vesicular stomatitis virus (VSV) glycoprotein in the presence of the α-glucosidase inhibitor 6-O-butyl-castanospermine (Bu-CAST), MDBK endomannosidase, like that of CHO cells, exhibited no activity, but *in vitro* studies demonstrated appreciable levels of activity (Karaivanova *et al*, 1998). This is explained by the substrate specificity of the enzyme – MDBK endomannosidase shows preference for monoglucosylated glycans as substrate, but cannot process

triglucosylated glycans, such as those produced in the presence of extensive α-glucosidase inhibition (Kukushkin *et al*, 2012).

1.1.5 Glycoprocessing enzymes as antiviral targets

Many viruses contain glycoproteins essential to their biogenesis and infectivity, and the potential of exploiting glycoprocessing enzymes as antiviral drug targets has been appreciated for some time. Inhibitors of ER α-glucosidases are known to inhibit maturation and secretion of mouse hepatitis virus and coronavirus (Repp *et al*, 1985), as well as Sindbis virus formation (Schlesinger *et al*, 1985), and BVDV and HCV secretion (Durantel *et al*, 2001; Steinmann *et al*, 2007). Conversely, glucosidase inhibition has previously been shown to reduce the infectivity, rather than secretion, of human immunodeficiency virus (HIV) and simian immunodeficiency virus (SIV) (Ratner *et al*, 1991), as well as cytomegalovirus (Taylor *et al*, 1988). In addition to effects on secretion, glucosidase inhibitors have also been shown to reduce BVDV infectivity (Durantel *et al*, 2001). Many glycoproteins from a variety of viruses have been shown to be dependent on calnexin and calreticulin, including hemagglutinin from influenza (Peterson *et al*, 1995), HN protein from Newcastle disease virus (McGinnes & Morrison, 1998), NSP4 from rotavirus (Mirazimi *et al*, 1998), M protein from hepatitis B virus (HBV) (Werr & Prange, 1998), and E1 and E2 proteins from hepatitis C virus (HCV) and BVDV (Dubuisson & Rice, 1996; Choukhi *et al*, 1998; Branza-Nichita *et al*, 2001), highlighting the potential of targeting the host glycosylation machinery as an antiviral therapeutic. Endomannosidase has also been demonstrated to be used by viral envelope glycoproteins (Karaivanova *et al*, 1998).

It is important to emphasise the potential benefit of targeting host cell machinery with antiviral compounds instead of directly interacting with viral proteins. This allows greater potential for the development of broad-spectrum antiviral drugs effective against a range of viruses, or a range of genotypes of a given virus, that rely on a common host cell pathway, whilst also reducing the likelihood of encouraging escape mutants within the viral genome. Strains from a number of viruses resistant to direct-acting antivirals have been reported, including influenza (McKimm-Breschkin, 2000), HCV (Susser *et al*, 2009; Hiraga *et al*, 2011) and HIV (Larder & Kemp, 1989).

1.2 Bovine viral diarrhea virus

Bovine viral diarrhea virus (BVDV) is a member of the Flaviviridae family of viruses. The Flaviviridae family are positive strand RNA viruses and comprise of four genera: *Flavivirus*, including yellow fever virus, dengue virus, West Nile virus and JEV; *Hepacivirus*, including HCV; *Pegivirus*, including pegivirus A; and *Pestivirus*, such as classical swine fever virus (CSFV) and BVDV (King *et al*, 2011).

Flaviviridae viruses are of major importance to global health, with the World Health Organization estimating about 150 million people worldwide to be chronically infected with HCV alone, resulting in more than 350,000 deaths from HCV-related liver disease each year.

Flaviviridae virions consist of a lipid bilayer envelope containing transmembrane glycoproteins, with a single-stranded positive-sense RNA genome packaged in a nucleocapsid core and all have similar life cycles (Figure 1.6) (Lindenbach *et al*, 2006). Virions bind to virus-specific cellular receptors and achieve uptake via receptor-mediated endocytosis. Upon entry into the endosomal pathway, low pH triggers fusion of the viral envelope with cellular membranes, allowing uncoating of the nucleocapsid and release of viral RNA into the cytoplasm.

Flaviviridae transcribe a single polyprotein which is subsequently cleaved into structural and non-structural proteins by host cell and viral-encoded proteases. Structural proteins are typically found at the N-terminal end of the polyprotein and followed by non-structural proteins. RNA replication occurs in the cytoplasm, and nascent virions are thought to assemble and bud from the ER membrane (Grummer *et al*, 2001; Miyanari *et al*, 2007; Roingeard *et al*, 2008; Welsch *et al*, 2009), before exiting the cell via the secretory pathway.

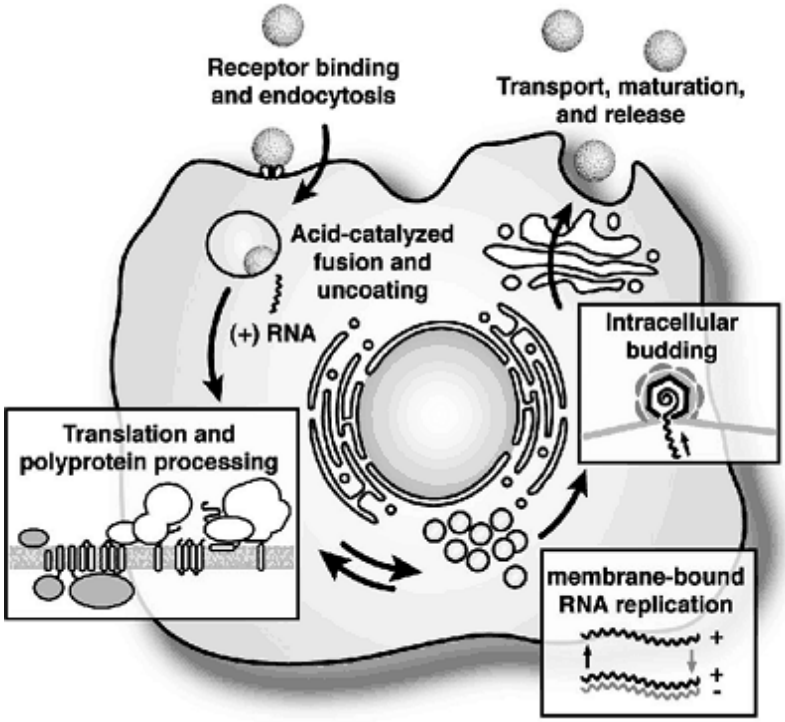

Figure 1.6 – Flaviviridae life cycle. Members of the Flaviviridae family share common life cycle components, from receptor binding and entry to replication and translation of the polyprotein, to budding and release from the host cell (figure adapted from Fields Virology, Fifth Edition).

1.2.1 BVDV encodes a single ORF that is processed into structural and non-structural proteins

The *Pestivirus* genus consists of four species, namely CSFV, BVDV 1, BVDV 2 and border disease virus (King *et al*, 2011). BVDV is a pathogen of economic significance, causing abortions, birth defects, reduced milk production and diarrhea in cattle. It is estimated to cause $10 to $40 million loss per million calvings in the United States (Houe, 2003). Two genotypes of BVDV – BVDV 1 and BVDV 2 – are defined based on nucleotide and antigenic differences. Within each genotype exist variants that can either trigger cell death in cell culture (cytopathic, cp), or fail to do so (non-cytopathic, ncp). Transmission of ncp BVDV commonly occurs from a mother to foetus in pregnancy, and can cause still birth or persistent infection. BVDV

in persistently infected calves can undergo a conversion of genotype from ncp to cp, which can lead to the development of mucosal disease.

Mucosal disease is associated with a high fatality rate in cattle, with death usually occurring within two weeks of the development of symptoms, with the animal suffering from bloody diarrhea and fever, and showing major ulceration of the gastrointestinal tract (Peterhans *et al*, 2010). Animals with mucosal disease are typically found to be infected with a virus pair: a ncp BVDV strain and an antigenically and genetically closely related cp strain (Brownlie, 1990). Most commonly, the cp biotype is a result of genomic changes, such as recombination or insertion of cellular RNA, to the ncp BVDV genome (Meyers & Thiel, 1996; Kummerer *et al*, 2000). Infection with a cp strain alone appears be insufficient to establish persistent infection (Brownlie *et al*, 1989).

An outline of the BVDV genome is shown in Figure 1.7. BVDV is a single-strand positive-sense RNA virus with a genome approximately 12.3 kb in length (Collett *et al*, 1988). It consists of a 5'-untranslated region (UTR) containing an internal ribosome entry site (IRES) allowing for cap-independent translation (Poole *et al*, 1995), a single, long open reading frame (ORF) that is translated into a polyprotein chain and a 3'-UTR. Both UTRs play important roles in replication (Yu *et al*, 1999; Yu *et al*, 2000). The polyprotein produced in translation is approximately 4,000 amino acids in length and is co- and post-translationally processed into individual viral proteins, with structural proteins towards the N-terminus and non-structural (NS) proteins downstream.

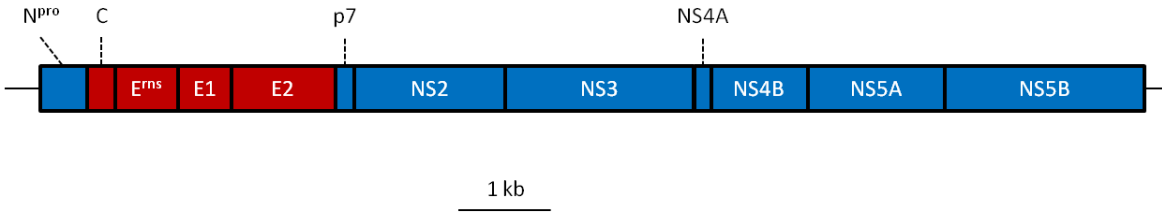

Figure 1.7 – Genomic organisation of BVDV, based on the cDNA sequence of NADL (National Animal Disease Laboratory) strain (GenBank Accession Number AJ133738). Untranslated regions are shown as horizontal lines; coding regions are shown as rectangles corresponding to the viral proteins produced from a single ORF. Red rectangles indicate structural proteins; blue rectangles indicate non-structural proteins. The diagram is to scale horizontally, with the length of 1-kb RNA indicated below the genome.

The first protein product of the ORF, N^{pro}, is a non-structural cysteine autoprotease that cleaves at its C-terminus exposing the N-terminus of the BVDV core (C) protein (Wiskerchen *et al*, 1991; Rumenapf *et al*, 1998). C protein is believed to be further processed by signal peptide peptidase to its mature form (Heimann *et al*, 2006), whilst the remaining structural proteins E^{rns} (envelope protein, RNase secreted), E1 and E2, as well as the putative ion channel p7, are most likely cleaved by host signal peptidase and, in the case of E^{rns}/E1, by a slower, as yet unidentified cellular protease (Rumenapf *et al*, 1993; Wegelt *et al*, 2009), although recently cleavage of CSFV E^{rns}/E1 has been attributed to signal peptidase albeit with an unusual recognition site that lacks a hydrophobic region upstream of the cleavage site (Bintintan & Meyers, 2010). In cp strains of BVDV, NS2/3 undergoes autoprocessing through the cysteine protease activity in NS2 (Lackner *et al*, 2004). The remaining non-structural proteins are processed by NS3-4A serine protease (Wiskerchen & Collett, 1991; Tautz *et al*, 1997; Xu *et al*, 1997).

In addition to and independent from its autoprotease activity, an immune evasion role has been identified for N^{pro} (Gil *et al*, 2006a). N^{pro} enhances degradation of interferon regulatory factor 3 (IRF-3) (Hilton *et al*, 2006), reducing stimulation of

interferon α/β (Baigent *et al*, 2002; Hilton *et al*, 2006). The ability of N^{pro} to bind zinc via a TRASH motif is essential for proteasomal degradation of IRF-3 (Szymanski *et al*, 2009), although whether N^{pro} interacts directly with IRF-3 remains to be determined.

1.2.2 BVDV virions contain three envelope glycoproteins

BVDV virions consist of a capsid containing C protein and genomic RNA, surrounded by a host-cell derived lipid bilayer with three envelope glycoproteins, E^{rns}, E1 and E2 (Thiel *et al*, 1991). C protein is highly basic, intrinsically disordered and binds to RNA non-specifically (Murray *et al*, 2008). Recent studies of CSFV have suggested C protein may not be essential for virion assembly, but is important for virulence (Riedel *et al*, 2012).

E^{rns} is a soluble glycoprotein that associates with the viral envelope via an unusual membrane anchor at its carboxy-terminus (Fetzer *et al*, 2005), as well as being secreted from infected cells (Rumenapf *et al*, 1993). It has been shown to bind to cell surface glycosaminoglycans (Iqbal *et al*, 2000). Amongst Flaviviridae, it is unique to the *Pestivirus* genus and possesses RNase activity (Schneider *et al*, 1993), and although it is has been shown to be dispensable for CSFV viral entry (Iqbal *et al*, 2004; Wang *et al*, 2004), it can inhibit double-stranded RNA-induced activation of interferon-β (Iqbal *et al*, 2004; Magkouras *et al*, 2008). Inactivation of RNase activity results in attenuation of infectious virus (Meyer *et al*, 2002).

E^{rns}, E1 and E2 all possess N-linked glycans, with eight, two and four potential glycosylation sites (with the sequence motif Asn-X-Ser/Thr, where X is any amino acid except proline) respectively (Weiland *et al*, 1990). There are no known O-linked glycosylation sites on the three envelope proteins. E2 has been shown to possess

intramolecular disulphide bonds, and additionally forms intermolecular disulphide bonds to stabilise homodimers and heterodimers with E1 (Branza-Nichita *et al*, 2001). E1E2 heterodimers have been shown to be essential for viral entry (Ronecker *et al*, 2008). E2 is the main determinant of cell culture tropism in pestiviruses, with chimeric BVDV expressing E2 from border disease virus exhibiting a reduced ability to propagate in bovine cells (Liang *et al*, 2003). Bovine CD46, a cell surface protein that acts as a cofactor for plasma serine protease factor I in cleaving complement proteins C3b and C4b, is a cellular receptor for BVDV, with expression of bovine CD46 in porcine cells sufficient to significantly increase susceptibility to BVDV infection (Maurer *et al*, 2004). Two structures of the ectodomain of BVDV E2 have recently been published (El Omari *et al*, 2013; Li *et al*, 2013), expressed in insect cells and HEK293T cells respectively. The structures show E2 to have an unusual architecture, suggesting the mechanism of pestivirus (and perhaps hepacivirus) entry is unique, whilst the lack of any recognizable fusion motif in the E2 structures suggests that E1 may play an important part in this step.

BVDV has been extensively used as a surrogate model of HCV for the study of potential antiviral compounds, sharing similar genomic and virion structure, and replication cycles (Buckwold *et al*, 2003). Although the use of BVDV has reduced in recent years with the development of HCV cell culture systems, it remains a useful tool for evaluating antiviral compounds and understanding more about viral biogenesis and the mammalian glycoprotein processing pathway.

1.3 Antiviral compounds

Antiviral compounds can be defined by two broad categories – direct-acting antivirals (DAAs), which directly target the virus or viral proteins, such as the HCV NS3/4A serine protease inhibitor telaprevir (Lin *et al*, 2006) and influenza neuraminidase inhibitor oseltamivir (Kim *et al*, 1997); and antivirals that effect an indirect antiviral response via a host-mediated mechanism, such as pegylated interferon-α (IFN-α). From 2001 until 2011, the standard of care (SOC) for patients with chronic hepatitis C infection has been a combination of pegylated IFN-α and ribavirin, which is only successful in inducing a sustained virological response (SVR) in less than half of patients with genotype 1 HCV. In 2011, two HCV protease inhibitors, telaprevir and boceprevir, were approved for use in combination with IFN-α and ribavirin, improving SVR rates up to 70% in treatment-naïve genotype 1 patients. More recently, in 2013, sofosbuvir, a HCV NS5B polymerase inhibitor (Sofia *et al*, 2010), has been approved for treatment of all HCV genotypes, either in combination with ribavirin alone, or as a triple therapy of sofosbuvir, ribavirin and IFN-α. Nevertheless, development of new drugs with greater efficacy and fewer side effects remains an important challenge, particularly with the rise of drug-resistant strains of various pathogens.

1.3.1 Thiazolides

Thiazolides are a class of small molecule antiparasitic, antibacterial and antiviral compounds, based on a thiazole ring coupled to a salicylic acid structure by a peptide bond. Nitazoxanide (NTZ) is the parent compound of these molecules (Figure 1.8) and in plasma is rapidly deacetylated to its active form, tizoxanide (TIZ) (Broekhuysen *et al*, 2000).

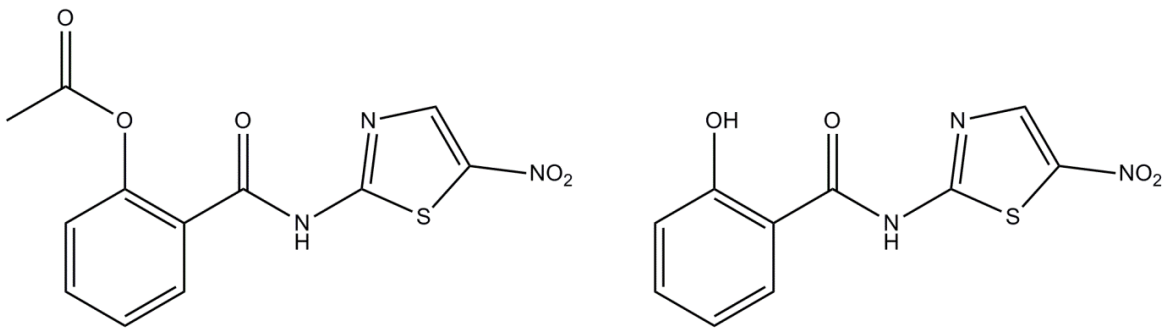

Figure 1.8 – Structures of nitazoxanide (NTZ) and its active metabolite, tizoxanide (TIZ).

NTZ was initially developed as part of a search for a broad spectrum antiparasitic drug (Rossignol & Cavier, 1976), and was found to be effective against *Cryptosporidium parvum*, an opportunistic pathogen that causes cryptosporidiosis in acquired immunodeficiency syndrome (AIDS) patients (Doumbo *et al*, 1997; Theodos *et al*, 1998; Rossignol *et al*, 2001a). In addition to this, it is highly effective against *Giardia lamblia* (Rossignol *et al*, 2001b), and is now licensed as Alinia™ for treatment of both these parasitic infections.

As well as being an anti-parasitic drug, NTZ shows antibacterial properties. Both NTZ and TIZ are highly effective against *Helicobacter pylori* (Megraud *et al*, 1998; Yamamoto *et al*, 1999), acting as an inhibitor of pyruvate oxidoreductase (Sisson *et al*, 2002; Hoffman *et al*, 2007). Furthermore, NTZ is effective against metronidazole-resistant strains of *H. pylori* (Megraud *et al*, 1998). Antibacterial activities of both NTZ and TIZ have also been shown against a broad range of anaerobic bacteria, both gram-positive and negative, including *Bacteriodes fragilis* and *Clostridium dificile* (Dubreuil *et al*, 1996). NTZ was also effective against the facultative anaerobe *Staphylococcus aureus* under anaerobic conditions (Dubreuil *et al*, 1996).

The nitro group of NTZ was initially considered to be essential for inhibition of pyruvate oxidoreductase (Sisson *et al*, 2002), with derivatives replacing the nitro group with a bromide showing no activity against a broad range of anaerobic species (Pankuch & Appelbaum, 2006). However, other non-nitro NTZ derivatives, including bromo-thiazolides, remained active against intracellular pathogens such as *Neospora caninum* (Esposito *et al*, 2005), suggesting a more complex structure-activity relationship. Modifications to the benzyl ring, particularly at the ortho-position, can also significantly alter activity (Esposito *et al*, 2005; Esposito *et al*, 2007).

During treatment of cryptosporidiosis in AIDS patients co-infected with HBV or HCV, the antiviral properties of NTZ were first observed (Rossignol & Keeffe, 2008). Since then, NTZ and other thiazolides have been shown to have antiviral potential against a number of different viruses, including enteric viruses (Rossignol *et al*, 2006; Rossignol & El-Gohary, 2006), JEV (Shi *et al*, 2014), HBV and HCV (Korba *et al*, 2008b).

The antiviral mechanisms of thiazolides appear varied yet remain unclear. NTZ has been shown to inhibit replication of subgenomic HCV replicon 1b and full-length HCV replicon 1a, and HBV replication in 2.2.15 cells (Korba *et al*, 2008b). It, however, had no effect on HBV RNA transcription, suggesting a post-transcriptional mechanism. NTZ has been shown to increase autophosphorylation of protein kinase activated by double-stranded RNA (PKR), which in turn phosphorylates eurokaryotic initiation factor 2α (eIF2α), inhibiting cap-dependent translation initiation (Elazar *et al*, 2009). Inhibition of cap-dependent translation would not be expected to directly affect HCV and BVDV replication, as both viruses possess IRES elements in their 5'-UTR, allowing cap-independent translation (Poole *et al*, 1995). Conversely, TIZ inhibits

influenza A virus replication but does not increase eIF2α phosphorylation in naive or influenza-infected cells (Rossignol *et al*, 2009), instead affecting hemagglutinin at a post-translation level. TIZ treatment disrupted hemagglutinin maturation, blocking transport to the trans-Golgi compartment and subsequent secretion.

With thiazolides having inhibitory activity against such a diverse range of parasites, bacteria and viruses, it is likely that any antiviral mechanisms will be host-mediated, rather than through direct interaction with virus. Further supporting this, no escape mutants have yet been observed in any study (Korba *et al*, 2008a).

1.3.2 Imino sugars

The origins of imino sugars as therapeutics dates back to ancient times and traditional Chinese herbal medicine (Compain & Martin, 2007). The first medication produced on an industrial scale, Haarlem oil, in the 17th century, recommended for the treatment of diabetes, contained, as a major component, extract from white mulberry (*Morus alba*) leaves, later found to be an extremely rich, natural source of imino sugars.

Imino sugars are monosaccharide mimics in which the endocyclic oxygen is replaced by nitrogen (Winchester & Fleet, 1992; Stutz, 1999). Nojirimycin is the parent compound of imino sugars and is an analogue of glucose. The 1-deoxy analogue of nojirimycin, 1-deoxynojirimycin (DNJ), is a stable, naturally occurring imino sugar found in mulberry plants, *Streptomyces* and *Bacillus*, and cannot be metabolized by mammals, and following its chemical synthesis in the 1960s (Paulsen, 1966), its biological activity as an α-glucosidase inhibitor was identified by Bayer chemists in 1976. In 1996, *N*-hydroxyethyl-DNJ (Miglitol) became the first imino sugar to become licensed for therapeutic use, as a treatment of type 2 diabetes, with *N*-butyl-DNJ

(*N*B-DNJ or Miglustat) following in 2003 as the first oral therapeutic for Gaucher disease (Figure 1.9).

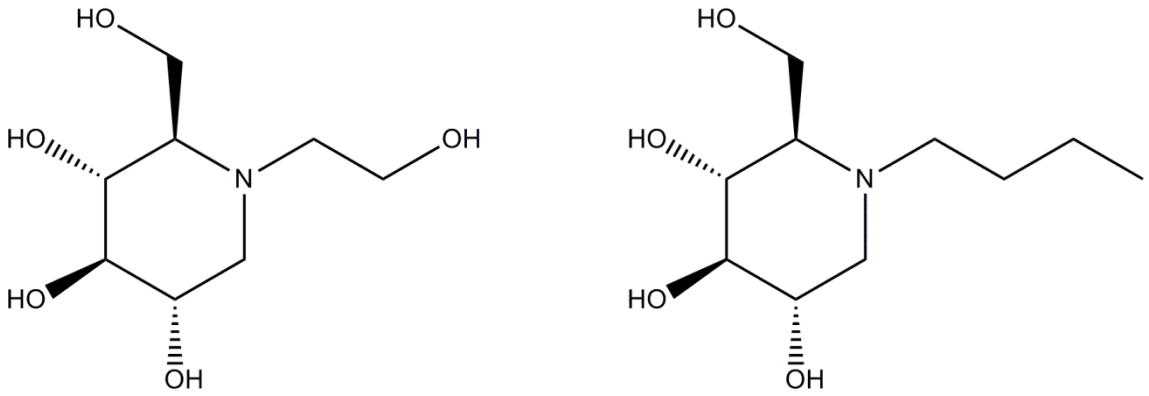

Figure 1.9 - Structures of Miglitol and Miglustat (*N*B-DNJ), licensed for treatment of type 2 diabetes and Gaucher disease respectively.

Imino sugars can mimic the natural substrates of carbohydrate-processing enzymes such as the ER-resident α-glucosidases I and II. Protonation of the imino sugar on the endocyclic nitrogen allows mimicry on the oxocarbonium ion transition state formed during carbohydrate hydrolysis, allowing the imino sugar to act as a competitive inhibitor binding to the active sites of carbohydrate-processing enzymes. Glucose mimics such as DNJ and castanospermine (CAST), and their derivatives, can bind to and inhibit glucose-hydrolysing enzymes such as α-glucosidases I and II in the ER. Mimics of other sugars, such as 1-deoxymannojirimycin (DMJ), an imino sugar mimic of mannose, can target other carbohydrate-processing enzymes.

By interrupting the glycoprocessing of nascent polypeptides in the ER through inhibition of α-glucosidases I and II, interaction with folding chaperones calnexin and calreticulin, which require the N-linked glycan to have been processed to a monoglucosylated state, can be prevented. Failure to fold correctly can lead to proteins being targeted for ERAD. Alternatively, some hyperglucosylated proteins

may be able to bypass the blockage to the calnexin cycle through endo-α-mannosidase processing in the Golgi (Moore & Spiro, 1990; Fujimoto & Kornfeld, 1991).

Imino sugars have a number of advantages for compound design and synthesis to define biological activity. As polyhydroxylated molecules, each chiral centre offers manipulation to generate isomers with restricted or enhanced mimicry, and the endocyclic nitrogen atom is readily modified to gain selectivity, increase potency or improve pharmacodynamics. The properties of imino sugars have considerable potential for treating a diverse range of diseases, including lysosomal storage disorders (Butters *et al*, 2000a), cystic fibrosis (Norez *et al*, 2006), and viral pathogenesis (Zitzmann *et al*, 1999; Chang *et al*, 2011), with a mechanism of action that is dictated by structural modification (Butters *et al*, 2000b).

DNJ is an imino sugar mimic of glucose, and its N-alkylated analogue *N*B-DNJ is an inhibitor of both the known cellular targets of DNJ-based imino sugars - ceramide glucosyl transferase (CGT), a key enzyme in the glycolipid biosynthetic pathway; and α-glucosidases I and II, N-glycan processing enzymes of the ER. *N*B-DNJ has been proposed as an effective treatment, known as 'substrate reduction therapy' (SRT), for a number of lysosomal storage diseases, in particular type I Gaucher disease for which clinical trials have been undertaken (Cox *et al*, 2000) and *N*B-DNJ (Miglustat, "Zavesca") is an approved medicine in USA, Europe and Israel for this disorder (Elstein *et al*, 2004).

The antiviral interest in imino sugars arose from studies with *N*B-DNJ, which underwent clinical trials for HIV therapy as a monotherapy (Tierney *et al*, 1995) and in combination with azidothymidine (AZT) (Fischl *et al*, 1994). Whilst these trials

were ultimately unsuccessful, *N*B-DNJ and other alkylated DNJ derivatives such as *N*-nonyl-DNJ (*N*N-DNJ) were further investigated using the BVDV cell culture system to study mechanism of action (Zitzmann *et al*, 1999). *N*N-DNJ was found to be almost 50 times more potent than *N*B-DNJ in antiviral assays despite similar inhibition constants against ER α-glucosidase I *in vitro* (Mellor *et al*, 2002). This improved efficacy was credited to the increased cellular uptake and enhanced membrane retention of the more hydrophobic nonyl chain, increasing availability of imino sugar to ER α-glucosidases.

Since these early antiviral studies, a variety of imino sugar derivatives have been developed in a search for more potent and less toxic antiviral compounds. Structures of a variety of imino sugars that have antiviral activities are shown in Table 1.1. These imino sugars have been shown to be antiviral against a broad range of enveloped viruses *in vitro*, and are summarised in Table 1.2.

.

Table 1.1 - Imino sugars with antiviral activities. See Table 1.2 for references.

Imino sugar	**Structure**
CAST	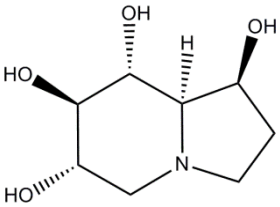
Bu-CAST	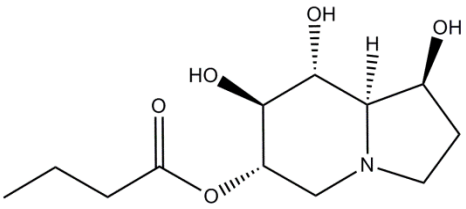
DNJ	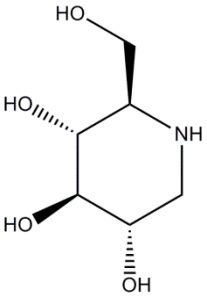
N-methyl-DNJ	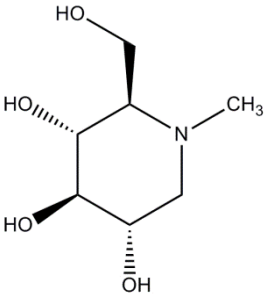
*N*B-DNJ	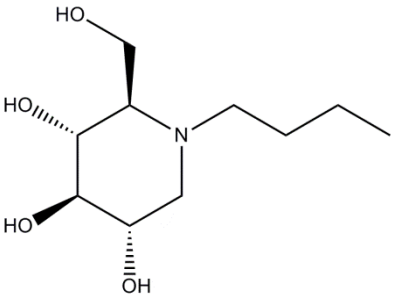
*N*N-DNJ	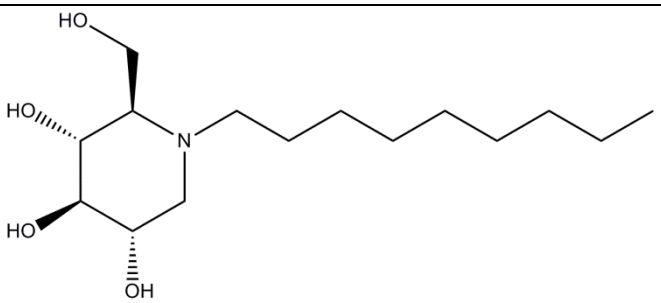

Imino sugar	Structure
*N*N-DGJ	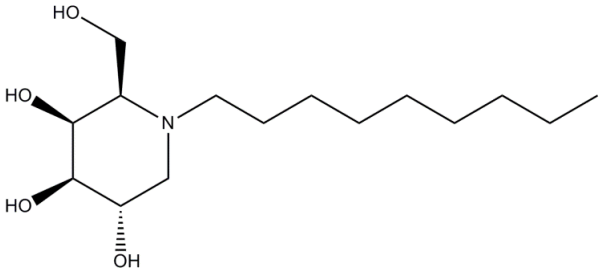
MON-DNJ	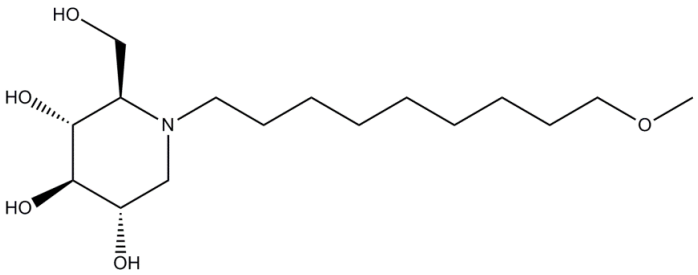
PBDNJ0804	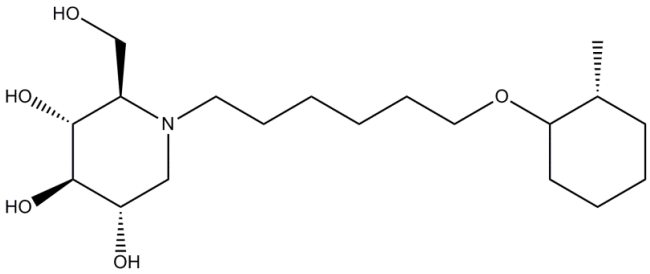
SP169	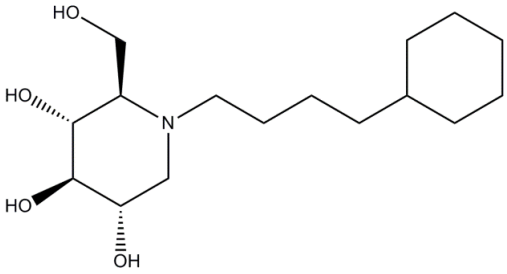
OSL-95II	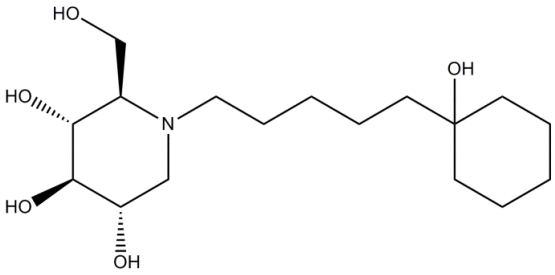
IHVR17028	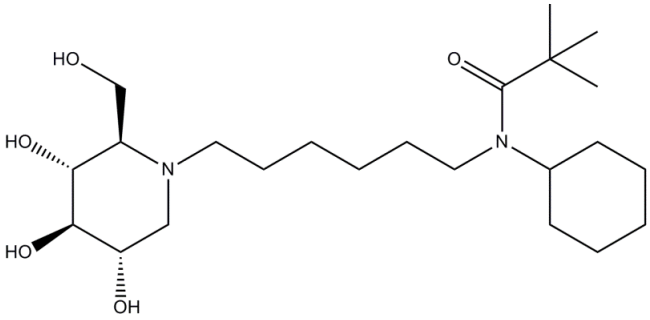

Table 1.2 - Viral targets of imino sugars shown in Table 1.1.

Virus	**Imino sugar**	**Reference**
Herpes simplex virus-2	Bu-CAST	(Ahmed *et al*, 1995)
Cytomegalovirus	CAST	(Taylor *et al*, 1988)
HBV	*N*B-DNJ, *N*N-DNJ, *N*N-DGJ	(Block *et al*, 1994; Lu *et al*, 2001; Mehta *et al*, 2001)
HIV	*N*B-DNJ, Bu-CAST	(Taylor *et al*, 1991; Taylor *et al*, 1994; Fischer *et al*, 1995; Fischer *et al*, 1996)
Moloney murine leukemia virus	Bu-CAST	(Taylor *et al*, 1991)
Rauscher murine leukemia virus	CAST	(Ruprecht *et al*, 1989)
Sindbis virus	DNJ	(Datema *et al*, 1984)
Semliki forest virus	*N*-methyl-DNJ	(Kaluza *et al*, 1990)
BVDV	*N*B-DNJ, MON-DNJ, *N*N-DNJ	(Zitzmann *et al*, 1999; Jordan *et al*, 2002; Mehta *et al*, 2002)
HCV	PBDNJ0804, *N*N-DNJ, *N*N-DGJ	(Steinmann *et al*, 2007; Qu *et al*, 2011)
Dengue virus	CAST, DNJ, SP169, OSL-95II, *N*N-DNJ, PBDNJ0804, MON-DNJ, NAP-DNJ	(Courageot *et al*, 2000; Wu *et al*, 2002; Whitby *et al*, 2005; Gu *et al*, 2007; Chang *et al*, 2009; Miller *et al*, 2012)
Japanese encephalitis virus	CAST, *N*N-DNJ	(Wu *et al*, 2002; Whitby *et al*, 2005)
West Nile virus	OSL-95II, PBDNJ0804	(Gu *et al*, 2007; Chang *et al*, 2009)
Severe acute respiratory syndrome coronavirus	*N*N-DNJ	(Fukushi *et al*, 2012)
Murine hepatitis virus	CAST, *N*-methyl-DNJ	(Repp *et al*, 1985)
Measles virus	CAST	(Bolt *et al*, 1999)
Vesicular stomatitis virus	DNJ, CAST	(Schlesinger *et al*, 1984)
Ebola virus	IHVR17028	(Chang *et al*, 2013)
Tacaribe virus	IHVR17028	(Chang *et al*, 2013)
Lassa virus	IHVR17028	(Chang *et al*, 2013)
Rift Valley fever virus	IHVR17028	(Chang *et al*, 2013)
Influenza A virus	CAST, DNJ	(Datema *et al*, 1984; Saito & Yamaguchi, 2000)

1.4 Project aims

This thesis will discuss the biological evaluation of a range of novel compounds against BVDV.

Chapter 2 will discuss a novel class of imino sugar α-glucosidase inhibitors based on a DNJ head group coupled to an adamantyl ring. This chapter establishes the ability of these compounds to inhibit BVDV infection and demonstrates the well-characterised correlation between α-glucosidase inhibition and antiviral activity. In addition to α-glucosidase inhibition, compounds with extended alkyl chain linkers between DNJ and the adamantyl ring show enhanced antiviral activity, suggesting a secondary antiviral mechanism. Indeed, this is further supported by antiviral effects observed with a non-α-glucosidase inhibiting galactose-derivative of one of the compounds.

Chapter 3 will discuss the biological evaluation of nitazoxanide (NTZ), an anti-microbial thiazolide currently licensed for treatment of parasitic infections. Here, the antiviral effects against BVDV are demonstrated. NTZ is shown to deplete ER and Golgi calcium stores, affecting cap-dependent translation, viral glycoprotein maturation and cell proliferation.

Chapter 4 will further investigate the effects of α-glucosidase inhibition on viral replication and glycosylation using the imino sugar NAP-DNJ, alongside and in combination with Golgi endomannosidase inhibition using glucose-isofagomine (GlcIFG). NAP-DNJ inhibits α-glucosidases I and II and enhances degradation of viral glycoproteins through ERAD. Inhibition of endomannosidase demonstrates it to be a valid antiviral target, and in combination with NAP-DNJ, enhances the antiviral effect observed from ER α-glucosidase inhibition alone, highlighting the potential of a

two-pronged approach to block viral glycoprocessing. In addition, this work uncovers the apparent use of endomannosidase by viral glycoproteins even in the absence of α-glucosidase inhibition, further emphasising the importance of this enzyme as part of the glycoprocessing pathway.

.

1.5 References

Ahmed SP, Nash RJ, Bridges CG, Taylor DL, Kang MS, Porter EA, Tyms AS (1995) Antiviral activity and metabolism of the castanospermine derivative MDL 28,574, in cells infected with herpes simplex virus type 2. *Biochemical and Biophysical Research Communications* **208:** 267-273

Anumula KR, Spiro RG (1983) Release of glucose-containing polymannose oligosaccharides during glycoprotein biosynthesis. Studies with thyroid microsomal enzymes and slices. *Journal of Biological Chemistry* **258:** 15274-15282

Apweiler R, Hermjakob H, Sharon N (1999) On the frequency of protein glycosylation, as deduced from analysis of the SWISS-PROT database. *Biochimica et Biophysica Acta - General Subjects* **1473:** 4-8

Baigent SJ, Zhang G, Fray MD, Flick-Smith H, Goodbourn S, McCauley JW (2002) Inhibition of beta interferon transcription by noncytopathogenic bovine viral diarrhea virus is through an interferon regulatory factor 3-dependent mechanism. *Journal of Virology* **76:** 8979-8988

Bannykh SI, Rowe T, Balch WE (1996) The organization of endoplasmic reticulum export complexes. *Journal of Cell Biology* **135:** 19-35

Bays NW, Gardner RG, Seelig LP, Joazeiro C, Hampton RY (2001) Hrd1p/Der3p is a membrane-anchored ubiquitin ligase required for ER-associated degradation. *Nature Cell Biology* **3:** 24-29

Bintintan I, Meyers G (2010) A new type of signal peptidase cleavage site identified in an RNA virus polyprotein. *Journal of Biological Chemistry* **285:** 8572-8584

Block TM, Lu X, Platt FM, Foster GR, Gerlich WH, Blumberg BS, Dwek RA (1994) Secretion of human hepatitis B virus is inhibited by the imino sugar N-butyldeoxynojirimycin. *Proc. Natl. Acad. Sci. USA* **91:** 2235-2239

Bolt G, Pedersen IR, Blixenkrone-Moller M (1999) Processing of N-linked oligosaccharides on the measles virus glycoproteins: importance for antigenicity and for production of infectious virus particles. *Virus Research* **61:** 43-51

Branza-Nichita N, Durantel D, Carrouee-Durantel S, Dwek RA, Zitzmann N (2001) Antiviral effect of N-butyldeoxynojirimycin against bovine viral diarrhea virus correlates with misfolding of E2 envelope proteins and impairment of their association into E1-E2 heterodimers. *Journal of Virology* **75:** 3527-3536

Broekhuysen J, Stockis A, Lins RL, De Graeve J, Rossignol JF (2000) Nitazoxanide: pharmacokinetics and metabolism in man. *International Journal of Clinical Pharmacology and Therapeutics* **38:** 387-394

Brownlie J (1990) Pathogenesis of mucosal disease and molecular aspects of bovine virus diarrhoea virus. *Veterinary Microbiology* **23:** 371-382

Brownlie J, Clarke MC, Howard CJ (1989) Experimental infection of cattle in early pregnancy with a cytopathic strain of bovine virus diarrhoea virus. *Research in Veterinary Science* **46:** 307-311

Buckwold VE, Beer BE, Donis RO (2003) Bovine viral diarrhea virus as a surrogate model of hepatitis C virus for the evaluation of antiviral agents. *Antiviral Research* **60:** 1-15

Buschhorn BA, Kostova Z, Medicherla B, Wolf DH (2004) A genome-wide screen identifies Yos9p as essential for ER-associated degradation of glycoproteins. *FEBS Letters* **577:** 422-426

Butters TD, Dwek RA, Platt FM (2000a) Inhibition of glycosphingolipid biosynthesis: application to lysosomal storage disorders. *Chemical Reviews* **100:** 4683-4696

Butters TD, van den Broek LAGM, Fleet GWJ, Krulle TM, Wormald MR, Dwek RA, Platt FM (2000b) Molecular requirements of imino sugars for the selective control of N-linked glycosylation and glycosphingolipid biosynthesis. *Tetrahedron: Asymmetry* **11:** 113-124

Cacan R, Dengremont C, Labiau O, Kmiecik D, Mir A, Verbert A (1996) Occurrence of a cytosolic neutral chitobiase activity involved in oligomannoside degradation: a study with Madin-Darby bovine kidney (MDBK) cells. *Biochemical Journal* **313:** 597-602

Cacan R, Duvet S, Labiau O, Verbert A, Krag SS (2001) Monoglucosylated oligomannosides are released during the degradation process of newly synthesized glycoproteins. *Journal of Biological Chemistry* **276:** 22307-22312

Caramelo JJ, Castro OA, Alonso LG, De Prat-Gay G, Parodi AJ (2003) UDP-Glc:glycoprotein glucosyltransferase recognizes structured and solvent accessible hydrophobic patches in molten globule-like folding intermediates. *Proc. Natl. Acad. Sci. USA* **100:** 86-91

Chang J, Schul W, Yip A, Xu X, Guo JT, Block TM (2011) Competitive inhibitor of cellular alpha-glucosidases protects mice from lethal dengue virus infection. *Antiviral Research* **92:** 369-371

Chang J, Wang L, Ma D, Qu X, Guo H, Xu X, Mason PM, Bourne N, Moriarty R, Gu B, Guo JT, Block TM (2009) Novel imino sugar derivatives demonstrate potent antiviral activity against flaviviruses. *Antimicrobial Agents and Chemotherapy* **53:** 1501-1508

Chang J, Warren TK, Zhao X, Gill T, Guo F, Wang L, Comunale MA, Du Y, Alonzi DS, Yu W, Ye H, Liu F, Guo JT, Mehta A, Cuconati A, Butters TD, Bavari S, Xu X, Block TM (2013) Small molecule inhibitors of ER alpha-glucosidases are active against multiple hemorrhagic fever viruses. *Antiviral Research* **98:** 432-440

Choukhi A, Ung S, Wychowski C, Dubuisson J (1998) Involvement of endoplasmic reticulum chaperones in the folding of hepatitis C virus glycoproteins. *Journal of Virology* **72:** 3851-3858

Christianson JC, Shaler TA, Tyler RE, Kopito RR (2008) OS-9 and GRP94 deliver mutant alpha1-antitrypsin to the Hrd1-SEL1L ubiquitin ligase complex for ERAD. *Nature Cell Biology* **10:** 272-282

Collett MS, Larson R, Gold C, Strick D, Anderson DK, Purchio AF (1988) Molecular cloning and nucleotide sequence of the pestivirus bovine viral diarrhea virus. *Virology* **165:** 191-199

Compain P, Martin OR (2007) *Iminosugars. From Synthesis to Therapeutic Applications,* Chichester, UK: John Wiley & Sons Ltd.

Courageot MP, Frenkiel MP, Dos Santos CD, Deubel V, Despres P (2000) Alpha-glucosidase inhibitors reduce dengue virus production by affecting the initial steps of virion morphogenesis in the endoplasmic reticulum. *Journal of Virology* **74:** 564-572

Cox T, Lachmann R, Hollak C, Aerts J, van Weely S, Hrebicek M, Platt F, Butters T, Dwek R, Moyses C, Gow I, Elstein D, Zimran A (2000) Novel oral treatment of Gaucher's disease with N-butyldeoxynojirimycin (OGT 918) to decrease substrate biosynthesis. *Lancet* **355:** 1481-1485

Daniels R, Kurowski B, Johnson AE, Hebert DN (2003) N-linked glycans direct the cotranslational folding pathway of influenza hemagglutinin. *Molecular Cell* **11:** 79-90

Datema R, Romero PA, Rott R, Schwarz RT (1984) On the role of oligosaccharide trimming in the maturation of Sindbis and influenza virus. *Archives of Virology* **81:** 25-39

Denic V, Quan EM, Weissman JS (2006) A luminal surveillance complex that selects misfolded glycoproteins for ER-associated degradation. *Cell* **126:** 349-359

Deprez P, Gautschi M, Helenius A (2005) More than one glycan is needed for ER glucosidase II to allow entry of glycoproteins into the calnexin/calreticulin cycle. *Molecular Cell* **19:** 183-195

Doumbo O, Rossignol JF, Pichard E, Traore HA, Dembele TM, Diakite M, Traore F, Diallo DA (1997) Nitazoxanide in the treatment of cryptosporidial diarrhea and other intestinal parasitic infections associated with acquired immunodeficiency syndrome in tropical Africa. *American Journal of Tropical Medicine and Hygiene* **56:** 637-639

Dubreuil L, Houcke I, Mouton Y, Rossignol JF (1996) In vitro evaluation of activities of nitazoxanide and tizoxanide against anaerobes and aerobic organisms. *Antimicrobial Agents and Chemotherapy* **40:** 2266-2270

Dubuisson J, Rice CM (1996) Hepatitis C virus glycoprotein folding: disulfide bond formation and association with calnexin. *Journal of Virology* **70:** 778-786

Durantel D, Branza-Nichita N, Carrouee-Durantel S, Butters TD, Dwek RA, Zitzmann N (2001) Study of the mechanism of antiviral action of iminosugar derivatives against bovine viral diarrhea virus. *Journal of Virology* **75:** 8987-8998

El Omari K, Iourin O, Harlos K, Grimes JM, Stuart DI (2013) Structure of a pestivirus envelope glycoprotein E2 clarifies its role in cell entry. *Cell Reports* **3:** 30-35

Elazar M, Liu M, McKenna SA, Liu P, Gehrig EA, Puglisi JD, Rossignol JF, Glenn JS (2009) The anti-hepatitis C agent nitazoxanide induces phosphorylation of eukaryotic initiation factor 2alpha via protein kinase activated by double-stranded RNA activation. *Gastroenterology* **137:** 1827-1835

Ellgaard L, Helenius A (2003) Quality control in the endoplasmic reticulum. *Nature Reviews Molecular Cell Biology* **4:** 181-191

Elstein D, Hollak C, Aerts JM, van Weely S, Maas M, Cox TM, Lachmann RH, Hrebicek M, Platt FM, Butters TD, Dwek RA, Zimran A (2004) Sustained therapeutic effects of oral miglustat (Zavesca, N -butyldeoxynojirimycin, OGT 918) in type I Gaucher disease. *Journal of Inherited Metabolic Disease* **27:** 757-766

Esposito M, Muller N, Hemphill A (2007) Structure-activity relationships from in vitro efficacies of the thiazolide series against the intracellular apicomplexan protozoan Neospora caninum. *International Journal of Parasitology* **37:** 183-190

Esposito M, Stettler R, Moores SL, Pidathala C, Muller N, Stachulski A, Berry NG, Rossignol JF, Hemphill A (2005) In vitro efficacies of nitazoxanide and other thiazolides against Neospora caninum tachyzoites reveal antiparasitic activity independent of the nitro group. *Antimicrobial Agents and Chemotherapy* **49:** 3715-3723

Fetzer C, Tews BA, Meyers G (2005) The carboxy-terminal sequence of the pestivirus glycoprotein E(rns) represents an unusual type of membrane anchor. *Journal of Virology* **79:** 11901-11913

Fischer PB, Collin M, Karlsson GB, James W, Butters TD, Davis SJ, Gordon S, Dwek RA, Platt FM (1995) The alpha-glucosidase inhibitor N-butyldeoxynojirimycin inhibits human immunodeficiency virus entry at the level of post-CD4 binding. *Journal of Virology* **69:** 5791-5797

Fischer PB, Karlsson GB, Dwek RA, Platt FM (1996) N-butyldeoxynojirimycin-mediated inhibition of human immunodeficiency virus entry correlates with impaired gp120 shedding and gp41 exposure. *Journal of Virology* **70:** 7153-7160

Fischl MA, Resnick L, Coombs R, Kremer AB, Pottage JC, Jr., Fass RJ, Fife KH, Powderly WG, Collier AC, Aspinall RL, et al. (1994) The safety and efficacy of combination N-butyl-deoxynojirimycin (SC-48334) and zidovudine in patients with HIV-1 infection and 200-500 CD4 cells/mm3. *Journal of Acquired Immune Deficiency Syndromes* **7:** 139-147

Frenkel Z, Gregory W, Kornfeld S, Lederkremer GZ (2003) Endoplasmic reticulum-associated degradation of mammalian glycoproteins involves sugar chain trimming to Man6-5GlcNAc2. *Journal of Biological Chemistry* **278:** 34119-34124

Frickel EM, Frei P, Bouvier M, Stafford WF, Helenius A, Glockshuber R, Ellgaard L (2004) ERp57 is a multifunctional thiol-disulfide oxidoreductase. *Journal of Biological Chemistry* **279:** 18277-18287

Fujimoto K, Kornfeld R (1991) alpha-Glucosidase II-deficient cells use endo alpha-mannosidase as a bypass route for N-linked oligosaccharide processing. *Journal of Biological Chemistry* **266:** 3571-3578

Fukushi M, Yoshinaka Y, Matsuoka Y, Hatakeyama S, Ishizaka Y, Kirikae T, Sasazuki T, Miyoshi-Akiyama T (2012) Monitoring of S protein maturation in the

endoplasmic reticulum by calnexin is important for the infectivity of severe acute respiratory syndrome coronavirus. *Journal of Virology* **86:** 11745-11753

Gauss R, Sommer T, Jarosch E (2006) The Hrd1p ligase complex forms a linchpin between ER-lumenal substrate selection and Cdc48p recruitment. *EMBO Journal* **25:** 1827-1835

Gil LH, Ansari IH, Vassilev V, Liang D, Lai VC, Zhong W, Hong Z, Dubovi EJ, Donis RO (2006a) The amino-terminal domain of bovine viral diarrhea virus Npro protein is necessary for alpha/beta interferon antagonism. *Journal of Virology* **80:** 900-911

Grinna LS, Robbins PW (1980) Substrate specificities of rat liver microsomal glucosidases which process glycoproteins. *Journal of Biological Chemistry* **255:** 2255-2258

Gross V, Tran-Thi TA, Schwarz RT, Elbein AD, Decker K, Heinrich PC (1986) Different effects of the glucosidase inhibitors 1-deoxynojirimycin, N-methyl-1-deoxynojirimycin and castanospermine on the glycosylation of rat alpha 1-proteinase inhibitor and alpha 1-acid glycoprotein. *Biochemical Journal* **236:** 853-860

Grummer B, Beer M, Liebler-Tenorio E, Greiser-Wilke I (2001) Localization of viral proteins in cells infected with bovine viral diarrhoea virus. *Journal of General Virology* **82:** 2597-2605

Gu B, Mason P, Wang L, Norton P, Bourne N, Moriarty R, Mehta A, Despande M, Shah R, Block T (2007) Antiviral profiles of novel iminocyclitol compounds against bovine viral diarrhea virus, West Nile virus, dengue virus and hepatitis B virus. *Antiviral Chemistry & Chemotherapy* **18:** 49-59

Hart GW, Brew K, Grant GA, Bradshaw RA, Lennarz WJ (1979) Primary structural requirements for the enzymatic formation of the N-glycosidic bond in glycoproteins. Studies with natural and synthetic peptides. *Journal of Biological Chemistry* **254:** 9747-9753

Harvey DJ, Merry AH, Royle L, Campbell MP, Dwek RA, Rudd PM (2009) Proposal for a standard system for drawing structural diagrams of N- and O-linked carbohydrates and related compounds. *Proteomics* **9:** 3796-3801

Heimann M, Roman-Sosa G, Martoglio B, Thiel HJ, Rumenapf T (2006) Core protein of pestiviruses is processed at the C terminus by signal peptide peptidase. *Journal of Virology* **80:** 1915-1921

Helenius A, Aebi M (2004) Roles of N-linked glycans in the endoplasmic reticulum. *Annual Review of Biochemistry* **73:** 1019-1049

Helenius J, Ng DT, Marolda CL, Walter P, Valvano MA, Aebi M (2002) Translocation of lipid-linked oligosaccharides across the ER membrane requires Rft1 protein. *Nature* **415:** 447-450

Hilton L, Moganeradj K, Zhang G, Chen YH, Randall RE, McCauley JW, Goodbourn S (2006) The NPro product of bovine viral diarrhea virus inhibits DNA binding by interferon regulatory factor 3 and targets it for proteasomal degradation. *Journal of Virology* **80:** 11723-11732

Hiraga N, Imamura M, Abe H, Hayes CN, Kono T, Onishi M, Tsuge M, Takahashi S, Ochi H, Iwao E, Kamiya N, Yamada I, Tateno C, Yoshizato K, Matsui H, Kanai A, Inaba T, Tanaka S, Chayama K (2011) Rapid emergence of telaprevir resistant hepatitis C virus strain from wildtype clone in vivo. *Hepatology* **54:** 781-788

Hoffman PS, Sisson G, Croxen MA, Welch K, Harman WD, Cremades N, Morash MG (2007) Antiparasitic drug nitazoxanide inhibits the pyruvate oxidoreductases of Helicobacter pylori, selected anaerobic bacteria and parasites, and Campylobacter jejuni. *Antimicrobial Agents and Chemotherapy* **51:** 868-876

Houe H (2003) Economic impact of BVDV infection in dairies. *Biologicals* **31:** 137-143

Huffaker TC, Robbins PW (1983) Yeast mutants deficient in protein glycosylation. *Proc. Natl. Acad. Sci. USA* **80:** 7466-7470

Iqbal M, Flick-Smith H, McCauley JW (2000) Interactions of bovine viral diarrhoea virus glycoprotein E(rns) with cell surface glycosaminoglycans. *Journal of General Virology* **81:** 451-459

Iqbal M, Poole E, Goodbourn S, McCauley JW (2004) Role for bovine viral diarrhea virus Erns glycoprotein in the control of activation of beta interferon by double-stranded RNA. *Journal of Virology* **78:** 136-145

Jakob CA, Burda P, Roth J, Aebi M (1998) Degradation of misfolded endoplasmic reticulum glycoproteins in Saccharomyces cerevisiae is determined by a specific oligosaccharide structure. *Journal of Cell Biology* **142:** 1223-1233

Jarosch E, Taxis C, Volkwein C, Bordallo J, Finley D, Wolf DH, Sommer T (2002) Protein dislocation from the ER requires polyubiquitination and the AAA-ATPase Cdc48. *Nature Cell Biology* **4:** 134-139

Jordan R, Nikolaeva OV, Wang L, Conyers B, Mehta A, Dwek RA, Block TM (2002) Inhibition of host ER glucosidase activity prevents Golgi processing of virion-associated bovine viral diarrhea virus E2 glycoproteins and reduces infectivity of secreted virions. *Virology* **295:** 10-19

Kaluza G, Repges S, McDowell W (1990) The significance of carbohydrate trimming for the antigenicity of the Semliki Forest virus glycoprotein E2. *Virology* **176:** 369-378

Karaivanova VK, Luan P, Spiro RG (1998) Processing of viral envelope glycoprotein by the endomannosidase pathway: evaluation of host cell specificity. *Glycobiology* **8:** 725-730

Kim CU, Lew W, Williams MA, Liu H, Zhang L, Swaminathan S, Bischofberger N, Chen MS, Mendel DB, Tai CY, Laver WG, Stevens RC (1997) Influenza neuraminidase inhibitors possessing a novel hydrophobic interaction in the enzyme active site: design, synthesis, and structural analysis of carbocyclic sialic acid analogues with potent anti-influenza activity. *Journal of the American Chemical Society* **119:** 681-690

King AMQ, Lefkowitz E, Adams MJ, Carstens EB. (2011) Virus Taxonomy Ninth Report of the International Committee on Taxonomy of Viruses. Elsevier Science, Burlington, p. 1 online resource (1462 p.).

Korba BE, Elazar M, Lui P, Rossignol JF, Glenn JS (2008a) Potential for hepatitis C virus resistance to nitazoxanide or tizoxanide. *Antimicrobial Agents & Chemotherapy* **52:** 4069-4071

Korba BE, Montero AB, Farrar K, Gaye K, Mukerjee S, Ayers MS, Rossignol JF (2008b) Nitazoxanide, tizoxanide and other thiazolides are potent inhibitors of hepatitis B virus and hepatitis C virus replication. *Antiviral Research* **77:** 56-63

Kornfeld R, Kornfeld S (1985) Assembly of asparagine-linked oligosaccharides. *Annual Review of Biochemistry* **54:** 631-664

Kukushkin NV, Easthope IS, Alonzi DS, Butters TD (2012) Restricted processing of glycans by endomannosidase in mammalian cells. *Glycobiology* **22:** 1282-1288

Kummerer BM, Tautz N, Becher P, Thiel H, Meyers G (2000) The genetic basis for cytopathogenicity of pestiviruses. *Veterinary Microbiology* **77:** 117-128

Lackner T, Muller A, Pankraz A, Becher P, Thiel HJ, Gorbalenya AE, Tautz N (2004) Temporal modulation of an autoprotease is crucial for replication and pathogenicity of an RNA virus. *Journal of Virology* **78:** 10765-10775

Larder BA, Kemp SD (1989) Multiple mutations in HIV-1 reverse transcriptase confer high-level resistance to zidovudine (AZT). *Science* **246:** 1155-1158

Leach MR, Cohen-Doyle MF, Thomas DY, Williams DB (2002) Localization of the lectin, ERp57 binding, and polypeptide binding sites of calnexin and calreticulin. *Journal of Biological Chemistry* **277:** 29686-29697

Lechner J, Wieland F (1989) Structure and biosynthesis of prokaryotic glycoproteins. *Annual Review of Biochemistry* **58:** 173-194

Li Y, Wang J, Kanai R, Modis Y (2013) Crystal structure of glycoprotein E2 from bovine viral diarrhea virus. *Proc. Natl. Acad. Sci. USA* **110:** 6805-6810

Liang D, Sainz IF, Ansari IH, Gil LH, Vassilev V, Donis RO (2003) The envelope glycoprotein E2 is a determinant of cell culture tropism in ruminant pestiviruses. *Journal of General Virology* **84:** 1269-1274

Lilley B, Ploegh H (2004) A membrane protein required for dislocation of misfolded proteins from the ER. *Nature* **429:** 834-840

Lin K, Perni RB, Kwong AD, Lin C (2006) VX-950, a novel hepatitis C virus (HCV) NS3-4A protease inhibitor, exhibits potent antiviral activities in HCV replicon cells. *Antimicrobial Agents and Chemotherapy* **50:** 1813-1822

Lindenbach BD, Thiel HJ, Rice CM (2006) Flaviviridae: The Viruses and Their Replication. In *Fields Virology, Fifth Edition*, Knipe DM, Howley PM, Griffin DE, Lamb RA, Martin MA, Roizman B, Straus SE (eds), 33, pp 1102-1152. Lippincott Williams and Wilkins

Lindquist JA, Hammerling GJ, Trowsdale J (2001) ER60/ERp57 forms disulfide-bonded intermediates with MHC class I heavy chain. *FASEB Journal* **15:** 1448-1450

Lu X, Lu Y, Geschwindt R, Dwek RA, Block TM (2001) Hepatitis B virus MHBs antigen is selectively sensitive to glucosidase-mediated processing in the endoplasmic reticulum. *DNA and Cell Biology* **20:** 647-656

Lubas WA, Spiro RG (1987) Golgi endo-alpha-D-mannosidase from rat liver, a novel N-linked carbohydrate unit processing enzyme. *Journal of Biological Chemistry* **262:** 3775-3781

Lubas WA, Spiro RG (1988) Evaluation of the role of rat liver Golgi endo-alpha-D-mannosidase in processing N-linked oligosaccharides. *Journal of Biological Chemistry* **263:** 3990-3998

Magkouras I, Matzener P, Rumenapf T, Peterhans E, Schweizer M (2008) RNase-dependent inhibition of extracellular, but not intracellular, dsRNA-induced interferon synthesis by Erns of pestiviruses. *Journal of General Virology* **89:** 2501-2506

Marshall RD (1972) Glycoproteins. *Annual Review of Biochemistry* **41:** 673-702

Matsuoka K, Orci L, Amherdt M, Bednarek SY, Hamamoto S, Schekman R, Yeung T (1998) COPII-coated vesicle formation reconstituted with purified coat proteins and chemically defined liposomes. *Cell* **93:** 263-275

Maurer K, Krey T, Moennig V, Thiel HJ, Rumenapf T (2004) CD46 is a cellular receptor for bovine viral diarrhea virus. *Journal of Virology* **78:** 1792-1799

McGinnes LW, Morrison TG (1998) Role of carbohydrate processing and calnexin binding in the folding and activity of the HN protein of Newcastle disease virus. *Virus Research* **53:** 175-185

McKimm-Breschkin JL (2000) Resistance of influenza viruses to neuraminidase inhibitors--a review. *Antiviral Research* **47:** 1-17

Megraud F, Occhialini A, Rossignol JF (1998) Nitazoxanide, a potential drug for eradication of Helicobacter pylori with no cross-resistance to metronidazole. *Antimicrobial Agents and Chemotherapy* **42:** 2836-2840

Mehta A, Carrouee S, Conyers B, Jordan R, Butters T, Dwek RA, Block TM (2001) Inhibition of hepatitis B virus DNA replication by imino sugars without the inhibition of the DNA polymerase: therapeutic implications. *Hepatology* **33:** 1488-1495

Mehta A, Ouzounov S, Jordan R, Simsek E, Lu X, Moriarty RM, Jacob G, Dwek RA, Block TM (2002) Imino sugars that are less toxic but more potent as antivirals, in vitro, compared with N-n-nonyl DNJ. *Antiviral Chemistry & Chemotherapy* **13:** 299-304

Mellor HR, Nolan J, Pickering L, Wormald MR, Platt FM, Dwek RA, Fleet GW, Butters TD (2002) Preparation, biochemical characterization and biological properties of radiolabelled N-alkylated deoxynojirimycins. *Biochemical Journal* **366:** 225-233

Messner P (1997) Bacterial glycoproteins. *Glycoconjugate Journal* **14:** 3-11

Meyer C, Von Freyburg M, Elbers K, Meyers G (2002) Recovery of virulent and RNase-negative attenuated type 2 bovine viral diarrhea viruses from infectious cDNA clones. *Journal of Virology* **76:** 8494-8503

Meyers G, Thiel HJ (1996) Molecular characterization of pestiviruses. *Advances in Virus Research* **47:** 53-118

Miller EA, Beilharz TH, Malkus PN, Lee MC, Hamamoto S, Orci L, Schekman R (2003) Multiple cargo binding sites on the COPII subunit Sec24p ensure capture of diverse membrane proteins into transport vesicles. *Cell* **114:** 497-509

Miller JL, Lachica R, Sayce AC, Williams JP, Bapat M, Dwek R, Beatty PR, Harris E, Zitzmann N (2012) Liposome-mediated delivery of iminosugars enhances efficacy against dengue virus in vivo. *Antimicrobial Agents and Chemotherapy* **56:** 6379-6386

Mirazimi A, Nilsson M, Svensson L (1998) The molecular chaperone calnexin interacts with the NSP4 enterotoxin of rotavirus in vivo and in vitro. *Journal of Virology* **72:** 8705-8709

Miyanari Y, Atsuzawa K, Usuda N, Watashi K, Hishiki T, Zayas M, Bartenschlager R, Wakita T, Hijikata M, Shimotohno K (2007) The lipid droplet is an important organelle for hepatitis C virus production. *Nature Cell Biology* **9:** 1089-1097

Moore SE, Spiro RG (1990) Demonstration that Golgi endo-alpha-D-mannosidase provides a glucosidase-independent pathway for the formation of complex N-linked oligosaccharides of glycoproteins. *Journal of Biological Chemistry* **265:** 13104-13112

Moore SE, Spiro RG (1994) Intracellular compartmentalization and degradation of free polymannose oligosaccharides released during glycoprotein biosynthesis. *Journal of Biological Chemistry* **269:** 12715-12721

Murray CL, Marcotrigiano J, Rice CM (2008) Bovine viral diarrhea virus core is an intrinsically disordered protein that binds RNA. *Journal of Virology* **82:** 1294-1304

Norez C, Noel S, Wilke M, Bijvelds M, Jorna H, Melin P, DeJonge H, Becq F (2006) Rescue of functional delF508-CFTR channels in cystic fibrosis epithelial cells by the alpha-glucosidase inhibitor miglustat. *FEBS Letters* **580:** 2081-2086

Orci L, Ravazzola M, Meda P, Holcomb C, Moore HP, Hicke L, Schekman R (1991) Mammalian Sec23p homologue is restricted to the endoplasmic reticulum transitional cytoplasm. *Proc. Natl. Acad. Sci. USA* **88:** 8611-8615

Pankuch GA, Appelbaum PC (2006) Activities of tizoxanide and nitazoxanide compared to those of five other thiazolides and three other agents against anaerobic species. *Antimicrobial Agents and Chemotherapy* **50:** 1112-1117

Parodi AJ (2000) Role of N-oligosaccharide endoplasmic reticulum processing reactions in glycoprotein folding and degradation. *Biochemical Journal* **348:** 1-13

Paulsen H (1966) Carbohydrates Containing Nitrogen or Sulfur in Hemiacetal Ring. *Angewandte Chemie-International Edition* **5:** 495-510

Pearse BR, Gabriel L, Wang N, Hebert DN (2008) A cell-based reglucosylation assay demonstrates the role of GT1 in the quality control of a maturing glycoprotein. *Journal of Cell Biology* **181:** 309-320

Peterhans E, Bachofen C, Stalder H, Schweizer M (2010) Cytopathic bovine viral diarrhea viruses (BVDV): emerging pestiviruses doomed to extinction. *Veterinary Research* **41:** 44

Peterson JR, Ora A, Van PN, Helenius A (1995) Transient, lectin-like association of calreticulin with folding intermediates of cellular and viral glycoproteins. *Molecular Biology of the Cell* **6:** 1173-1184

Pierce RJ, Spik G, Montreuil J (1979) Cytosolic location of an endo-N-acetyl-beta-D-glucosaminidase activity in rat liver and kidney. *Biochemical Journal* **180:** 673-676

Poole TL, Wang C, Popp RA, Potgieter LN, Siddiqui A, Collett MS (1995) Pestivirus translation initiation occurs by internal ribosome entry. *Virology* **206:** 750-754

Qu X, Pan X, Weidner J, Yu W, Alonzi D, Xu X, Butters T, Block T, Guo JT, Chang J (2011) Inhibitors of endoplasmic reticulum alpha-glucosidases potently suppress hepatitis C virus virion assembly and release. *Antimicrobial Agents and Chemotherapy* **55:** 1036-1044

Ratner L, vander Heyden N, Dedera D (1991) Inhibition of HIV and SIV infectivity by blockade of alpha-glucosidase activity. *Virology* **181:** 180-192

Repp R, Tamura T, Boschek CB, Wege H, Schwarz RT, Niemann H (1985) The effects of processing inhibitors of N-linked oligosaccharides on the intracellular migration of glycoprotein E2 of mouse hepatitis virus and the maturation of coronavirus particles. *Journal of Biological Chemistry* **260:** 15873-15879

Riedel C, Lamp B, Heimann M, Konig M, Blome S, Moennig V, Schuttler C, Thiel HJ, Rumenapf T (2012) The core protein of classical Swine Fever virus is dispensable for virus propagation in vitro. *PLoS Pathogens* **8:** e1002598

Roingeard P, Hourioux C, Blanchard E, Prensier G (2008) Hepatitis C virus budding at lipid droplet-associated ER membrane visualized by 3D electron microscopy. *Histochemistry and Cell Biology* **130:** 561-566

Ronecker S, Zimmer G, Herrler G, Greiser-Wilke I, Grummer B (2008) Formation of bovine viral diarrhea virus E1-E2 heterodimers is essential for virus entry and depends on charged residues in the transmembrane domains. *Journal of General Virology* **89:** 2114-2121

Rossanese OW, Soderholm J, Bevis BJ, Sears IB, O'Connor J, Williamson EK, Glick BS (1999) Golgi structure correlates with transitional endoplasmic reticulum organization in Pichia pastoris and Saccharomyces cerevisiae. *Journal of Cell Biology* **145:** 69-81

Rossignol JF, Abu-Zekry M, Hussein A, Santoro MG (2006) Effect of nitazoxanide for treatment of severe rotavirus diarrhoea: randomised double-blind placebo-controlled trial. *Lancet* **368:** 124-129

Rossignol JF, Ayoub A, Ayers MS (2001a) Treatment of diarrhea caused by Cryptosporidium parvum: a prospective randomized, double-blind, placebo-controlled study of Nitazoxanide. *Journal of Infectious Diseases* **184:** 103-106

Rossignol JF, Ayoub A, Ayers MS (2001b) Treatment of diarrhea caused by Giardia intestinalis and Entamoeba histolytica or E. dispar: a randomized, double-blind, placebo-controlled study of nitazoxanide. *Journal of Infectious Diseases* **184:** 381-384

Rossignol JF, Cavier R. (1976) New derivatives of 2-benzamido-5-nitrothiazoles. In Patent US (ed.), Vol. 3950351.

Rossignol JF, El-Gohary YM (2006) Nitazoxanide in the treatment of viral gastroenteritis: a randomized double-blind placebo-controlled clinical trial. *Alimentary Pharmacology & Therapeutics* **24:** 1423-1430

Rossignol JF, Keeffe EB (2008) Thiazolides: a new class of drugs for the treatment of chronic hepatitis B and C. *Future Microbiology* **3:** 539-545

Rossignol JF, La Frazia S, Chiappa L, Ciucci A, Santoro MG (2009) Thiazolides, a new class of anti-influenza molecules targeting viral hemagglutinin at the post-translational level. *Journal of Biological Chemistry* **284:** 29798-29808

Rumenapf T, Stark R, Heimann M, Thiel HJ (1998) N-terminal protease of pestiviruses: identification of putative catalytic residues by site-directed mutagenesis. *Journal of Virology* **72:** 2544-2547

Rumenapf T, Unger G, Strauss JH, Thiel HJ (1993) Processing of the envelope glycoproteins of pestiviruses. *Journal of Virology* **67:** 3288-3294

Ruprecht RM, Mullaney S, Andersen J, Bronson R (1989) In vivo analysis of castanospermine, a candidate antiretroviral agent. *Journal of Acquired Immune Deficiency Syndromes* **2:** 149-157

Saint-Pol A, Bauvy C, Codogno P, Moore SE (1997) Transfer of free polymannose-type oligosaccharides from the cytosol to lysosomes in cultured human hepatocellular carcinoma HepG2 cells. *Journal of Cell Biology* **136:** 45-59

Saint-Pol A, Codogno P, Moore SE (1999) Cytosol-to-lysosome transport of free polymannose-type oligosaccharides. Kinetic and specificity studies using rat liver lysosomes. *Journal of Biological Chemistry* **274:** 13547-13555

Saito T, Yamaguchi I (2000) Effect of glycosylation and glucose trimming inhibitors on the influenza A virus glycoproteins. *Journal of Veterinary Medical Science* **62:** 575-581

Schlesinger S, Koyama AH, Malfer C, Gee SL, Schlesinger MJ (1985) The effects of inhibitors of glucosidase I on the formation of Sindbis virus. *Virus Research* **2:** 139-149

Schlesinger S, Malfer C, Schlesinger MJ (1984) The formation of vesicular stomatitis virus (San Juan strain) becomes temperature-sensitive when glucose residues are retained on the oligosaccharides of the glycoprotein. *Journal of Biological Chemistry* **259:** 7597-7601

Schneider R, Unger G, Stark R, Schneider-Scherzer E, Thiel HJ (1993) Identification of a structural glycoprotein of an RNA virus as a ribonuclease. *Science* **261:** 1169-1171

Shailubhai K, Pratta MA, Vijay IK (1987) Purification and characterization of glucosidase I involved in N-linked glycoprotein processing in bovine mammary gland. *Biochemical Journal* **247:** 555-562

Shailubhai K, Pukazhenthi BS, Saxena ES, Varma GM, Vijay IK (1991) Glucosidase I, a transmembrane endoplasmic reticular glycoprotein with a luminal catalytic domain. *Journal of Biological Chemistry* **266:** 16587-16593

Shi Z, Wei J, Deng X, Li S, Qiu Y, Shao D, Li B, Zhang K, Xue F, Wang X, Ma Z (2014) Nitazoxanide inhibits the replication of Japanese encephalitis virus in cultured cells and in a mouse model. *Virology Journal* **11:** 10

Sisson G, Goodwin A, Raudonikiene A, Hughes NJ, Mukhopadhyay AK, Berg DE, Hoffman PS (2002) Enzymes associated with reductive activation and action of nitazoxanide, nitrofurans, and metronidazole in Helicobacter pylori. *Antimicrobial Agents and Chemotherapy* **46:** 2116-2123

Sofia MJ, Bao D, Chang W, Du J, Nagarathnam D, Rachakonda S, Reddy PG, Ross BS, Wang P, Zhang HR, Bansal S, Espiritu C, Keilman M, Lam AM, Steuer HM, Niu C, Otto MJ, Furman PA (2010) Discovery of a beta-d-2'-deoxy-2'-alpha-fluoro-2'-beta-C-methyluridine nucleotide prodrug (PSI-7977) for the treatment of hepatitis C virus. *Journal of Medicinal Chemistry* **53:** 7202-7218

Sousa M, Parodi AJ (1995) The molecular basis for the recognition of misfolded glycoproteins by the UDP-Glc:glycoprotein glucosyltransferase. *EMBO Journal* **14:** 4196-4203

Steinmann E, Whitfield T, Kallis S, Dwek RA, Zitzmann N, Pietschmann T, Bartenschlager R (2007) Antiviral effects of amantadine and iminosugar derivatives against hepatitis C virus. *Hepatology* **46:** 330-338

Stutz AE (1999) *Iminosugars as Glycosidase Inhibitors*, Weinheim: Wiley-VCH.

Susser S, Welsch C, Wang Y, Zettler M, Domingues FS, Karey U, Hughes E, Ralston R, Tong X, Herrmann E, Zeuzem S, Sarrazin C (2009) Characterization of resistance to the protease inhibitor boceprevir in hepatitis C virus-infected patients. *Hepatology* **50:** 1709-1718

Suzuki T, Park H, Lennarz W (2002a) Cytoplasmic peptide: N-glycanase (PNGase) in eukaryotic cells: occurrence, primary structure, and potential functions. *FASEB Journal* **16:** 635-641

Suzuki T, Yano K, Sugimoto S, Kitajima K, Lennarz WJ, Inoue S, Inoue Y, Emori Y (2002b) Endo-beta-N-acetylglucosaminidase, an enzyme involved in processing of free oligosaccharides in the cytosol. *Proc. Natl. Acad. Sci. USA* **99:** 9691-9696

Szymanski MR, Fiebach AR, Tratschin JD, Gut M, Ramanujam VM, Gottipati K, Patel P, Ye M, Ruggli N, Choi KH (2009) Zinc binding in pestivirus N(pro) is required for interferon regulatory factor 3 interaction and degradation. *Journal of Molecular Biology* **391:** 438-449

Tamura T, Cormier JH, Hebert DN (2008) Sweet bays of ERAD. *Trends in Biochemical Sciences* **33:** 298-300

Tautz N, Elbers K, Stoll D, Meyers G, Thiel HJ (1997) Serine protease of pestiviruses: determination of cleavage sites. *Journal of Virology* **71:** 5415-5422

Taylor DL, Fellows LE, Farrar GH, Nash RJ, Taylor-Robinson D, Mobberley MA, Ryder TA, Jeffries DJ, Tyms AS (1988) Loss of cytomegalovirus infectivity after treatment with castanospermine or related plant alkaloids correlates with aberrant glycoprotein synthesis. *Antiviral Research* **10:** 11-26

Taylor DL, Kang MS, Brennan TM, Bridges CG, Sunkara PS, Tyms AS (1994) Inhibition of alpha-glucosidase I of the glycoprotein-processing enzymes by 6-O-butanoyl castanospermine (MDL 28,574) and its consequences in human immunodeficiency virus-infected T cells. *Antimicrobial Agents and Chemotherapy* **38:** 1780-1787

Taylor DL, Sunkara PS, Liu PS, Kang MS, Bowlin TL, Tyms AS (1991) 6-0-butanoylcastanospermine (MDL 28,574) inhibits glycoprotein processing and the growth of HIVs. *AIDS* **5:** 693-698

Theodos CM, Griffiths JK, D'Onfro J, Fairfield A, Tzipori S (1998) Efficacy of nitazoxanide against Cryptosporidium parvum in cell culture and in animal models. *Antimicrobial Agents and Chemotherapy* **42:** 1959-1965

Thiel HJ, Stark R, Weiland E, Rumenapf T, Meyers G (1991) Hog cholera virus: molecular composition of virions from a pestivirus. *Journal of Virology* **65:** 4705-4712

Tierney M, Pottage J, Kessler H, Fischl M, Richman D, Merigan T, Powderly W, Smith S, Karim A, Sherman J, et al. (1995) The tolerability and pharmacokinetics of

N-butyl-deoxynojirimycin in patients with advanced HIV disease (ACTG 100). The AIDS Clinical Trials Group (ACTG) of the National Institute of Allergy and Infectious Diseases. *Journal of Acquired Immune Deficiency Syndromes and Human Retrovirology* **10:** 549-553

Torossi T, Roth J, Ziak M (2007) A single tryptophan residue of endomannosidase is crucial for Golgi localization and in vivo activity. *Cellular and Molecular Life Sciences* **64:** 1881-1889

Totani K, Ihara Y, Tsujimoto T, Matsuo I, Ito Y (2009) The recognition motif of the glycoprotein-folding sensor enzyme UDP-Glc:glycoprotein glucosyltransferase. *Biochemistry* **48:** 2933-2940

Trombetta ES, Simons JF, Helenius A (1996) Endoplasmic reticulum glucosidase II is composed of a catalytic subunit, conserved from yeast to mammals, and a tightly bound noncatalytic HDEL-containing subunit. *Journal of Biological Chemistry* **271:** 27509-27516

Varki A, Cummings RD, Esko JD, Freeze HH, Stanley P, Bertozzi CR, Hart GW, Etzler ME (2009) *Essentials of Glycobiology*, Cold Spring Harbor, NY: Cold Spring Harbor Laboratory Press.

Wang L, Dobberstein B (1999) Oligomeric complexes involved in translocation of proteins across the membrane of the endoplasmic reticulum. *FEBS Letters* **457:** 316-322

Wang Z, Nie Y, Wang P, Ding M, Deng H (2004) Characterization of classical swine fever virus entry by using pseudotyped viruses: E1 and E2 are sufficient to mediate viral entry. *Virology* **330:** 332-341

Ware FE, Vassilakos A, Peterson PA, Jackson MR, Lehrman MA, Williams DB (1995) The molecular chaperone calnexin binds Glc1Man9GlcNAc2 oligosaccharide as an initial step in recognizing unfolded glycoproteins. *Journal of Biological Chemistry* **270:** 4697-4704

Wegelt A, Reimann I, Zemke J, Beer M (2009) New insights into processing of bovine viral diarrhea virus glycoproteins E(rns) and E1. *Journal of General Virology* **90:** 2462-2467

Weiland E, Stark R, Haas B, Rumenapf T, Meyers G, Thiel HJ (1990) Pestivirus glycoprotein which induces neutralizing antibodies forms part of a disulfide-linked heterodimer. *Journal of Virology* **64:** 3563-3569

Welsch S, Miller S, Romero-Brey I, Merz A, Bleck CK, Walther P, Fuller SD, Antony C, Krijnse-Locker J, Bartenschlager R (2009) Composition and three-dimensional architecture of the dengue virus replication and assembly sites. *Cell Host & Microbe* **5:** 365-375

Weng S, Spiro RG (1993) Demonstration that a kifunensine-resistant alpha-mannosidase with a unique processing action on N-linked oligosaccharides occurs in rat liver endoplasmic reticulum and various cultured cells. *Journal of Biological Chemistry* **268:** 25656-25663

Weng S, Spiro RG (1996) Endoplasmic reticulum kifunensine-resistant α-mannosidase is enzymatically and immunologically related to the cytosolic α-mannosidase. *Archives of Biochemistry and Biophysics* **325:** 113-123

Weng S, Spiro RG (1997) Demonstration of a peptide: N-glycosidase in the endoplasmic reticulum of rat liver. *Biochemical Journal* **322:** 655-661

Werr M, Prange R (1998) Role for calnexin and N-linked glycosylation in the assembly and secretion of hepatitis B virus middle envelope protein particles. *Journal of Virology* **72:** 778-782

Whitby K, Pierson TC, Geiss B, Lane K, Engle M, Zhou Y, Doms RW, Diamond MS (2005) Castanospermine, a potent inhibitor of dengue virus infection in vitro and in vivo. *Journal of Virology* **79:** 8698-8706

Wiertz E, Tortorella D, Bogyo M, Yu J, Mothes W, Jones T, Rapoport T, Ploegh H (1996) Sec61-mediated transfer of a membrane protein from the endoplasmic reticulum to the proteasome for destruction. *Nature* **384:** 432-438

Winchester B, Fleet GW (1992) Amino-sugar glycosidase inhibitors: versatile tools for glycobiologists. *Glycobiology* **2:** 199-210

Wiskerchen M, Belzer SK, Collett MS (1991) Pestivirus gene expression: the first protein product of the bovine viral diarrhea virus large open reading frame, p20, possesses proteolytic activity. *Journal of Virology* **65:** 4508-4514

Wiskerchen M, Collett MS (1991) Pestivirus gene expression: protein p80 of bovine viral diarrhea virus is a proteinase involved in polyprotein processing. *Virology* **184:** 341-350

Wu SF, Lee CJ, Liao CL, Dwek RA, Zitzmann N, Lin YL (2002) Antiviral effects of an iminosugar derivative on flavivirus infections. *Journal of Virology* **76:** 3596-3604

Xu J, Mendez E, Caron PR, Lin C, Murcko MA, Collett MS, Rice CM (1997) Bovine viral diarrhea virus NS3 serine proteinase: polyprotein cleavage sites, cofactor requirements, and molecular model of an enzyme essential for pestivirus replication. *Journal of Virology* **71:** 5312-5322

Yamamoto Y, Hakki A, Friedman H, Okubo S, Shimamura T, Hoffman PS, Rossignol J (1999) Nitazoxanide, a nitrothiazolide antiparasitic drug, is an anti-Helicobacter pylori agent with anti-vacuolating toxin activity. *Chemotherapy* **45:** 303-312

Yan Q, Lennarz WJ (1999) Oligosaccharyltransferase: a complex multisubunit enzyme of the endoplasmic reticulum. *Biochemical and Biophysical Research Communications* **266:** 684-689

Yanagida K, Natsuka S, Hase S (2006) Structural diversity of cytosolic free oligosaccharides in the human hepatoma cell line, HepG2. *Glycobiology* **16:** 294-304

Yu H, Grassmann CW, Behrens SE (1999) Sequence and structural elements at the 3' terminus of bovine viral diarrhea virus genomic RNA: functional role during RNA replication. *Journal of Virology* **73:** 3638-3648

Yu H, Isken O, Grassmann CW, Behrens SE (2000) A stem-loop motif formed by the immediate 5' terminus of the bovine viral diarrhea virus genome modulates translation as well as replication of the viral RNA. *Journal of Virology* **74:** 5825-5835

Zitzmann N, Mehta AS, Carrouee S, Butters TD, Platt FM, McCauley J, Blumberg BS, Dwek RA, Block TM (1999) Imino sugars inhibit the formation and secretion of bovine viral diarrhea virus, a pestivirus model of hepatitis C virus: implications for the development of broad spectrum anti-hepatitis virus agents. *Proc. Natl. Acad. Sci. USA* **96:** 11878-11882

2 Novel imino sugar α-glucosidase inhibitors as antiviral compounds

2.1 Introduction

Imino sugars are monosaccharide mimics in which the endocyclic oxygen has been replaced by nitrogen (Stutz, 1999). They have a number of advantages for compound design and synthesis to define biological activity. As polyhydroxylated molecules, each chiral centre offers manipulation to generate isomers with restricted or enhanced mimicry, whilst the endocyclic nitrogen atom can be readily modified to gain selectivity, increase potency or improve pharmacodynamics. The properties of imino sugars have considerable potential for treating a diverse range of diseases, including lysosomal storage disorders (Butters *et al*, 2000a), cystic fibrosis (Norez *et al*, 2006), and viral pathogenesis (Zitzmann *et al*, 1999; Chang *et al*, 2011), with a mechanism of action that is dictated by structural modification (Butters *et al*, 2000b). Two N-alkylated imino sugars, miglitol and miglustat, are approved medicines for the treatment of type 2 diabetes and Gaucher disease, respectively (Compain & Martin, 2007).

Deoxynojirimycin (DNJ) is an imino sugar mimic of glucose, and its N-alkylated derivative *N*-butyl deoxynojirimycin (*N*B-DNJ) is an inhibitor of both the known cellular targets of DNJ-based imino sugars – ceramide glucosyl transferase (CGT), a key enzyme in the glycolipid biosynthetic pathway and the N-glycan processing enzymes of the ER, α-glucosidases I and II.

The class of imino sugar derivatives discussed in this chapter has been generated through click chemistry, using alkyl linkers of varying length, to attach functionalised adamantyl rings to the endocyclic nitrogen of a DNJ or deoxygalactonojirimycin

(DGJ) head group (Figure 2.1). Adamantyl-DNJ conjugates have previously been shown to be potent inhibitors of glucose-processing enzymes (Overkleeft *et al*, 1998), whilst other adamantyl structures have been shown to inhibit HCV p7 and influenza M2 ion channels (Wang *et al*, 1993; Griffin *et al*, 2003). Combining a DNJ head group with an adamantyl structure may potentially allow a two-pronged antiviral approach, targeting both α-glucosidases and viral ion channels. The DNJ conjugates have previously been studied to gain structure-activity relationship insights into their potential to inhibit both CGT and ER α-glucosidases I and II (Ardes-Guisot *et al*, 2011). All compounds inhibited rice α-glucosidase with sub-micromolar IC_{50} values, which decreased with increasing alkyl linker length. Inhibition of β-glucosidases was less potent, with only longer chain compounds inhibiting almond β-glucosidase and only one compound (compound **8** in Figure 2.1) showing enhanced inhibition over miglitol against rat intestinal cellobiase (Ardes-Guisot *et al*, 2011). No inhibition was observed against α-galactosidase, α- or β-mannosidase.

Following on from the initial investigation of these compounds into the enzyme targets discussed above (Ardes-Guisot *et al*, 2011), this chapter attempts to consolidate our knowledge on this class of compounds by focusing on their potential to be antiviral, using the HCV surrogate model, bovine viral diarrhea virus (BVDV) (Buckwold *et al*, 2003). The antiviral mechanism of action remains to be fully understood but in the case of DNJ-based imino sugars, the inhibition of the ER glucosidases resulting in the disruption of the N-linked oligosaccharide processing pathway in the cell is a key factor (Greimel *et al*, 2003; Norton *et al*, 2007). However, the ability of these compounds to inhibit CGT, any viral ion channels (such as p7 of HCV and BVDV) plus any other unknown mechanisms of action provided by these intriguing molecules cannot be discounted.

This chapter expands on previous work showing the *in vitro* CGT and ER α-glucosidase inhibition of seven adamantyl-DNJ structures (Ardes-Guisot *et al*, 2011), and relates the *in cellulo* ER α-glucosidase inhibition to the antiviral activity of these compounds, alongside a novel adamantyl-DGJ analogue (Howe *et al*, 2013), and aims to further our understanding of these compounds as novel antivirals using the cell culture BVDV model. DGJ structures are incapable of inhibiting α-glucosidases and as such provide a valuable control for investigating the effects of α-glucosidase inhibition on viral output. Initially analysing the α-glucosidase inhibition by FOS analysis, it is possible to differentiate in a cellular context the relative inhibitions of both α-glucosidases I and II and compare them to the antiviral capacity against BVDV to reveal the antiviral potential of these compounds. Whilst α-glucosidase inhibition appears to be the major mechanism via which antiviral effects are observed, for longer chain derivatives of the adamantyl-DNJ compounds, and the DGJ analogue for which no α-glucosidase inhibition is observed, additional antiviral activity is noted, indicating a secondary antiviral mechanism is likely to be involved.

The work presented in this chapter has been published in Bioorganic & Medicinal Chemistry (Howe *et al*, 2013).

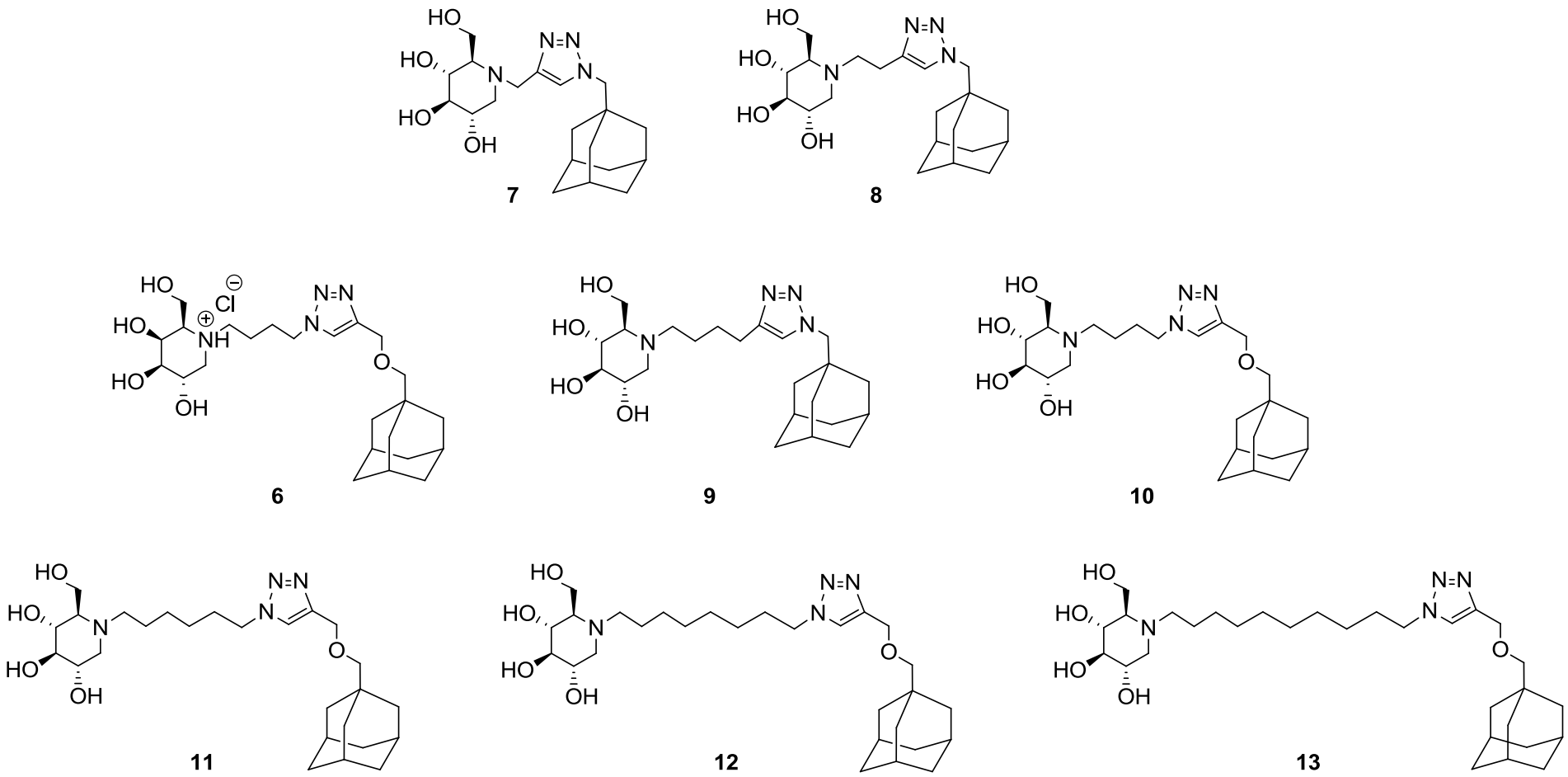

Figure 2.1 - Structures of the adamantyl-imino sugar conjugates **6-13**, previously synthesised (Ardes-Guisot *et al*, 2011; Howe *et al*, 2013). Compounds are numbered for consistency as detailed in (Howe *et al*, 2013).

2.2 Materials and methods

2.2.1 Materials

Adamantyl-DNJ conjugates **7-13** and adamantyl-DGJ conjugate **6** were kindly provided by Dr. Nicolas Ardes-Guisot (Laboratoire de Glycochimie Moléculaire et Macromoléculaire, Institut de Chimie Moléculaire et des Matériaux d'Orsay, France) and Dr. Yves Bleriot (Institut de Chimie des Milieux et Matériaux de Poitiers, France). Compounds were resuspended in dimethyl sulfoxide (DMSO) as 1000x stocks. All other reagents were supplied by Sigma-Aldrich, unless otherwise specified.

2.2.2 Cell culture

MDBK cells (European Collection of Animal Cell Cultures, Porton Down, United Kingdom) were cultured in RPMI-1640 medium (PAA Laboratories, Teddington, UK) supplemented with 10% BVDV-free fetal calf serum (Invitrogen), 2 mM L-glutamine (PAA) and 1x penicillin-streptomycin (PAA), at 37°C in a humidified atmosphere containing 5% CO2 (v/v).

BVDV-1 (cytopathic NADL strain) was provided by Professor Nicole Zitzmann (Oxford Glycobiology Institute, University of Oxford, UK).

MDBK cells and fetal calf serum were verified to be free from BVDV contamination by reverse transcriptase (RT)-PCR.

2.2.3 Cell proliferation assays

A CellTiter 96R aqueous non-radioactive cell proliferation assay kit (Promega) was used to measure the effect of compounds on cell proliferation, according to manufacturer protocol. MDBK cells were seeded in 96 well plates (5 x 10^3/well) and incubated for 24 h. Media was removed from wells and replaced with fresh media

containing different concentrations of imino sugars shown in Figure 2.1, and then incubated for a further 72 h.

Next, 40 µl of 3-(4,5-dimethylthiazol-2-yl)-5-(3-carboxymethoxyphenyl)-2-(4-sulfophenyl-2H tetrazolium) (MTS):phenazine methosulfate (PMS) mixture (20:1) were added to each well and the samples incubated for 2 h. The absorbance of formazan product was measured at 490 nm with a UVmax plate reader (Molecular Devices). Samples were analysed in triplicate and the concentrations at which absorbance at 490 nm was 50% of 0.1% DMSO-treated controls (CC_{50}) were determined.

2.2.4 Carbohydrate analysis

MDBK cells were seeded in 6-well plates (1 x 10^6 cells/well) in medium containing different concentrations of imino sugars and incubated at 37°C, 5% CO_2 atmosphere, for 24 h. After incubation, cells were washed with phosphate-buffered saline (PBS) and collected, then centrifuged at 1,000 x g for 5 m. Pellets were frozen briefly at -20°C, then resuspended in 1 ml H_2O and dounce-homogenised. Free oligosaccharides (FOS) were extracted and purified as previously described (Alonzi *et al*, 2008). Samples were desalted and deproteinated by mixed bed ion-exchange chromatography, and FOS were then labelled with 2-anthranilic acid (2-AA) (Neville *et al*, 2004) for 1 h at 80°C. Next, 2-AA-labelled FOS were purified by chromatography using Discovery Speed Amide-2 columns (Alonzi *et al*, 2008), and then further purified by affinity chromatography using Concanavalin A (ConA)-Sepharose 4B columns (100 ml packed resin) as described previously (Alonzi *et al*, 2008). Finally, 2-AA-labelled FOS species were separated by normal phase high performance liquid chromatography (NP-HPLC) using a 4.6 x 250 mm TSKgel

Amide-80 column (Anachem) (Neville *et al*, 2004), as described previously (Alonzi *et al*, 2009). Amounts of each FOS were calculated against oligosaccharide standards of known concentration by measuring peak areas and expressed relative to protein concentration, determined by standard bicinchoninic acid assay.

2.2.5 Fluorescence focus assay

MDBK cells were seeded in 6-well plates (1.75 x 10^6 cells/well) and infected with BVDV at a multiplicity of infection (MOI) of 1, followed by incubation with different concentrations of imino sugars for 24 h. Cell culture medium was then harvested and clarified by centrifugation at 1,000 x g for 10 m to remove cell debris. Serial dilutions were made and used to infect naive MDBK cells seeded in 96-well plates (7 x 10^4/well). Cells were incubated for 24 h, then washed twice with ice-cold PBS and fixed with 4% (v/v) paraformaldehyde in PBS for 30 m at room temperature. Cells were washed again and blocked for 2 h in 5% (w/v) milk in PBS. Cells were then permeabilised with 1% (v/v) Triton-X-100 in PBS for 20 m, washed with 1% (v/v) Tween20 in PBS and incubated with MAb103/105 (2 µg/ml in 5% milk-PBS; Animal Health Veterinary Laboratories Agency, Weybridge, UK) for 1 h. Cells were washed three times with 1% Tween20-PBS then incubated with anti-mouse fluorescein isothiocyanate (FITC)-conjugated secondary antibody (2 µg/ml in 5% milk-PBS; Sigma). Finally, cells were washed again with 1% Tween20-PBS, and nuclei stained with 4',6-diamidino-2-phenylindole (DAPI; Vector Laboratories Inc.). Cells were observed and evaluated using an inverted Nikon Eclipse TE200-U microscope, equipped with a Fluor 10X objective lens, and FITC and UV filter sets. Fluorescent foci were counted, and virus titres (fluorescent focus units (FFU)/ml) calculated.

2.2.6 Real-time RT-PCR analysis

MDBK cells were seeded in 6-well plates (1.75 x 10^6 cells/well) and infected with BVDV at an MOI of 1, followed by incubation with different concentrations of imino sugars for 24 h. Cell culture medium was then harvested and clarified by centrifugation at 5000 rpm for 10 m to remove cell debris.

A QIAamp viral RNA mini kit (Qiagen, Crawley, UK) was used to purify viral RNA from cell culture medium, according to the manufacturer's protocol. The purified RNA samples were treated with DNase (20 m at 37°C, followed by 10 m at 75°C for deactivation). Real time reverse transcriptase (RT)-PCR was carried out with a Qiagen SYBR green Quantitect RT-PCR kit, using primers that amplify a 334-bp portion of the NS2 coding sequence (forward primer, 5'-AGA AAA CAC AGA AAC CCG ACA GAC-3'; reverse primer 5'-TTC CAC CAC TAT TGT AGC ATC CG-3'). An Opticon 2 real time PCR machine (Bio-Rad) was used to perform the PCR reaction as follows: 50°C incubation for 30 m, then 95°C incubation for 15 m, followed by 35 cycles of 95°C for 15 s, 50°C for 1 m and 72°C for 1 m, with a final extension incubation at 72°C for 7 m. Viral copy numbers were measured and calibrated against a standard curve produced using serial dilutions of a concentrated BVDV stock.

2.2.7 Immunoblotting

MDBK cells were seeded in 6-well plates (1.75 x 10^6 cells/well) and infected with BVDV at an MOI of 1, followed by incubation with different concentrations of imino sugars for 24 h. Cells were harvested by scraping in PBS and centrifuged at 2000 rpm for 5 m. The resulting pellet was briefly frozen at -20°C then resuspended in PBS. The suspension was sonicated on ice using a Branson Sonifier S-250A (20 s,

50% duty cycle) to lyse cells. Protein concentrations were determined using a standard bicinchoninic acid protein assay. Proteins were then separated by sodium dodecyl sulfate-polyacrylamide gel electrophoresis (SDS-PAGE) under non-reducing conditions and transferred to Immobilon-P PVDF membrane (Millipore) by semi-dry electroblotting, then blocked overnight in 5% (w/v) milk, 0.2% (v/v) Tween20 in PBS. The membrane was incubated with MAb214 primary antibody (1 µg/ml in blocking solution; Animal Health Veterinary Laboratories Agency) for 2 h at room temperature, washed extensively with PBS-0.1% (v/v) Tween20, then incubated with anti-mouse horseradish peroxidase-conjugated secondary antibody (1 µg/ml; Dako) for 1 h. Antibody binding to BVDV E2 protein was detected using Pierce ECL Western Blotting Substrate (Thermo Scientific, UK) and X-ray film (GE Healthcare, UK) by following the manufacturer's instructions.

All assays were carried out on at least three independent occasions and data shown is representative of at least three experiments.

2.3 Results

2.3.1 Effect on cell proliferation increases with N-alkyl chain length

An MTS-based cell proliferation assay was carried out to determine the maximum concentrations of imino sugar derivatives that could be used without causing a significant effect on cell proliferation (Figure 2.2). The concentrations of compounds **6** to **13** required to reduce proliferation in MDBK cells by 50% (CC_{50}) in 72 h are shown in Table 2.1. No significant effect on proliferation was observed for compounds **6, 7**, **8**, **9** and **10** up to 250 μM. More hydrophobic compounds showed greater anti-proliferative effects, with CC_{50} values below 250 μM: compound **11** was 205 ± 1.1 μM, **12** was 51.7 ± 4.4 μM and **13** was 29.2 ± 1.0 μM. As the length of the alkyl linker between the imino sugar and the triazole ring increased, the CC_{50} decreased markedly, a property that has been noted for other N-alkylated imino sugars (Durantel *et al*, 2001).

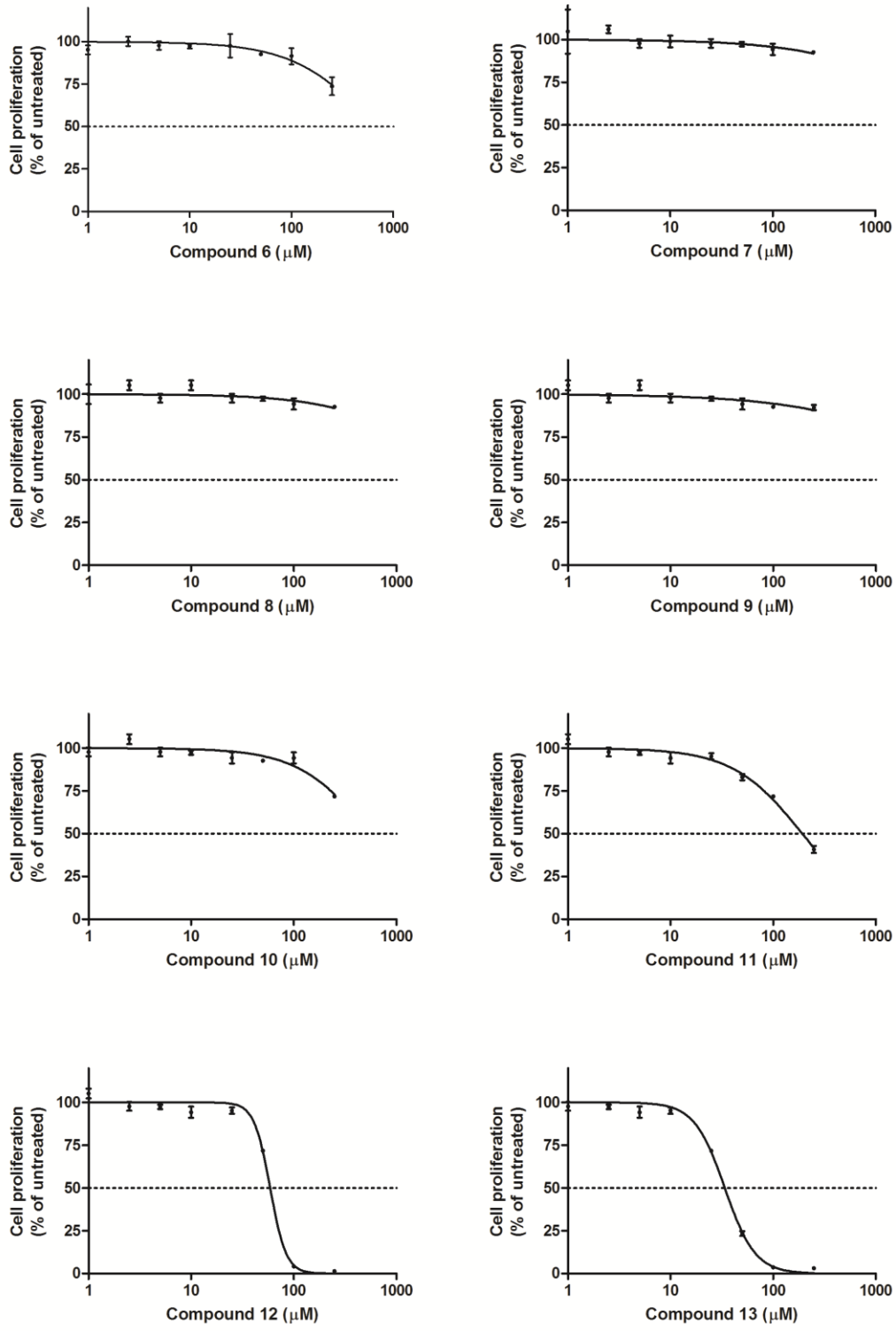

Figure 2.2 - MTS assay of MDBK cells treated with compounds **6-13**. MDBK cells were incubated with compound at various concentrations for 72 h (0.1% DMSO-treated samples were used as untreated controls). After 72 h, cells were incubated with MTS/PMS for 2 h and absorption measured (λ = 490 nm). Samples were run in triplicates, error bars represent standard deviation. CC_{50} values were calculated by non-linear regression, with equation y=100/(1+10^((LogIC50-x)*HillSlope)).

2.3.2 ER α-glucosidase inhibition correlates with N-alkyl chain length

The adamantyl-DNJ conjugates used in this chapter have previously been shown to inhibit ER α-glucosidases *in vitro* (Ardes-Guisot *et al*, 2011). FOS analysis of MDBK cells following inhibitor treatment was used to determine the level of *in cellulo* inhibition of ER α-glucosidases I & II. Inhibition of α-glucosidase II is known to cause an accumulation of monoglucosylated FOS, with inhibition of α-glucosidase I resulting in triglucosylated FOS accumulation (Alonzi *et al*, 2008). FOS species were purified from cells and separated by NP-HPLC for analysis (Figure 2.3). $Man_4GlcNAc_1$, which remained in constant amount over all concentrations of inhibitor used in this study, was used as standard and the relative amounts of mono- and tri-glucosylated $Man_5GlcNAc_1$ species were measured as representative markers of α-glucosidase II and I inhibition respectively.

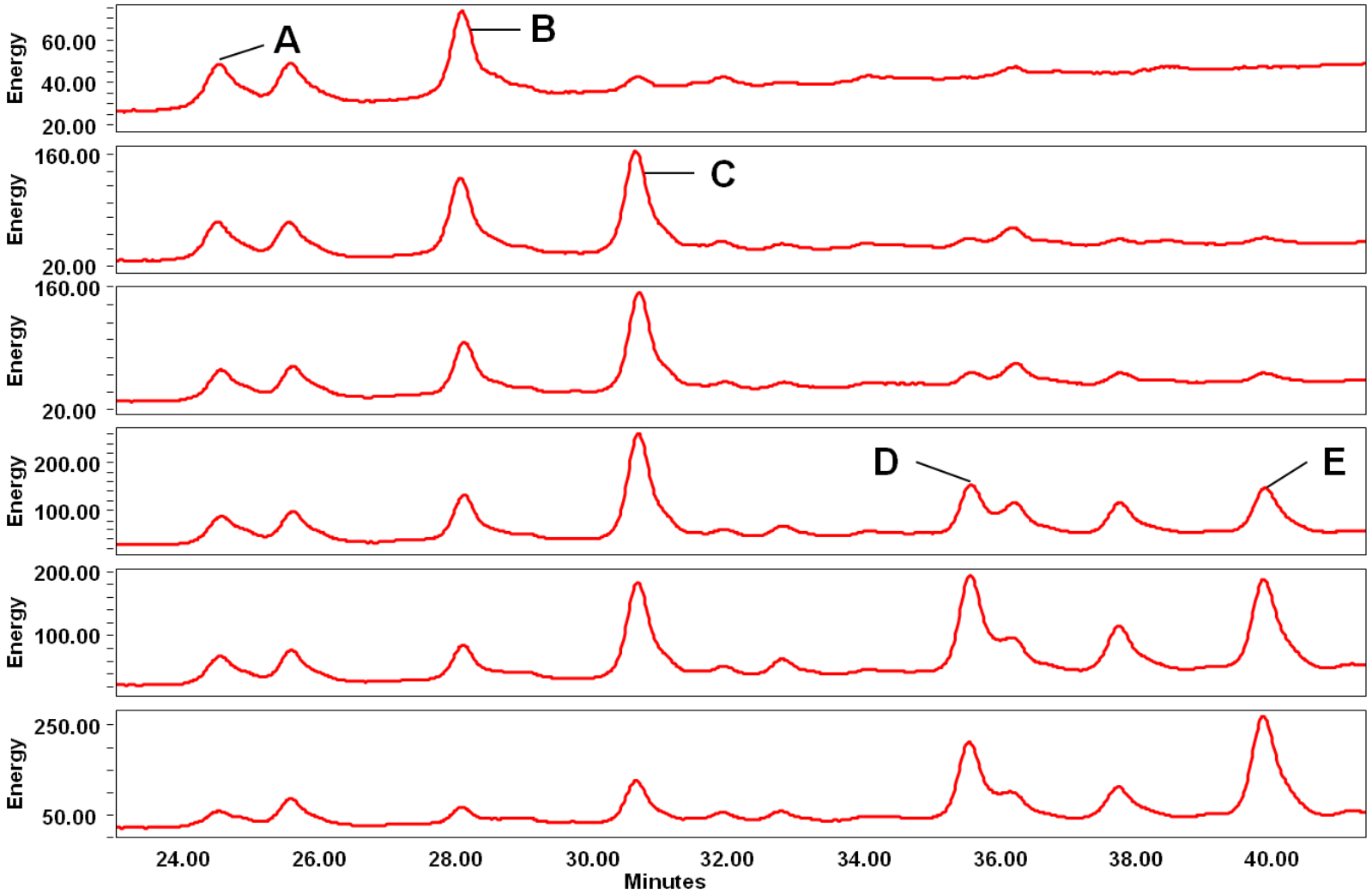

Figure 2.3 – Free oligosaccharide analysis of MDBK cells treated with DNJ-adamantyl compounds. Representative HPLC profiles of treatment with compound **11**, which gave the highest levels of α-glucosidase inhibition. From top, MDBK cells treated with 0 μM, 5, 10, 25, 50 and 100 μM compound **11**. A – $Man_4GlcNAc_1$. B – $Man_5GlcNAc_1$. C – $Glc_1Man_5GlcNAc_1$. D – $Glc_3Man_5GlcNAc_1$. E – $Glc_3Man_7GlcNAc_2$.

Concentrations for maximal α-glucosidase I and II inhibition for each compound are shown in Table 2.1. α-Glucosidase I inhibition occurred at higher concentrations than inhibition of α-glucosidase II, and little inhibition of α-glucosidase I was observed for compounds with short alkyl linkers. Treatment with 100 μM **11** showed the highest level of α-glucosidase I inhibition (Figure 2.4), more than three times higher than any other compound tested (Table 2.1). Compounds **9** and **10** have alkyl linkers of the same length, differing only in the introduction of an ether bond between the triazole and the adamantyl group in **10**. The two compounds exhibited very similar ER α-glucosidase inhibition. Compound **6**, the DGJ-analogue of compound **10**, had no effect on α-glucosidase activity up to the maximum concentration tested of 100 μM, in agreement with previously published data using N-alkylated-DGJ compounds (Butters *et al*, 2000b).

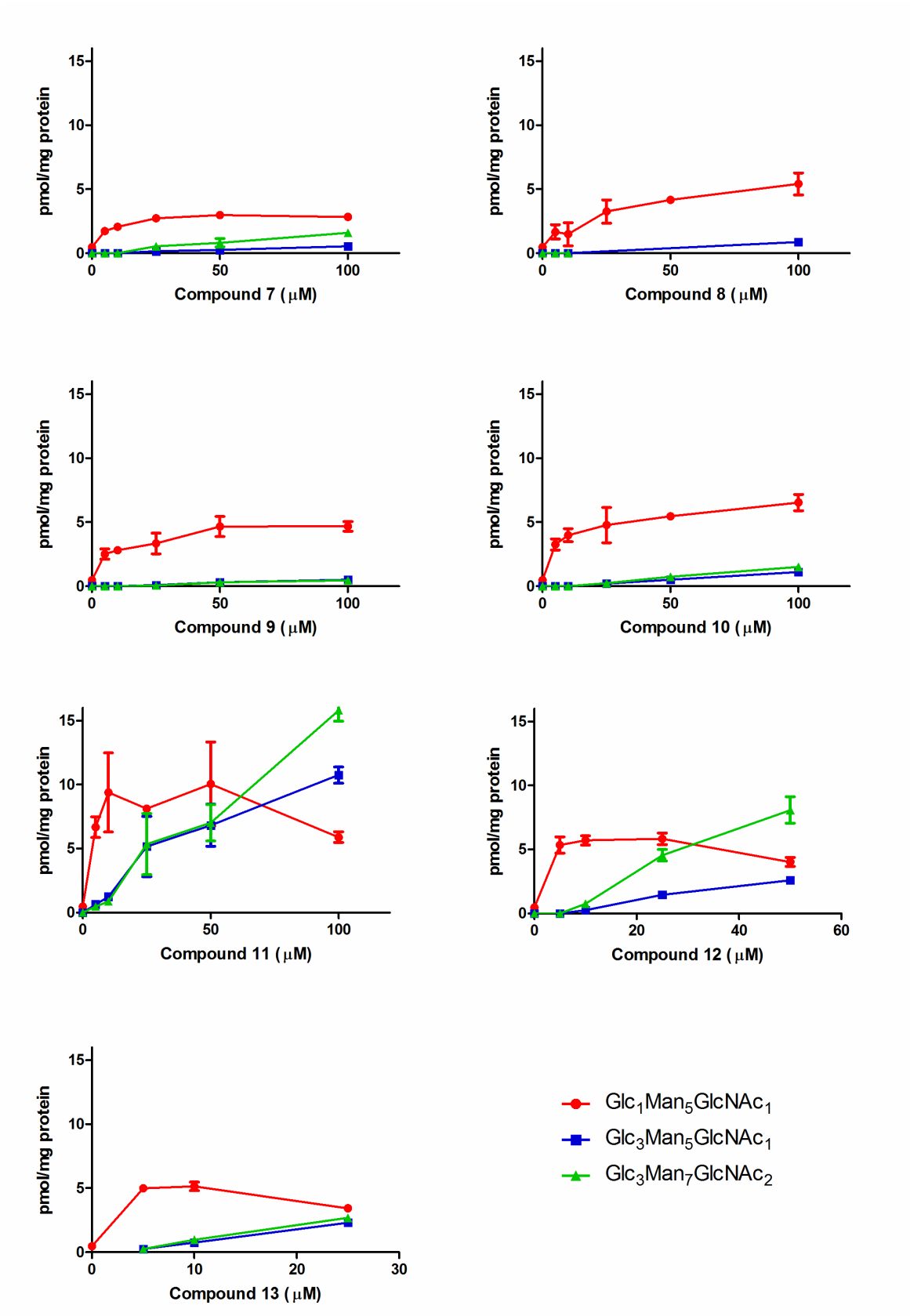

Figure 2.4 - Free oligosaccharide analysis of MDBK cells treated with DNJ-adamantyl compounds. Cells were incubated with compound for 24 h up to 100 μM. Free oligosaccharides were purified, labelled and analysed by NP-HPLC. Error bars indicate standard deviation of samples ran in triplicate.

Table 2.1 - Antiproliferative effects and glucosidase inhibition of compounds **6-13**.

CC_{50} values are shown for each compound used in MDBK cells. FOS HPLC analysis was used to determine peak areas of mono- or tri-glucosylated $Man_5GlcNAc_1$ as indicators of inhibition of α-glucosidase II and I enzymes, respectively. Relative amounts in comparison to a control species $Man_4GlcNAc_1$ are shown. NI, no inhibition observed.

		24 h FOS Analysis in MDBK cells			
Compound (alkyl linker C atoms)	**CC_{50} (μM)**	**Maximal† α-glucosidase II inhibition (μM) and relative amount**		**Maximal† α-glucosidase I inhibition (μM) and relative amount**	
6 (C4)	> 250	NI	NI	NI	NI
7 (C1)	> 250	100	3.0	100	0.54
8 (C2)	> 250	100	5.1	100	0.82
9 (C4)	> 250	50	5.2	100	1.44
10 (C4)	> 250	100	6.0	100	1.52
11 (C6)	205 ± 1.1	10	8.3	100	11.4
12 (C8)	51.7 ± 4.4	10	5.4	25	2.0
13 (C10)	29.2 ± 1.0	5	5.8	10	0.26

† Values indicate concentration tested that gave highest amount of each FOS relative to $Man_5GlcNAc_1$.

2.3.3 Antiviral activity correlates with ER α-glucosidase inhibition

Compounds were screened for their ability to inhibit the biogenesis and infectivity of BVDV. Viral production and release from MDBK cells was determined using RT-PCR to measure viral RNA copies secreted (Figure 2.5a). Compounds were initially administered at 10 μM and at this concentration, short alkyl chain compounds **7**, **8** and **9** showed no antiviral activity, although **8** and **9** were effective when a higher concentration was used (50 μM). Reduction in RNA copies increased as alkyl chain length increased, with 10 μM **13** treatment reducing viral RNA four-fold. At 10 μM, compound **10** reduced RNA copies approximately two-fold whereas compound **9** showed no effect, suggesting that, despite showing similar inhibition of α-glucosidases, the introduction of the ether bond between the triazole and the adamantyl group increases antiviral activity.

Infectivity of viral particles secreted from MDBK cells was determined as focus-forming units/ml (FFU/ml), by inoculating naive MDBK cells with virus secreted from cells administered with compound, then probing for BVDV NS2/3 protein (Figure 2.5b). Compounds were tested at the same concentrations as for RT-PCR analysis, and reduction in FFU/ml largely mirrors the reduction in viral RNA copies for compounds **7** through **13**. Treatment with the galactose analogue **6** at 10 μM however showed no significant reduction in viral RNA yet a small reduction in infectivity (FFU/ml) compared to the untreated control.

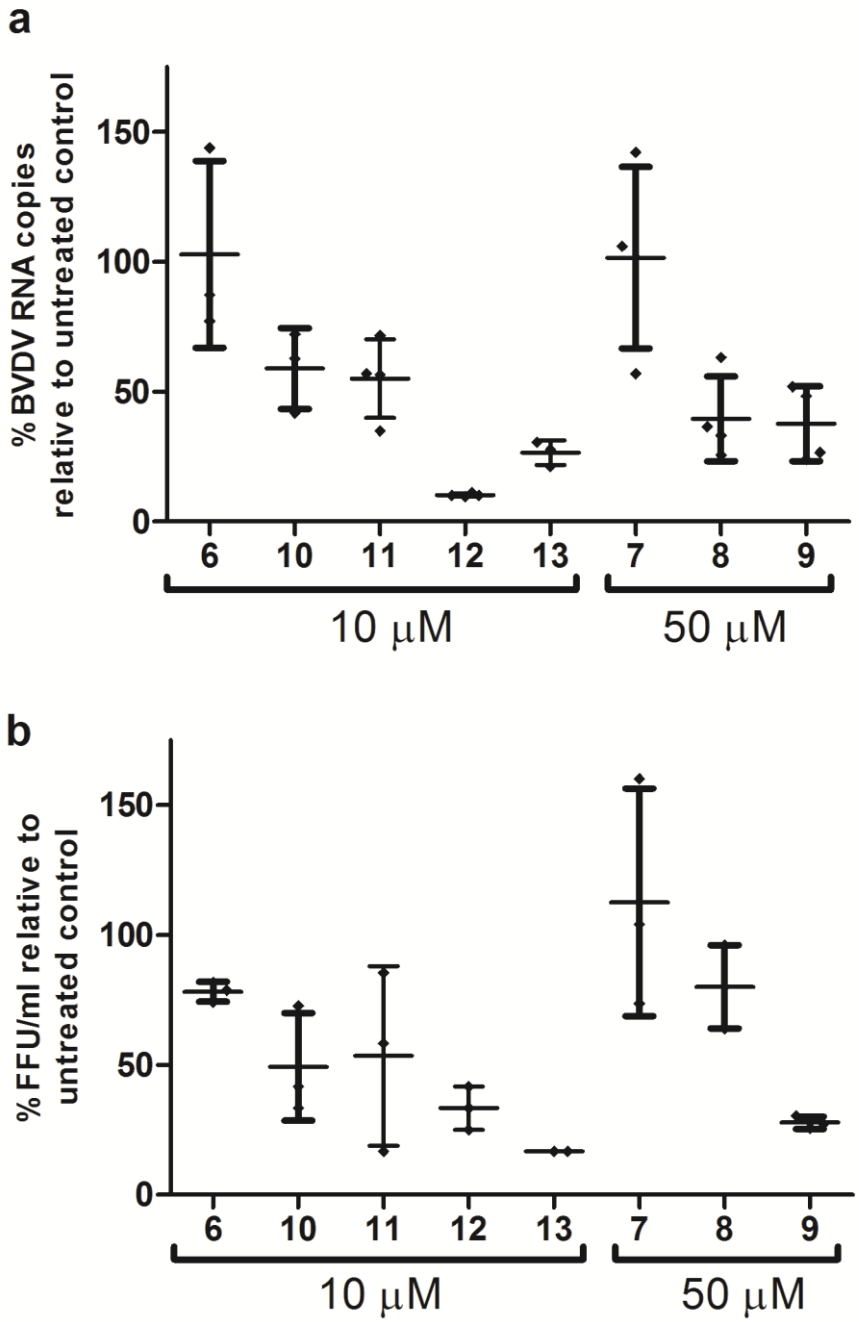

Figure 2.5 - Antiviral effects of compounds **6-13**. MDBK cells were infected with BVDV (MOI=1), then incubated with compound at 10 μM concentration for 24 h. Viral supernatant was then harvested and viral RNA copies determined by RT-PCR (a). Supernatant was also used to infect naive cells in a fluorescent focus assay, using α-BVDV NS2/3 antibody MAb103/105 (b). Experiments were performed in triplicate, error bars represent standard deviation. For compounds **7-9**, no antiviral activity was observed with 10 μM treatment (data not shown), and therefore a higher concentration (50 μM) was used.

2.3.4 ER α-glucosidase inhibition increases glucosylation of intracellular BVDV E2 protein

Inhibition of ER α-glucosidases I and II by N-alkylated DNJ prevents deglucosylation of BVDV E2 protein (Jordan *et al*, 2002). MDBK cells were infected with BVDV (MOI=1), then administered with compounds **10**, **11**, **13** and **6** for 24 h. Compounds were used at concentrations that gave maximal α-glucosidase I inhibition by FOS analysis (Table 2.1). Proteins from cell lysate were separated by SDS-PAGE and probed for BVDV E2 protein (Figure 2.6). Treatment with 100 μM **11** caused an increase in apparent molecular weight for all E2 species, due to increased glucosylation, whilst all other compounds showed little or no bandshift. For E1E2 heterodimer, the main band detected, there are six potential N-linked glycosylation sites (Dubuisson & Rice, 1996). A change in glycan structure from deglucosylated to triglucosylated could therefore increase the molecular weight of the heterodimer by up to 3.2 kDa (180.14 g/mol x 3 glucose residues x 6 glycosylation sites), which is in agreement with the bandshift observed.

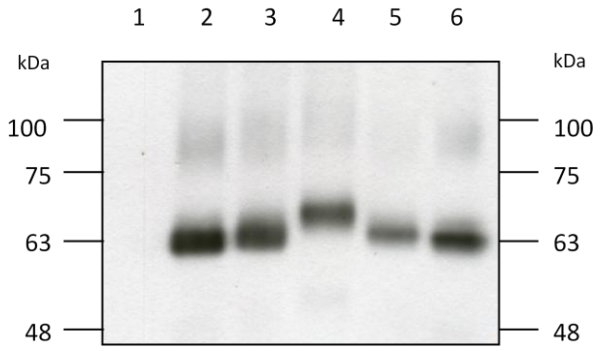

Figure 2.6 - Western Blot analysis of BVDV glycoprotein E2. MDBK cells were infected with BVDV (MOI=1), then incubated with compound for 24 h. Viral supernatants were collected and concentrated by ultracentrifugation, and viral particles lysed by sonication. Proteins were separated by non-reducing SDS-PAGE and probed by Western Blot with α-BVDV E2 antibody MAb214. Lane 1 - uninfected, untreated control; Lanes 2-6 – (2) BVDV-infected, untreated. (3) 100 μM compound **10**, (4) 50 μM compound **11**, (5) 25 μM compound **13** and (6) 100 μM compound **6**.

2.4 Discussion

DNJ and its derivatives have shown antiviral activity against the pestivirus BVDV (Zitzmann *et al*, 1999), as well as a number of other viruses including HBV (Block *et al*, 1994), and HCV pseudoparticles (Chapel *et al*, 2007). DNJ-based imino sugars reversibly inhibit ER α-glucosidases I and II by competing with glucose substrates for their active site, thereby perturbing the folding of viral glycoproteins in the N-linked glycosylation pathway and impeding viral biogenesis by hindering their assembly (Parodi, 2000).

Disruption of the folding of envelope glycoproteins E1 and E2, essential for virus entry (Ronecker *et al*, 2008), by ER α-glucosidase inhibition can induce misassembly of glycoprotein pre-budding complexes (Chapel *et al*, 2007).

The novel DNJ derivatives discussed here have been shown to inhibit ER α-glucosidases and to possess antiviral activity against BVDV, with a distinct correlation observed between the increasing length of the alkyl chain linker between the DNJ head group and the triazole ring and their antiviral efficacy. Compounds **7** and **8** demonstrate low levels of α-glucosidase II inhibition and little inhibition of α-glucosidase I even at the highest concentrations tested. Compounds **9** and **10**, which both possess a 4-carbon alkyl linker, show similar levels of inhibition of both enzymes, suggesting that the introduction of an ether bond in **10** between the triazole and adamantyl group has little effect on glucosidase inhibition. Longer alkyl chain compounds **11**, **12** and **13** efficiently inhibited α-glucosidase II at low concentrations (5 to 10 μM) and α-glucosidase I at high concentrations (25 to 100 μM). The more hydrophobic compounds **12** and **13** were limited in their ability to inhibit α-glucosidase I due to their effects on cell proliferation. The 6-carbon linker compound **11** could be administered to cells at higher concentrations and therefore

proved to be the most effective at inhibiting α-glucosidase I. In comparison to NAP-DNJ, an imino sugar which also contains a six carbon linker and is known to potently inhibit both α-glucosidases (Rawlings *et al*, 2009), compound **11** achieves a comparable level of α-glucosidase I inhibition. Increasing alkyl chain length in N-alkylated DNJ compounds has previously been shown to increase cellular uptake (Mellor *et al*, 2003), and an increase in the alkyl chain length linker between DNJ and phenyl or cyclohexyl groups increases ER α-glucosidase inhibition (Alonzi *et al*, 2009). Here, increasing the alkyl chain length of the linker between DNJ and triazole group similarly increases α-glucosidase inhibition.

DNJ-based imino sugars have previously been shown to demonstrate antiviral activity against BVDV (Zitzmann *et al*, 1999). The longer alkyl chain N-nonyl-DNJ has shown tenfold greater potency than N-butyl-DNJ (Durantel *et al*, 2001), with branching and cyclisation of side chains able to increase potency further (Mehta *et al*, 2002). Compound **7**, with a single carbon linker between DNJ and triazole, showed no antiviral activity at the concentrations tested. As the length of the alkyl linker is increased, the amount of viral RNA in culture medium decreases, with 10 μM **12** reducing viral titre approximately tenfold. Compound **13**, despite having a longer alkyl chain, reduced viral titre less than compound **12**, suggesting an upper limit to alkyl linker length may have been reached. Subsequent infection of naive MDBK cells with virus secreted from cells administered with compound followed a similar pattern to α-glucosidase inhibition and viral secretion levels, although despite showing higher viral titre levels than **12**, less infection was observed following treatment with **13**. These results suggest that the antiviral effects of these compounds are largely a result of reduced viral biogenesis or secretion, rather than as a result of reduced infectivity, although an additional reduction is observed with

13. In addition to this, treatment with adamantyl-DGJ **6**, a galactose analogue of adamantyl-DNJ **10** that does not inhibit α-glucosidases, failed to reduce viral titre but partially reduced infectivity. Long-alkyl-chain DGJ derivatives have previously been shown to exert their antiviral effect solely via the production of viral particles with reduced infectivity (Durantel *et al*, 2001), which has been proposed to be through interaction with p7 ion channel (Pavlovic *et al*, 2003).

A direct effect on BVDV glycoprotein E2 is observed with Western blot analysis. Treatment with **11**, shown by FOS analysis to be the most potent α-glucosidase I inhibitor, resulted in increased glucosylation of intracellular E2 protein. These results taken together lead to the following proposal for the antiviral effects observed with compounds **7** to **13**. With the shorter alkyl chain compounds, antiviral activity is a result of ER α-glucosidase inhibition, which prevents efficient and successful processing of viral glycoproteins, resulting in a reduction in the formation of pre-budding complexes and a subsequent reduction in virion formation and release. Increased hydrophobicity of longer alkyl linker derivatives facilitates their uptake and results in a prolonged period of retention in the intracellular environment where they can exert inhibition of α-glucosidases in the ER (Alonzi *et al*, 2009), resulting in greater antiviral activity. Separately, as alkyl linker length increases, an antiviral effect unrelated to α-glucosidase inhibition begins to appear, producing non- or less infectious virions. Interactions between more hydrophobic adamantyl conjugates and p7 (Pavlovic *et al*, 2003) may explain the reduction in infectivity. Altogether, this novel family of imino sugars further demonstrate the potential of α-glucosidases as an antiviral target, whilst also highlighting the possibility of developing imino sugars capable of targeting more than one component of the viral life cycle.

2.5 References

Alonzi DS, Dwek RA, Butters TD (2009) Improved cellular inhibitors for glycoprotein processing α-glucosidases: biological characterisation of alkyl- and arylalkyl-N-substituted deoxynojirimycins. *Tetrahedron: Asymmetry* **20:** 897-901

Alonzi DS, Neville DC, Lachmann RH, Dwek RA, Butters TD (2008) Glucosylated free oligosaccharides are biomarkers of endoplasmic- reticulum alpha-glucosidase inhibition. *Biochemical Journal* **409:** 571-580

Ardes-Guisot N, Alonzi DS, Reinkensmeier G, Butters TD, Norez C, Becq F, Shimada Y, Nakagawa S, Kato A, Bleriot Y, Sollogoub M, Vauzeilles B (2011) Selection of the biological activity of DNJ neoglycoconjugates through click length variation of the side chain. *Organic & Biomolecular Chemistry* **9:** 5373-5388

Block TM, Lu X, Platt FM, Foster GR, Gerlich WH, Blumberg BS, Dwek RA (1994) Secretion of human hepatitis B virus is inhibited by the imino sugar N-butyldeoxynojirimycin. *Proc. Natl. Acad. Sci. USA* **91:** 2235-2239

Buckwold VE, Beer BE, Donis RO (2003) Bovine viral diarrhea virus as a surrogate model of hepatitis C virus for the evaluation of antiviral agents. *Antiviral Research* **60:** 1-15

Butters TD, Dwek RA, Platt FM (2000a) Inhibition of glycosphingolipid biosynthesis: application to lysosomal storage disorders. *Chemical Reviews* **100:** 4683-4696

Butters TD, van den Broek LAGM, Fleet GWJ, Krulle TM, Wormald MR, Dwek RA, Platt FM (2000b) Molecular requirements of imino sugars for the selective control of N-linked glycosylation and glycosphingolipid biosynthesis. *Tetrahedron: Asymmetry* **11:** 113-124

Chang J, Schul W, Yip A, Xu X, Guo JT, Block TM (2011) Competitive inhibitor of cellular alpha-glucosidases protects mice from lethal dengue virus infection. *Antiviral Research* **92:** 369-371

Chapel C, Garcia C, Bartosch B, Roingeard P, Zitzmann N, Cosset FL, Dubuisson J, Dwek RA, Trepo C, Zoulim F, Durantel D (2007) Reduction of the infectivity of hepatitis C virus pseudoparticles by incorporation of misfolded glycoproteins induced by glucosidase inhibitors. *Journal of General Virology* **88:** 1133-1143

Compain P, Martin OR (2007) *Iminosugars. From Synthesis to Therapeutic Applications*: John Wiley & Sons Ltd.

Dubuisson J, Rice CM (1996) Hepatitis C virus glycoprotein folding: disulfide bond formation and association with calnexin. *Journal of Virology* **70:** 778-786

Durantel D, Branza-Nichita N, Carrouee-Durantel S, Butters TD, Dwek RA, Zitzmann N (2001) Study of the mechanism of antiviral action of iminosugar derivatives against bovine viral diarrhea virus. *Journal of Virology* **75:** 8987-8998

Greimel P, Spreitz J, Stutz AE, Wrodnigg TM (2003) Iminosugars and relatives as antiviral and potential anti-infective agents. *Current Topics in Medicinal Chemistry* **3:** 513-523

Griffin SD, Beales LP, Clarke DS, Worsfold O, Evans SD, Jaeger J, Harris MP, Rowlands DJ (2003) The p7 protein of hepatitis C virus forms an ion channel that is blocked by the antiviral drug, Amantadine. *FEBS Letters* **535:** 34-38

Howe JD, Smith N, Lee MJR, Ardes-Guisot N, Vauzeilles B, Desire J, Baron A, Bleriot Y, Sollogoub M, Alonzi DS, Butters TD (2013) Novel imino sugar alpha-glucosidase inhibitors as antiviral compounds. *Bioorganic & Medicinal Chemistry* **21:** 4831-4838

Jordan R, Nikolaeva OV, Wang L, Conyers B, Mehta A, Dwek RA, Block TM (2002) Inhibition of host ER glucosidase activity prevents Golgi processing of virion-associated bovine viral diarrhea virus E2 glycoproteins and reduces infectivity of secreted virions. *Virology* **295:** 10-19

Mehta A, Ouzounov S, Jordan R, Simsek E, Lu X, Moriarty RM, Jacob G, Dwek RA, Block TM (2002) Imino sugars that are less toxic but more potent as antivirals, in vitro, compared with N-n-nonyl DNJ. *Antiviral Chemistry & Chemotherapy* **13:** 299-304

Mellor HR, Platt FM, Dwek RA, Butters TD (2003) Membrane disruption and cytotoxicity of hydrophobic N-alkylated imino sugars is independent of the inhibition of protein and lipid glycosylation. *Biochemical Journal* **374:** 307-314

Neville DC, Coquard V, Priestman DA, te Vruchte DJ, Sillence DJ, Dwek RA, Platt FM, Butters TD (2004) Analysis of fluorescently labeled glycosphingolipid-derived oligosaccharides following ceramide glycanase digestion and anthranilic acid labeling. *Analytical Biochemistry* **331:** 275-282

Norez C, Noel S, Wilke M, Bijvelds M, Jorna H, Melin P, DeJonge H, Becq F (2006) Rescue of functional delF508-CFTR channels in cystic fibrosis epithelial cells by the alpha-glucosidase inhibitor miglustat. *FEBS Letters* **580:** 2081-2086

Norton A, Gu B, Block TM (2007) Iminosugars as antiviral agents. In *Iminosugars. From Synthesis to Therapeutic Applications*, Compain P, Martin OR (eds), pp 209-224. Chichester: John Wiley & Sons Ltd

Overkleeft HS, Renkema GH, Neele J, Vianello P, Hung IO, Strijland A, van der Burg AM, Koomen GJ, Pandit UK, Aerts JM (1998) Generation of specific deoxynojirimycin-type inhibitors of the non-lysosomal glucosylceramidase. *Journal of Biological Chemistry* **273:** 26522-26527

Parodi AJ (2000) Role of N-oligosaccharide endoplasmic reticulum processing reactions in glycoprotein folding and degradation. *Biochemical Journal* **348:** 1-13

Pavlovic D, Neville DC, Argaud O, Blumberg B, Dwek RA, Fischer WB, Zitzmann N (2003) The hepatitis C virus p7 protein forms an ion channel that is inhibited by long-alkyl-chain iminosugar derivatives. *Proc. Natl. Acad. Sci. USA* **100:** 6104-6108

Rawlings AJ, Lomas H, Pilling AW, Lee MJ, Alonzi DS, Rountree JS, Jenkinson SF, Fleet GW, Dwek RA, Jones JH, Butters TD (2009) Synthesis and biological characterisation of novel N-alkyl-deoxynojirimycin alpha-glucosidase inhibitors. *ChemBioChem* **10:** 1101-1105

Ronecker S, Zimmer G, Herrler G, Greiser-Wilke I, Grummer B (2008) Formation of bovine viral diarrhea virus E1-E2 heterodimers is essential for virus entry and depends on charged residues in the transmembrane domains. *Journal of General Virology* **89:** 2114-2121

Stutz AE (1999) *Iminosugars as Glycosidase Inhibitors*, Weinheim: Wiley-VCH.

Wang C, Takeuchi K, Pinto LH, Lamb RA (1993) Ion channel activity of influenza A virus M2 protein: characterization of the amantadine block. *Journal of Virology* **67:** 5585-5594

Zitzmann N, Mehta AS, Carrouee S, Butters TD, Platt FM, McCauley J, Blumberg BS, Dwek RA, Block TM (1999) Imino sugars inhibit the formation and secretion of bovine viral diarrhea virus, a pestivirus model of hepatitis C virus: implications for the development of broad spectrum anti-hepatitis virus agents. *Proc. Natl. Acad. Sci. USA* **96:** 11878-11882

3 Nitazoxanide

3.1 Introduction

Thiazolides are a class of small molecules that share a common structure of a benzene ring coupled to a thiazole by an amide bond. The benzene ring and the thiazole both offer opportunities for the development of derivatives through modification of side chains. The parent compound of the thiazolide family is nitazoxanide (NTZ), which possesses a nitro group attached to the thiazole ring and an acetyl group attached to the benzene. In plasma, NTZ is readily deacetylated to tizoxanide (TIZ), where the benzene ring simply possesses a hydroxyl group. Further modifications to both components of the thiazolide have resulted in the development of a series of molecules with overlapping activities that as a whole display antiparasitic, antibacterial and antiviral properties.

Initially developed as antiparasitic compounds, and licensed for the treatment of *Cryptosporidium parvum* and *Giardia lamblia*, NTZ was later identified as a potential antiviral whilst being used to treat *C. parvum* in AIDS patients co-infected with HBV or HCV. Since this discovery, thiazolides have been found to display antiviral activity against a broad range of viruses, including HBV, HCV, rotavirus, influenza and JEV (Rossignol *et al*, 2006; Korba *et al*, 2008b; Rossignol *et al*, 2009; Shi *et al*, 2014).

In cells supporting HCV RNA replication, NTZ has previously been shown to upregulate autophosphorylation of protein kinase activated by double-stranded (ds)RNA (PKR), which in turn phosphorylates the alpha-subunit of eukaryotic initiation factor-2 (eIF2α) (Elazar *et al*, 2009). PKR is well-characterised as an interferon-stimulated mediator of antiviral responses (Garcia *et al*, 2007), inhibiting cap-dependent translation through phosphorylation of eIF2α. Phosphorylation of

eIF2α results in sequestration and inhibition of the guanine nucleotide exchange factor eIF2β, preventing nucleotide exchange and formation of active eIF2-GTP, which is required for pre-initiation complex formation at 5' mRNA cap structures (Rowlands *et al*, 1988). HCV translation, like that of BVDV, is mediated via an IRES element however, and is unaffected by eIF2α phosphorylation (Robert *et al*, 2006).

Additionally, NTZ and TIZ have been found to be antiviral against influenza A. NTZ disrupts the maturation and trafficking of influenza surface glycoprotein hemagglutinin (HA) (Rossignol *et al*, 2009). NTZ treatment prevents complex glycan formation and insertion of HA into the host cell membrane, a key step in virion formation. More recently, antiviral activity of NTZ has been demonstrated against JEV, protecting against the JEV-induced cytopathic effect (Shi *et al*, 2014). For both influenza and JEV, NTZ was found to work exclusively via a post-viral entry mechanism (Rossignol *et al*, 2009; Shi *et al*, 2014).

Other thiazolides have been studied to enhance our understanding of the structure-activity relationship of NTZ and its derivatives (Table 3.1). RM4819, a bromo-derivative of the thiazolide family, has previously been shown to have pro-apoptotic properties, in a glutathione-S-transferase P1-dependent manner, mediated through Bim expression (Muller *et al*, 2008; Sidler *et al*, 2012), although this appears to be cell-line dependent – RM4819 induced apoptosis in Caco2 and Ls174T cells, whereas HT29 and Colo205 cells were resistant, despite all four cell lines being derived from human colorectal cancers (Sidler *et al*, 2012). Whilst NTZ has been shown to be anti-proliferative in Caco2 cells (Muller *et al*, 2008), NTZ appears to protect against proteasome inhibitor-mediated apoptosis (Ashiru *et al*, 2014).

NTZ does, however, stimulate apoptosis-like cell death, or eryptosis, in erythrocytes (Arnold *et al*, 2014). Although NTZ did not trigger an increase in cytosolic Ca^{2+} levels, a common stimulus of eryptosis, increases in ceramide formation, phosphatidylserine exposure and haemolysis were observed. Interestingly however, the eryptotic effects of NTZ were significantly diminished in the absence of extracellular Ca^{2+}, indicating that the changes observed were at least in part due to sensitization of erythrocytes to Ca^{2+}. The effect of NTZ on Ca^{2+} mobilisation in cells with intracellular Ca^{2+} stores including the ER and the Golgi apparatus is still unknown, and is investigated here.

Although the antiviral potential of NTZ has been demonstrated against a number of different viruses, our understanding of the mechanistic details of thiazolides in an antiviral capacity still lacks depth.

In this chapter, the antiviral effects of NTZ against BVDV are investigated. NTZ is shown to be anti-proliferative in MDBK cells, but protects against proteasome inhibitor-mediated apoptosis. NTZ treatment rapidly depletes ATP-sensitive Ca^{2+} stores, disrupting ER-Golgi trafficking and viral glycoprotein glycosylation. Virion secretion is also reduced, and the formation of complex glycans on secreted viral glycoproteins is inhibited. Overall, this furthers our understanding of the antiviral mechanism of action of thiazolides, and highlights Ca^{2+} mobilisation as a major and rapid effect of NTZ treatment, potentially responsible for a wide range of antiviral effects observed to date.

The work presented in this chapter has been published in Virology (Ashiru *et al*, 2014). Figures produced by Dr. Omodele Ashiru are individually identified in figure legends.

Table 3.1 - Structures and anti-microbial activities of selected thiazolides. See main text for references.

Name	Structure	Activity
Nitazoxanide (NTZ)	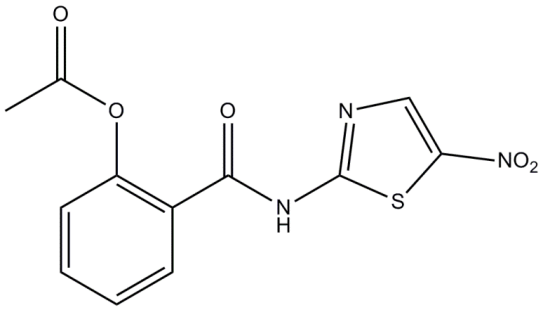	C. parvum HBV replication HCV replication Influenza A JEV
Tizoxanide (TIZ)	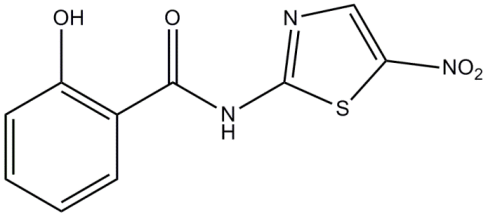	C. parvum HBV replication HCV replication Influenza A
RM5014	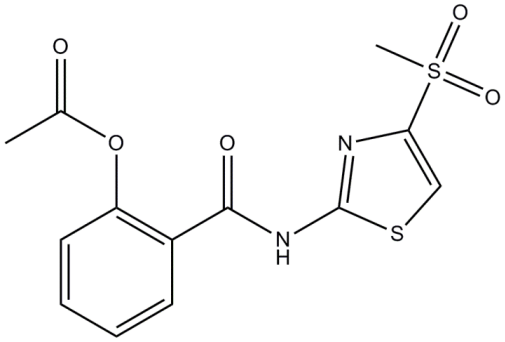	Influenza A No effect on HCV replication
RM5038	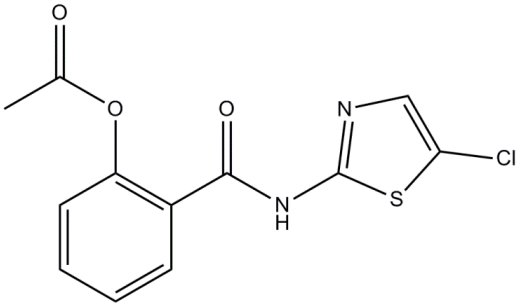	C. parvum
RM4819	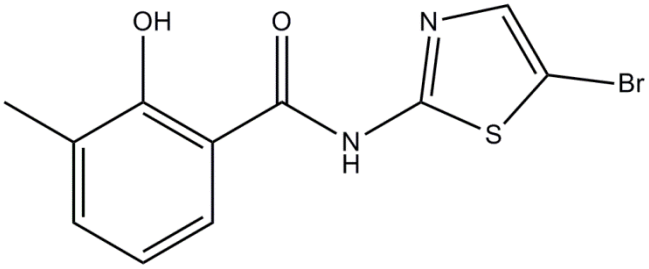	Pro-apoptotic

3.2 Materials and methods

3.2.1 Materials

The following drugs were supplied as follows: NTZ and TIZ (Romark Pharmaceuticals); thapsigargin (Calbiochem); kifunensine (Sigma-Aldrich); 1,2-bis(2-aminophenoxy)ethane-N,N,N',N'-tetraacetic acid tetrakis (acetoxymethyl ester) (BAPTA-AM; Invitrogen); ionomycin (Enzo Life Sciences); carbonyl cyanide 3-chlorophenylhydrazone (CCCP; Sigma-Aldrich); and adenosine-5'-triphosphate disodium salt (ATP; Enzo Life Sciences). All compounds except ATP were dissolved in DMSO (Sigma-Aldrich) as 1000x stocks, to maintain DMSO concentrations below 0.2% for all experiments. ATP was dissolved in deionised water.

3.2.2 Cell culture

Mardin-Darby Bovine Kidney (MDBK) cells (European Collection of Animal Cell Cultures, Porton Down, United Kingdom) were cultured in RPMI-1640 media (PAA Laboratories, Teddington, UK) supplemented with 10% BVDV-free foetal calf serum (FCS; Invitrogen), 2 mM L-glutamine (PAA), 20 U/ml penicillin (PAA) and 50 µg/ml streptomycin (PAA). Cells were grown at 37°C in a humidified atmosphere containing 5% (v/v) CO_2 and passaged using trypsin-EDTA (PAA), 1:10 every three days.

BVDV strains Pe515 (non-cytopathic) and NADL (cytopathic) were kind gifts from Dr. Bryan Charleston (The Pirbright Institute, UK) and Professor Nicole Zitzmann (Oxford Glycobiology Institute, University of Oxford, UK) respectively. To propagate BVDV, MDBK cells were infected with virus at a multiplicity of infection (MOI) of 0.01 and cultured for 72 h at 37°C. Virus-containing media was then collected and clarified by centrifugation at 1,000 x g for 10 m to remove cellular debris.

Supernatants were aliquoted and stored at -70°C, with virus titres determined by fluorescent focus-forming assay (FFA).

3.2.3 Cell proliferation assays

3.2.3.1 Cell metabolism

MDBK cells were seeded in 96-well plates (10^4 cells/well) and allowed to adhere for 4 h at 37°C. Media was aspirated and replaced with 200 µl/well fresh media containing NTZ or TIZ up to 250 µM in concentration. Following incubation at 37°C for 24 or 72 h, a CellTiter 96R aqueous non-radioactive cell proliferation assay kit (Promega) was used to measure cellular cytotoxicity of compounds according to manufacturer protocol. To each well, 40 µl of MTS:PMS mixture (20:1) was added and then incubated for 2 h. Absorbance was measured at 490 nm with a UVmax plate reader (Molecular Devices). Empty wells containing only media were used as blanks. Samples were analysed in triplicate and the concentrations at which absorbance at 490 nm was 50% of DMSO-treated controls (CC_{50}) were determined.

3.2.3.2 Cell division

MDBK cells (1 x 10^6/well) in 6-well plates were incubated with 10 µM carboxyfluorescein succinimidyl ester (CFSE; eBioscience) for 15 m at 37°C in humidified 5% CO_2, then incubated in media for a further 30 m. To measure the CFSE level of undivided cells (designated “Day 0”), untreated CFSE-labelled MDBK cells were detached using trypsin, fixed in 4% formaldehyde for 15 m at room temperature, then analysed by flow cytometry (FACSCalibur; BD Biosciences). The remaining CFSE-labelled cells were washed in PBS, incubated with media containing DMSO or NTZ for 24 h at 37°C in humidified 5% CO_2, then analysed by flow cytometry. The geometric mean of the fluorescent intensity (MFI) was

determined for each treatment, and normalised to the MFI of “Day 0” cells.

3.2.4 Translation reporter assay

Triplicate wells of MDBK cells (4 x 10^4/ well) in white 96-well plates were transfected with psiCHECK2-HCV IRES (Wang *et al*, 2011), which was a kind gift from Dr. Michael Lai (Academia Sinica, Taiwan). psiCHECK2-HCV IRES is a bicistronic plasmid carrying firefly luciferase (FLuc) and renilla luciferase (RLuc) genes driven by HCV IRES- and cap-dependent translation, respectively. At 20 h post-transfection, cells were treated with DMSO or NTZ for 24 h. FLuc and RLuc activities were determined using the Dual-Glo® Luciferase Assay System (Promega) and a SpectraMax M5 plate reader (Molecular Devices). For each well, the ratio of FLuc to RLuc activity was calculated.

3.2.5 Focus-forming assay

MDBK cells were seeded in 6-well plates (1.5 x 10^6/well) and allowed to adhere for 4 h at 37°C. Media was removed and cells then infected with BVDV (MOI=1) for 1 h at 37°C. Cells were then washed with PBS and incubated with complete media containing DMSO or NTZ at different concentrations for 24 h. Following this incubation, media was removed and clarified, then serially diluted (eight 10-fold dilutions) and used to infect naive MDBK cells in 96-well plates. After a 1 h infection period, viral inoculum was removed and replaced with fresh RPMI media. After 16 h overnight incubation to allow virus replication to occur, cells were washed with ice-cold PBS twice and fixed with 4% (v/v) paraformaldehyde (30 m, rt). Cells were washed again with PBS, then blocked with blocking solution for 2 h. Cells were then permeabilised with 1% Triton-X-100 in PBS (20 m, rt), washed with 1% Tween20 in PBS, and then incubated with primary monoclonal antibody MAb103/105 (2 µg/ml in

blocking solution, 1h, rt; AHVLA). After washing again in 1% Tween20-PBS, cells were incubated with Alexa Fluor® 488 Goat Anti-Mouse IgG (H+L) Antibody (2 µg/ml in blocking solution, 1 h, rt, dark; Life Technologies, Thermo Fisher Scientific, Paisley, UK). Cells were then washed again with Tween20-PBS, nuclei stained with DAPI and viewed using a inverted Nikon Eclipse TE200-U microscope, equipped with a Fluor 10X objective lens, and FITC and UV filter sets. Fluorescent foci were counted, and virus titres (focus forming units (FFU)/ml) calculated.

3.2.6 Endo H digests of BVDV E2 glycoprotein

Confluent MDBK cells in 25 cm^2 flasks were infected with BVDV at an MOI of 1. After virus adsorption, cells were incubated in 5 ml media containing DMSO, NTZ, thapsigargin or kifunensine for 24 h at 37°C in humidified 5% CO_2. Virus-containing supernatants were centrifuged for 10 m at 2000 rpm to remove cell debris, then ultracentrifuged for 2 h at 20,000 rpm at 4°C. Viral pellets were resuspended in 500 µl PBS, and then sonicated using a Branson Sonifier S-250A (50% duty cycle, 20 s) to lyse virions. Lysates were incubated with endoglycosidase H (Endo H; NEB) or water at 37°C for 24 h. Non-reduced proteins were run on an 8% SDS-PAGE gel then analysed by Western blot.

3.2.7 Western blot analysis

Lysates were reduced and denatured by addition of β-mercaptoethanol (Sigma-Aldrich) and heating at 90°C for 5 m, respectively. Lysates for analysis of BVDV E2 using MAb214 were not reduced. Proteins were separated on 8% or 10% SDS-PAGE gels, and transferred onto Immobilon-P membranes (Millipore). PVDF membranes were blocked overnight at 4°C in 5% bovine serum albumin (BSA) or milk/0.1% Tween 20/PBS (Sigma-Aldrich), which was designated WB blocking

solution. This was followed by hour-long incubations with primary antibody then species-specific HRP-conjugated secondary, diluted in WB blocking solution. Unless otherwise stated, all incubations were carried out at room temperature on a rocking platform. Washes using 0.1% Tween 20/PBS were carried out between each step. Protein bands were visualised by chemiluminescence using ECL Western Blotting Substrate or SuperSignal West Pico Chemiluminescent Substrate (Pierce Biotechnology) and Amersham Hyperfilm MP (GE Healthcare). Where necessary, membranes were reprobed for a different antigen. Firstly, membranes were incubated in stripping buffer [1 M Tris-HCL (pH 6.8), 10% SDS, 0.8% β-mercaptoethanol] (Sigma-Aldrich) for 30 m to 1 h at 80°C. Following washes in 0.1% Tween 20/PBS, stripped membranes were incubated in WB blocking solution overnight at 4°C, then probed for proteins of interest.

3.2.8 Carbohydrate analysis

Free oligosaccharide (FOS) analysis of MDBK cells treated with NAP-DNJ and NTZ or thapsigargin for 24 h was performed, with FOS purified, labelled and analysed as described in Chapter 2. Inhibitor treatments were performed in triplicate, with the amounts of $Glc_3Man_5GlcNAc_1$ and $Glc_3Man_7GlcNAc_2$ measured, relative to protein concentration or $Man_4GlcNAc_1$ levels, which remained constant for all treatments. Protein concentrations were determined by standard bicinchoninic acid assay, calibrated against a BSA (Sigma-Aldrich) standard curve.

3.2.9 Measurement of cytosolic Ca^{2+}

All fluorometric determinations of cytosolic Ca^{2+} were carried out at room temperature using Hank's Balanced Salt Solution (HBSS; Invitrogen) with or without 1.3 mM $CaCl_2$. MDBK or Huh-7 cells (4 x 10^4/well) in µClear black 96-well plates

(Greiner) were loaded with Fura-2 acetoxymethyl (AM; Invitrogen) and pluronic acid (Invitrogen) for 30 m in the dark. The cells were washed twice with HBSS, then incubated in 200 µl HBSS for a further 30 m to allow complete de-esterification of intracellular Fura-2 AM esters. Where necessary, the de-esterification step was carried out in the presence of 10 µM BAPTA-AM or DMSO. Baseline emissions of intracellular Fura-2 were measured for 5 m, at 1 m intervals using a SpectraMax M5 plate reader (Molecular Devices). Fura-2 was alternatively excited at wavelengths of 340 nm and 380 nm, and emissions at 510 nm were measured. Compounds of interest (including vehicle/diluent) were diluted 1:25 in HBSS in order to reduce cell damage from DMSO-containing compounds. Each diluted compound (5 µl) was added to Fura-2 loaded cells in triplicate, such that a final 1:1000 dilution of each compound stock was achieved. Following compound addition, Fura-2 emissions were measured for 10 m. Where necessary, this was followed by the addition of a second compound and a further 10 m measurement of Fura-2 emissions. For each well and time point, the ratio of emission at 510 nm following 340/380 nm excitation was measured then normalised to the average baseline 340/380 ratio. Note that no compartmentalisation of Fura-2 was observed, as determined by the IonOptix Fluorescence Measurement System.

All assays were carried out on at least three independent occasions and data shown is representative of at least three experiments.

3.3 Results

3.3.1 NTZ inhibits BVDV replication

MDBK cells were infected with cytopathic BVDV (MOI=1) and treated post-infection for 24 h with NTZ. Secreted virus was then used to infect naïve MDBK cells to determine the effect of NTZ on BVDV replication (Figure 3.1a). NTZ was highly antiviral against BVDV, with a concentration required to reduce infection by 50% relative to DMSO-treated controls (IC_{50}) of 12.8 ± 4.1 µM. Treatment with 25 µM NTZ resulted in an approximate 100-fold reduction in infectivity. At 25 µM, a similar effect on secretion (viral load) was observed as on infectious virus (data not shown).

In addition to this, a significant reduction in the proportion of MDBK cells expressing BVDV NS2/3 protein, as determined by immunofluorescence staining, was observed following 24 h post-infection treatment with 25 µM NTZ (Figure 3.1b). No such decrease was observed at lower concentrations.

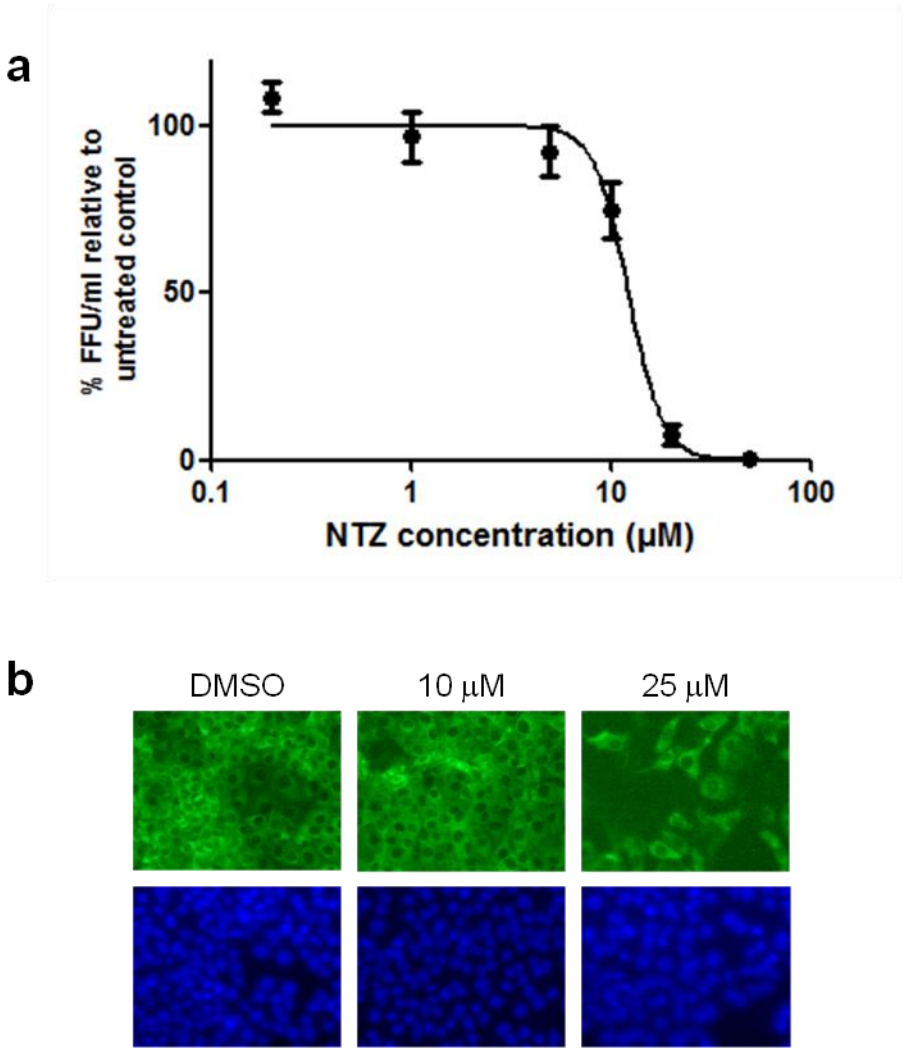

Figure 3.1 - NTZ inhibits BVDV replication. (a) MDBK cells were infected with BVDV (MOI=1) and treated with NTZ for 24 h. Viral progeny was harvested, serially diluted and used to infect naïve cells. After a further 18 h, cells were fixed and stained with anti-BVDV NS2/3 antibody MAb103/105. Fluorescent focus units were then counted across triplicate wells. (b) MDBK cells infected with cytopathic BVDV were incubated with DMSO or NTZ for 24 h, then stained with anti-NS2/3 antibody MAb103/105 and FITC-conjugated secondary (green). Cell nuclei were stained with DAPI (blue). Cells were viewed using an inverted Nikon Eclipse TE200-U microscope, equipped with a Fluor 10X objective lens, and FITC and UV filter sets.

3.3.2 NTZ reduces cell proliferation

The effect of NTZ treatment on cell proliferation in MDBK cells was determined following incubation with compound for 24 h, with DMSO-treated MDBK cells serving as a control (Figure 3.2a). NTZ significantly inhibited cell proliferation, reducing proliferation to 50% of DMSO-treated controls (CC_{50}) at 20.11 ± 7.7 µM. In addition, the effect on cell division was measured by flow cytometry of CFSE-labelled MDBK cells treated with NTZ (Figure 3.2b). NTZ treatment upwards of 10 µM resulted in significantly elevated amounts of CFSE, indicating a reduction in cell division.

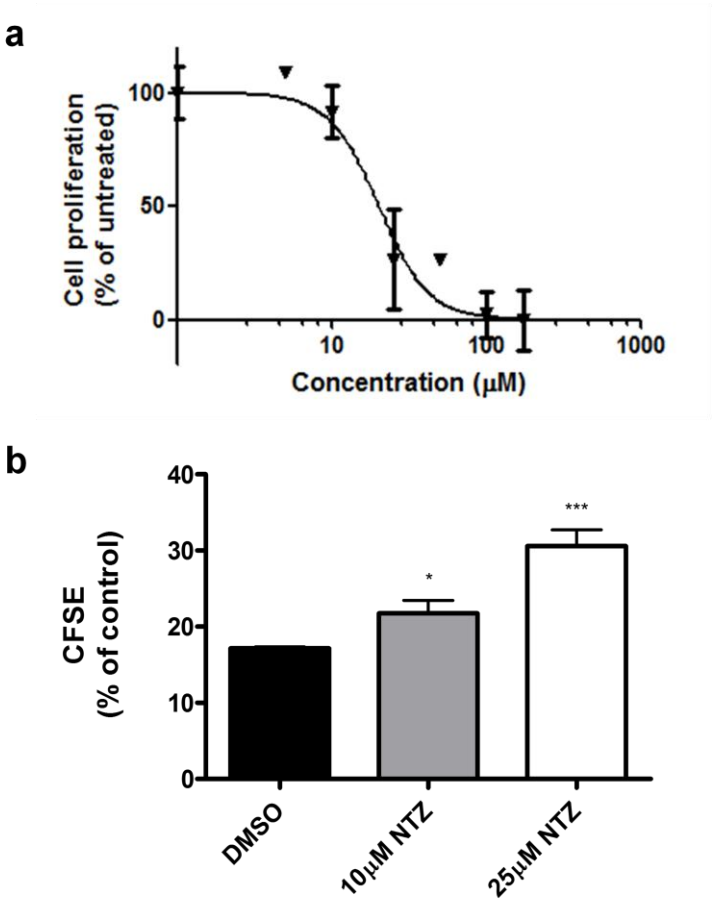

Figure 3.2 – NTZ reduces cell proliferation in MDBK cells. (a) MTS assay of MDBK cells incubated with NTZ for 24 h. Cell proliferation at each concentration normalized to DMSO-treated controls. Error bars indicate standard deviation. (b) CFSE assay of MDBK cells incubated with DMSO, 10 µM and 25 µM NTZ for 24 h. Amount of CFSE normalized to DMSO-treated control at 0 h. Error bars indicate standard deviation. * $p<0.05$, *** $p<0.001$; two-tailed student's t-test.

3.3.3 NTZ increases PKR and eIF2α phosphorylation

As previously discussed, NTZ has been shown to induce autophosphorylation of PKR, activating its kinase activity (Elazar *et al*, 2009). This results in phosphorylation of eIF2α and a subsequent global inhibition of cap-dependent translation.

In MDBK cells, infection with cytopathic BVDV (NADL strain) induced PKR phosphorylation, whilst non-cytopathic BVDV (Pe515 strain) did not, in agreement with previously published data (Figure 3.3a) (Gil *et al*, 2006b). Interestingly, in the absence of infection, NTZ also induced phosphorylation of PKR, and subsequently eIF2α, in the absence of dsRNA. The effect of NTZ treatment on cap-dependent translation was then investigated using a translation reporter assay (Figure 3.3b). MDBK cells were transfected with a bicistronic plasmid encoding firefly and renilla luciferases expressed via HCV IRES- and cap-mediated translation respectively. NTZ treatment resulted in a dose-dependent reduction in cap-dependent translation relative to IRES-mediated translation as determined by luciferase activity. No effect on the absolute level of IRES-mediated translation was observed. With NTZ activating PKR phosphorylation, even in the absence of viral dsRNA, expression of translationally controlled tumour protein (TCTP) and ER stress marker BiP was investigated (Figure 3.3a). TCTP is a cellular protein encoded by a highly structured mRNA that can activate PKR phosphorylation (Bommer *et al*, 2002). NTZ treatment, as well as cytopathic BVDV infection, induced TCTP and BiP expression in MDBK cells.

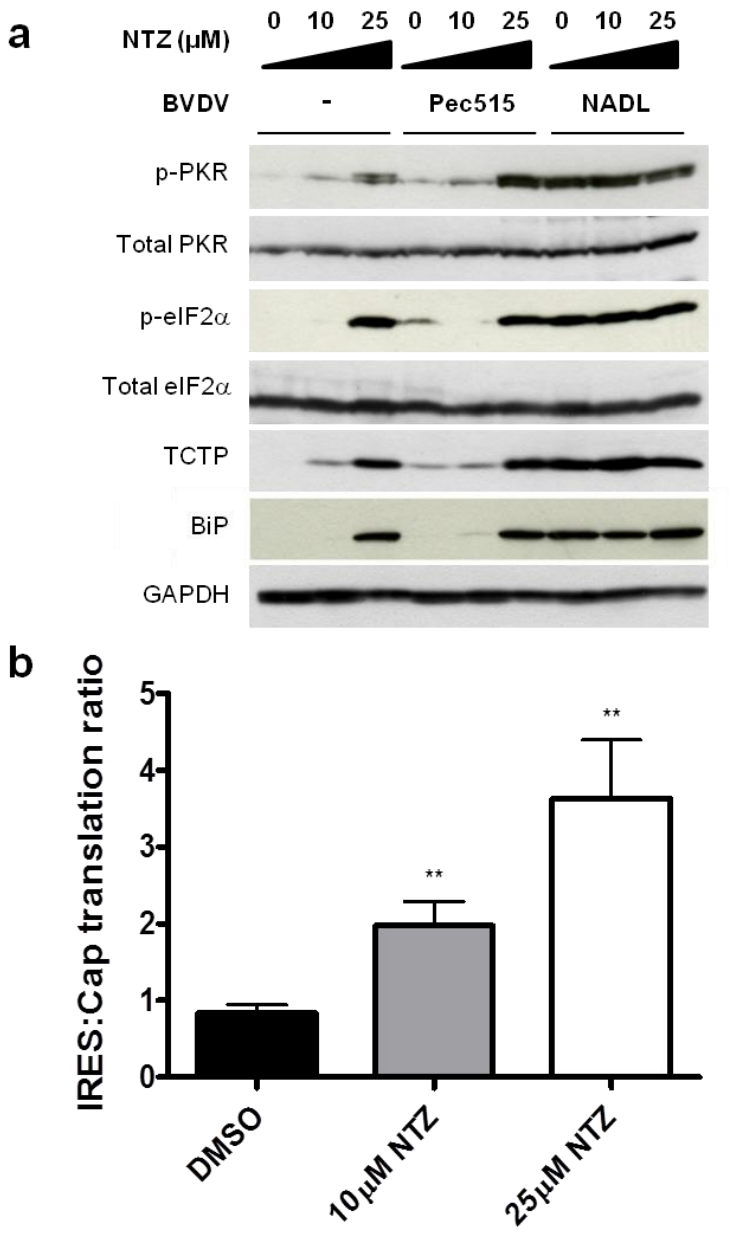

Figure 3.3 – (a) NTZ increases PKR and eIF2a phosphorylation and upregulates TCTP. MDBK cells (either uninfected or infected with BVDV strains Pec515 or NADL) were treated with DMSO, 10 μM or 25 μM NTZ for 24 h, then lysed and analysed by Western blotting. Protein lysates were separated by SDS-PAGE under reducing conditions, transferred to Immobilon-P membranes and probed with antibodies against phosphorylated PKR (p-PKR), total PKR, phosphorylated eIF2α (p-eIF2α), total eIF2α, TCTP and BiP, with GAPDH used as a loading control. (b) NTZ inhibits cap-dependent translation relative to IRES-mediated translation. MDBK cells were transfected with psiCHECK2-HCV IRES, expressing FLuc and RLuc under IRES- and cap-dependent translational control respectively. FLuc and RLuc activities were measured using the Dual-Glo® Luciferase Assay System and FLuc:RLuc (IRES:cap) ratio calculated. Figure 3.3b was produced by Dr. Omodele Ashiru.

3.3.4 NTZ depletes intracellular ATP-sensitive Ca^{2+} stores

Thapsgargin, which has previously been shown to inhibit HCV replication (Nakagawa *et al*, 2005), also induces PKR autophosphorylation in the absence of dsRNA, via a mechanism involving the depletion of ER Ca^{2+} stores (Prostko *et al*, 1995). In addition, TCTP levels are known to be upregulated in response to increased cytosolic Ca^{2+} levels (Xu *et al*, 1999). Consequently, the effect of NTZ on intracellular Ca^{2+} levels and mobilisation was investigated. Cytosolic Ca^{2+} concentration ($[Ca^{2+}]$) in MDBK cells was measured using Fura-2 AM, a cell permeable ratiometric fluorescent Ca^{2+} indicator. Emission at wavelength 510 nm is measured following excitation at wavelengths 340 and 380 nm, with the 340/380nm absorbance ratio directly correlating to intracellular free $[Ca^{2+}]$.

Addition of 1-50 μM NTZ to Fura-2 AM-labelled MDBK cells resulted in a rapid (< 1 m), dose-dependent increase in cytosolic $[Ca^{2+}]$ (Figure 3.4a). As expected, pretreatment with the cell permeable Ca^{2+} chelator BAPTA-AM prevented NTZ-mediated increase in cytosolic $[Ca^{2+}]$ (Figure 3.4b).

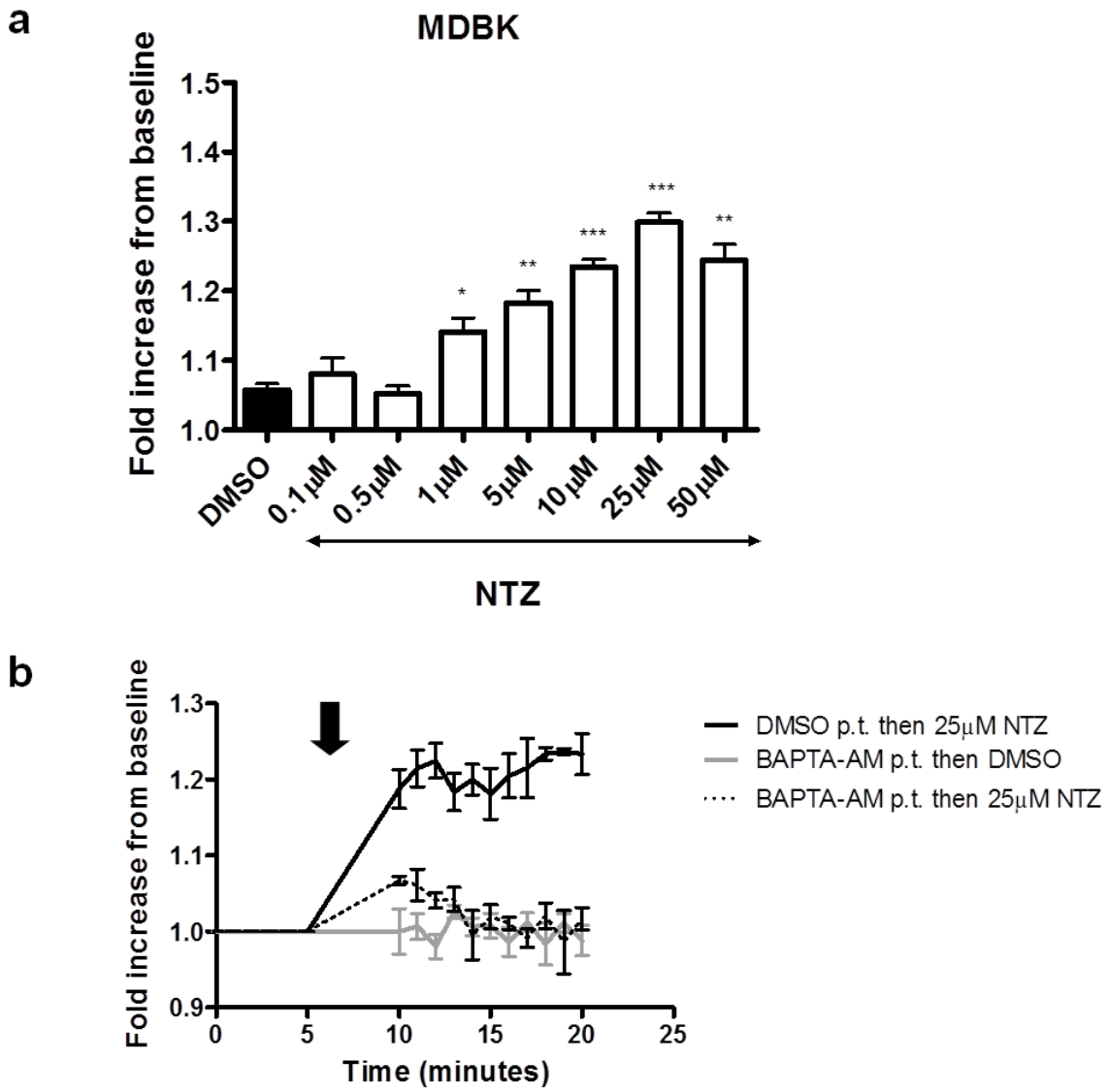

Figure 3.4 - NTZ elevates cytosolic Ca^{2+} levels. (a) MDBK cells were labelled with Fura-2 and incubated with up to 50 μM NTZ. Absorbance at 510 nm was measured after excitation at 340 and 390 nm, with the 340/390 nm absorbance ratio calculated. (b) MDBK cells were labelled with Fura2 AM and pretreated with DMSO or BAPTA-AM, then incubated with DMSO or NTZ (addition indicated by black arrow). Absorbance at 510 nm was measured at 1 m intervals. Error bars indicate standard deviation of at least three replicates. *p<0.05; ** p<0.01; *** p<0.001 student's t-test. This figure was produced by Dr. Omodele Ashiru.

By probing the effect of NTZ on [Ca^{2+}] in Ca^{2+}-free HBSS buffer, extracellular influx of Ca^{2+} was ruled out as the source of the observed increase (Figure 3.5b), indicating the increased cytosolic levels were a result of depletion of intracellular Ca^{2+} stores only. To subsequently identify the intracellular Ca^{2+} stores that are depleted by NTZ, a series of Ca^{2+}-mobilising compounds were used in combination with NTZ.

Thapsigargin is known to deplete ER Ca^{2+} stores by inhibiting sarcoplasmic/endoplasmic reticulum calcium ATPase (SERCA) (Thastrup *et al*, 1990), which maintains the Ca^{2+} gradient between the ER and the cytosol by pumping Ca^{2+} into the ER lumen. Thapsigargin-sensitive SERCA pumps are also located in the Golgi apparatus, in addition to thapsigargin-insensitive inositol 1,3,4-triphosphate receptors (Pinton *et al*, 1998). MDBK cells were pre-incubated with thapsigargin prior to NTZ treatment and [Ca^{2+}] monitored (Figure 3.5a). Thapsigargin treatment induced an immediate increase in free intracellular [Ca^{2+}], and subsequent addition of NTZ failed to increase [Ca^{2+}] further, indicating NTZ mobilises Ca^{2+} from the same intracellular stores as thapsigargin. Similarly, the effect of NTZ on Ca^{2+} mobilisation following ionomycin, CCCP and ATP treatment were investigated. Ionomycin exclusively depletes non-acidic Ca^{2+} stores (i.e. ER (pH 7.2) and mitochondria (pH 7.8) but not Golgi (pH 6-6.7) or lysosomes (pH 5.5)). Following ionomycin pretreatment, addition of NTZ resulted in a further increase in [Ca^{2+}], indicating the depletion of an acidic store (either the Golgi apparatus or lysosomes) by NTZ. CCCP pretreatment, which depletes the mitochondrial matrix of Ca^{2+}, had no effect on NTZ-mediated Ca^{2+} mobilisation. Finally, pretreatment with ATP, which depletes stores possessing ATP-sensitive inositol 1,4,5-triphosphate (IP_3R) channels, entirely prevented any subsequent increase in [Ca^{2+}] on addition of NTZ. Altogether, these data indicate NTZ induces the depletion of ATP-sensitive intracellular Ca^{2+} stores i.e. the ER and Golgi apparatus.

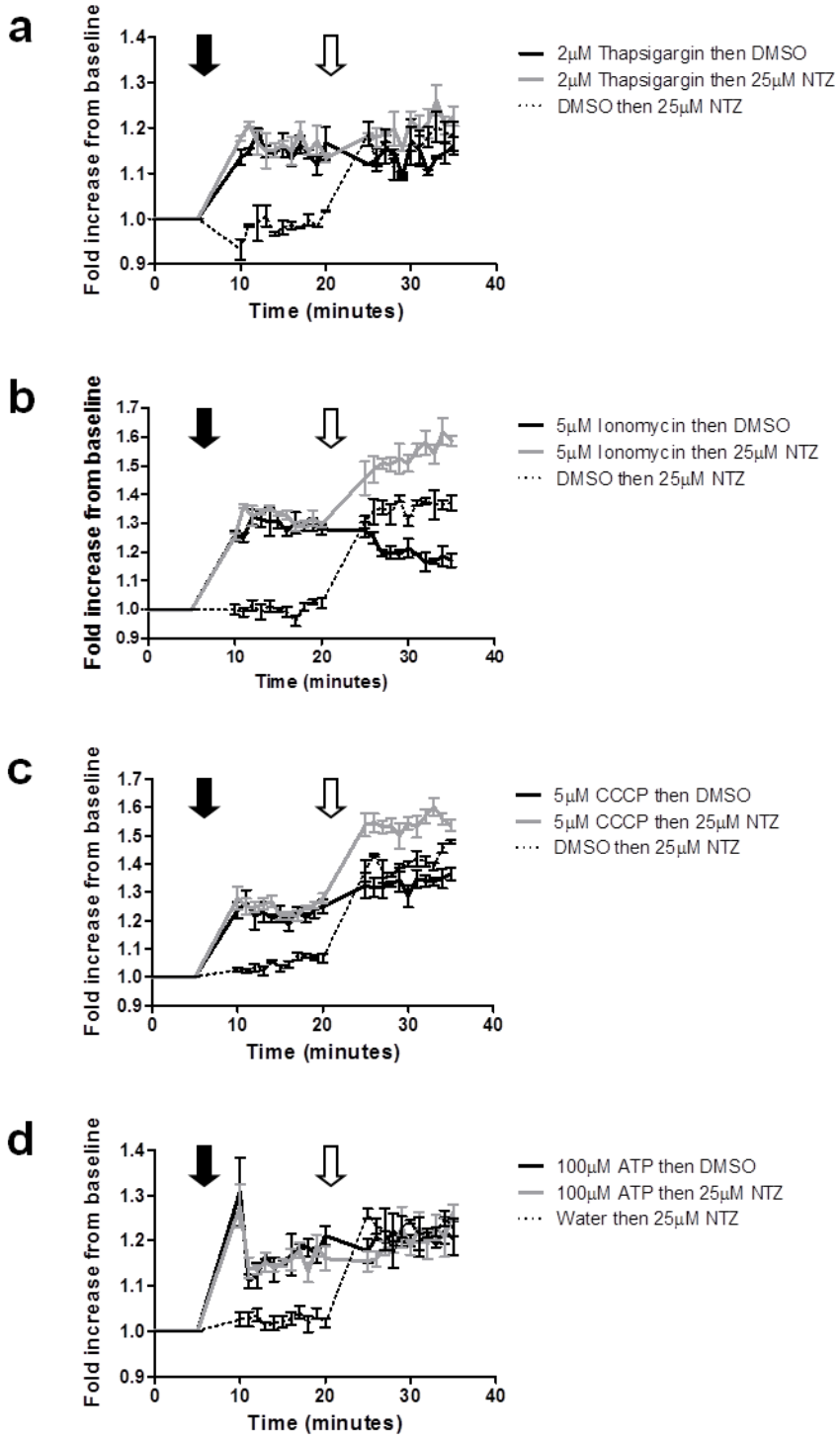

Figure 3.5 – NTZ depletes intracellular Ca^{2+} stores. Cytosolic Ca^{2+} levels were measured in Fura-2-labelled MDBK cells treated with two consecutive compounds: (a) thapsigargin followed by NTZ; (b) ionomycin followed by NTZ; (c) CCCP followed by NTZ; (d) ATP followed by NTZ. DMSO and water were used as controls as indicated. Filled and open arrows indicate addition of the first and second compounds, respectively. Experiments with ionomycin (b) were performed in the absence of extracellular Ca^{2+}. This figure was produced by Dr. Omodele Ashiru.

3.3.5 NTZ disrupts glycoprocessing and viral glycosylation

With NTZ depleting ER/Golgi Ca^{2+} stores, and having previously been shown to affect HA maturation in influenza A (Rossignol *et al*, 2009), the effect of NTZ on BVDV glycoprotein glycosylation and processing in the secretory pathway was investigated. Virus secreted from MDBK cells treated with NTZ was analysed by Western blot to detect BVDV envelope glycoprotein E2 (Figure 3.6). E2 protein showed increased electrophoretic mobility with increasing NTZ concentration, which was confirmed by Endo H digests to be a result of altered glycosylation. In agreement with previously published data, native E2 from untreated MDBK cells was partially digested by Endo H treatment, indicating a mixed glycan population of oligomannose and complex structures (Jordan *et al*, 2002). Using kifunensine, which inhibits complex glycan formation, as a positive control, E2 was shown to be more susceptible to Endo H digestion following NTZ treatment, indicating a loss of complex glycan species on the protein. The effect of thapsigargin on E2 glycosylation was also investigated, and resulted in a minor increase in Endo H sensitivity at 0.5 µM. Higher concentrations of thapsigargin were investigated to determine if this further increased Endo H sensitivity, but the greatly reduced output of virus from thapsigargin-treated cells made E2 protein undetectable by Western blot.

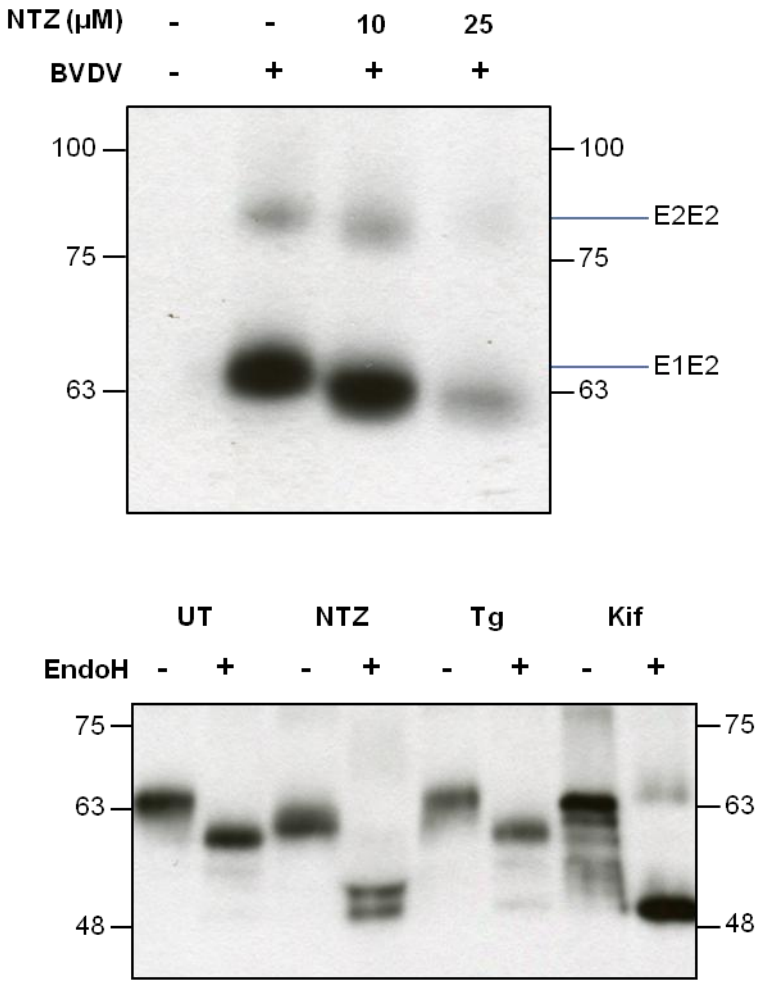

Figure 3.6 - Western blot analysis of BVDV E2 protein. (top) MDBK cells were infected with BVDV and treated with NTZ up to 25 μM for 24 h. Secreted virions were concentrated and lysed by sonication. Viral proteins were then separated by non-reducing SDS-PAGE and analysed by Western blot using anti-BVDV E2 antibody MAb214. (bottom) Viral lysates from samples treated with DMSO (untreated, UT), 10 μM NTZ, 0.5 μM thapsigargin (Tg) and 10 μM kifunensine (Kif) were digested with EndoH for 24 h, then subjected to SDS-PAGE and Western blot analysis as above.

To investigate whether NTZ treatment caused a disruption of ER-Golgi trafficking, which could explain the inhibition of complex glycan formation, MDBK cells were treated with either NTZ or thapsigargin in the presence of ER α-glucosidase inhibitor NAP-DNJ (Rawlings *et al*, 2009). Free oligosaccharides (FOS) were purified and analysed by normal-phase HPLC. Inhibition of ER α-glucosidases increases the level of cytosolic FOS $Glc_3Man_5GlcNAc_1$, a marker of ERAD (Alonzi *et al*, 2008) and ER luminal FOS $Glc_3Man_7GlcNAc_2$, a marker of a secondary degradation pathway for

Golgi-retrieved proteins (Alonzi *et al*, 2013). Treatment of MDBK cells with either NTZ or thapsigargin, in the presence of glucosidase inhibitor NAP-DNJ, resulted in a dose-dependent reduction in ER-localised but not cytosolic FOS, indicating a disruption to ER-Golgi trafficking of glycoproteins (Figure 3.7). Thapsigargin, which was less effective in modulating E2 glycosylation at the concentration used, affected FOS to a similar extent to NTZ, suggesting that a global analysis of disruption of ER-Golgi transport may mask protein-specific effects on BVDV E2 glycosylation induced by NTZ.

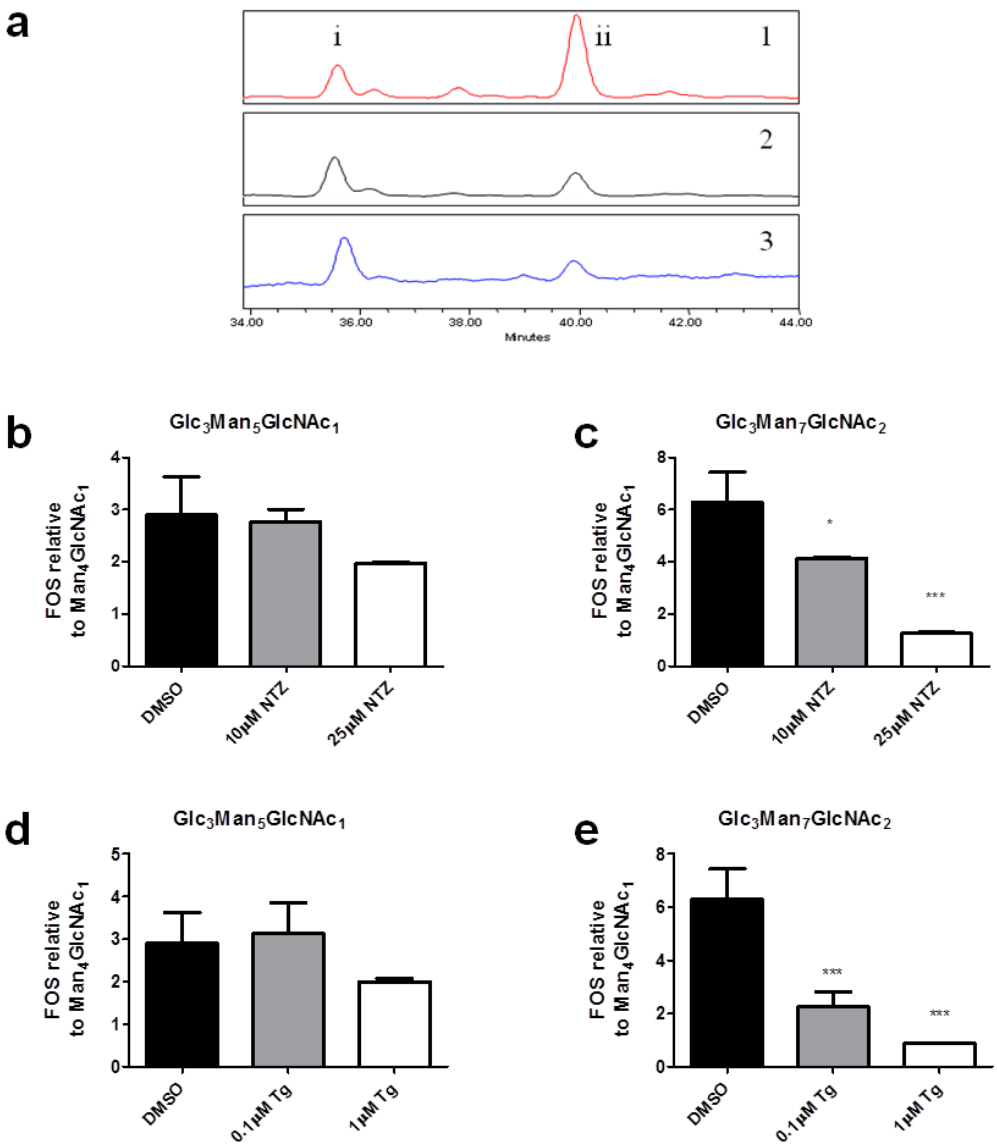

Figure 3.7 - Free oligosaccharide (FOS) analysis of MDBK cells. MDBK cells were incubated with NAP-DNJ and either NTZ or thapsigargin (Tg) for 24 h. FOS were extracted and purified, labelled with 2-AA and analysed by NP-HPLC. (a) Representative FOS profiles showing (i) $Glc_3Man_5GlcNAc_1$ and (ii) $Glc_3Man_7GlcNAc_2$ – MDBK cells with (1) 50 μM NAP-DNJ and DMSO control; (2) 50 μM NAP-DNJ and 25 μM NTZ; and (3) 50 μM NAP-DNJ and 1 μM Tg. (b)-(e) Amounts of $Glc_3Man_5GlcNAc_1$ and $Glc_3Man_7GlcNAc_2$, relative to $Man_4GlcNAc_1$, which remained constant for all treatments, from MDBK cells incubated with 50 μM NAP-DNJ and either DMSO vehicle, NTZ or Tg as indicated.

3.4 Discussion

3.4.1 Antiviral properties of NTZ

The antiviral properties of the thiazolide NTZ have been demonstrated previously, against a variety of viruses including HBV and the Flaviviridae members HCV and JEV (Korba *et al*, 2008b; Shi *et al*, 2014). Here, NTZ is shown to inhibit replication of another member of the Flaviviridae family, BVDV. Treatment with 25 μM NTZ, below the peak plasma concentration observed in man following oral administration of 500 mg NTZ (Stockis *et al*, 2002), resulted in an approximate 100-fold reduction in infectivity of the cytopathic NADL strain of BVDV.

3.4.2 Effect of NTZ on cell survival and proliferation

MG132 induces apoptotic cell death through the formation of reactive oxygen species (Emanuele *et al*, 2002). NTZ treatment protects against MG132-induced apoptosis (Ashiru *et al*, 2014), indicating that although NTZ is highly anti-proliferative, it potentiates strong survival/anti-apoptotic signals, unlike its bromo-derivative RM4819, which demonstrates Bim-mediated pro-apoptotic properties in colorectal cancer cells (Sidler *et al*, 2012). Thapsigargin has been reported to protect against cycloheximide-induced apoptosis, via depletion of intracellular Ca^{2+} stores (Chacon-Cruz *et al*, 1998). Additionally, overexpression of TCTP, shown here to upregulated by NTZ, also protects against cycloheximide-induced cell death (Wei *et al*, 2012).

NTZ treatment downregulates cell metabolism and cell division and induces global shutoff of cap-dependent translation via eIF2α phosphorylation. Hence it is likely that NTZ treatment leads to a block in the synthesis of cellular proteins involved in the cell cycle, thereby reducing proliferation. Interestingly, NTZ-mediated eIF2α

phosphorylation has been shown to promote translation of ATF4 (Elazar *et al*, 2009), which drives expression of pro-survival functions (Harding *et al*, 2003). Thus, it is likely that, whilst NTZ is highly anti-proliferative, it promotes cell survival by upregulating ATF4, TCTP and BiP. It therefore seems plausible that NTZ holds cells in stasis until Ca^{2+} homoeostasis and cellular functions are restored. Altogether, these data indicate that 24 h NTZ treatment does not induce lethal acute ER stress, but instead induces chronic sub-lethal ER stress that cells can adapt to via multiple mechanisms.

3.4.3 NTZ-mediated mobilisation of intracellular Ca^{2+}

As reported for HCV, NTZ-mediated anti-BVDV activity also involved PKR phosphorylation. Unexpectedly, NTZ induced PKR phosphorylation in uninfected MDBK cells i.e. even in the absence of viral dsRNA. As PKR phosphorylation is also known to be induced by ER stress, ER stress markers BiP and TCTP were investigated, and both found to rapidly upregulated following NTZ treatment. TCTP levels are regulated at both the transcriptional and post-transcriptional levels, by cytosolic and ER [Ca^{2+}] respectively (Xu *et al*, 1999). With TCTP upregulation identified as a potential precursor to PKR phosphorylation, NTZ was subsequently found to elevate cytosolic [Ca^{2+}] through depletion of intracellular Ca^{2+} stores and did not elicit an influx of extracellular Ca^{2+}. Interestingly, NTZ is reported to have no effect on cytosolic [Ca^{2+}] in erythrocytes, which lack an ER and Golgi (Arnold *et al*, 2014). NTZ treatment upregulated BiP expression (a hallmark of ER stress), and also upregulated TCTP expression. Both TCTP and BiP genes possess calcium-responsive promoter elements (Li *et al*, 1993; Lee *et al*, 2004). Thus, depletion of ER Ca^{2+} stores is likely to be the primary signal for NTZ-mediated induction of BiP and TCTP expression. Similarly, thapsigargin has been shown to upregulate TCTP and

BiP expression within 4-6 h of initiation of treatment (Xu *et al*, 1999; Chen *et al*, 2000). Consequently, the ability of NTZ to induce ER stress and upregulate TCTP expression further suggests that NTZ raises cytosolic Ca^{2+} levels by depleting (in part) ER Ca^{2+} stores. Ionomycin pretreatment experiments indicated that NTZ also depletes Ca^{2+} sequestered in an acidic compartment, most likely the Golgi apparatus. Ca^{2+} plays a role in regulating intra-Golgi transport (Micaroni, 2012) and is a key factor for many Golgi resident enzymes, including glycosyltransferases. Interestingly, elevation of cytosolic Ca^{2+} concentration above 100 nM is reported to inhibit intra-Golgi transport (Porat & Elazar, 2000). Thus, NTZ-mediated increase of cytosolic Ca^{2+} might be expected to inhibit protein trafficking. This could also offer a partial explanation as to why such a marked contrast in antiviral activity is observed between 10 and 25 μM treatment with NTZ. If 10 μM treatment is incapable of elevating cytosolic Ca^{2+} sufficiently, inhibition of Golgi trafficking and hence viral secretion might not be observed. Indeed, only a small effect is observed on FOS composition following 10 μM NTZ treatment.

3.4.4 NTZ-mediated PKR phosphorylation

Previously, NTZ has been shown to directly enhance viral dsRNA-mediated autophosphorylation of PKR *in vitro* (Elazar *et al*, 2009). However, with NTZ capable of inducing PKR autophosphorylation *in cellulo* in the absence of viral dsRNA, the cellular mechanism for NTZ-mediated phosphorylation of PKR likely involves additional or alternative mechanisms. In addition to viral dsRNA, PKR can be activated by a number of cellular factors, including PKR activating protein (PACT) and TCTP mRNA. Indeed, PACT is directly responsible for PKR activation during thapsigargin treatment (Lee *et al*, 2007). The TCTP mRNA is a cellular mRNA with extensive secondary structure that is also known to activate PKR (Bommer *et al*,

2002). Increased TCTP mRNA transcription and upregulated TCTP protein expression are induced by depletion of ER Ca^{2+} stores and the resultant increase in cytosolic Ca^{2+}, respectively (Xu *et al*, 1999). NTZ-mediated PKR phosphorylation might involve the upregulation of TCTP mRNA as well as any direct interaction between PKR and NTZ itself.

In the study by Elazar *et al*, it was also observed that interferon (IFN) enhances NTZ-mediated phosphorylation of PKR and eIF2α (Elazar *et al*, 2009). The eif2ak2 gene, which encodes PKR, is an interferon-stimulated gene (ISG). Thus, IFN-mediated upregulation of PKR gene expression could result in increased PKR protein that would be available for NTZ-mediated phosphorylation. However, activation of PKR and subsequent phosphorylation of eIF2α would ultimately inhibit translation of mRNAs encoding PKR itself, other ISGs and IFN, allowing, via a negative-feedback mechanism, the re-establishment of cap-dependent translation. It is possible that this may allow MDBK cells to adapt and recover from NTZ treatment and avoid becoming apoptotic.

3.4.5 NTZ and the UPR

Regardless of how NTZ mediates PKR phosphorylation, it is clear that NTZ-mediated activation of PKR results in the phosphorylation of eIF2α. eIF2α can also be phosphorylated by PKR-like ER kinase (PERK), which is one of three inducers of the UPR. Interestingly, phosphorylation of eIF2α favours translation of activating transcription factor 4 (ATF4), which drives expression of pro-survival functions (Harding *et al*, 2003). Importantly, NTZ treatment is reported to induce translational activation of ATF4 in a PKR-dependent manner (Elazar *et al*, 2009). Hence it appears that upregulation of ATF4 is a mechanism employed by the cell to adapt to

NTZ. Cells can also adapt to ER stress by inducing ER-associated degradation and autophagy in order to clear misfolded proteins accumulated in the ER. Preliminary experiments with proteasome inhibitors MG132 and ALLN suggest that ERAD is not induced by NTZ treatment (Ashiru, unpublished), however NTZ has been shown to induce autophagy (Lam *et al*, 2012).

3.4.6 Effect of NTZ on BVDV glycosylation

NTZ has previously been shown to affect maturation and trafficking of the influenza envelope HA protein, impairing trafficking to the cell surface and preventing complex glycan formation (Rossignol *et al*, 2009). A similar effect is observed with BVDV envelope glycoprotein E2. NTZ treatment results in near-total loss of complex glycans from virion-associated E2 protein secreted from MDBK cells. The effect of NTZ on glycoprocessing can be observed through FOS analysis. NTZ treatment results in a decrease in ER-localised FOS that are derived from Golgi-retrieved misfolded proteins. Together, these effects indicate a disruption to trafficking and processing of viral glycoproteins through the Golgi apparatus. Elevation of cytosolic [Ca^{2+}] has previously been shown to disrupt Golgi trafficking (Porat & Elazar, 2000), whilst a number of ER and Golgi resident glycoprocessing enzymes are dependent on Ca^{2+} for activity. It is therefore likely that NTZ-mediated Ca^{2+} depletion from ER and Golgi stores would perturb viral glycosylation and trafficking through the secretory pathway. Interestingly, the effect of thapsigargin on viral glycosylation appears to be much lower than that of NTZ, despite corresponding concentrations of both compounds having a similar level of effect on FOS composition. Treatment with 1 μM thapsigargin greatly reduced $Glc_3Man_7GlcNAc_2$ levels, yet only induced a slight increase in sensitivity of BVDV E2 protein to Endo H digestion. Contrastingly, 10 μM NTZ reduced $Glc_3Man_7GlcNAc_2$ levels to a lesser extent than 1 μM thapsigargin, but

was sufficient to almost complete abolish complex glycan formation. The explanation for this discrepancy requires further investigation, but may arise from the different mechanisms of the two compounds in depleting intracellular Ca^{2+} stores. Thapsigargin is known to inhibit SERCA pumps, to principally deplete the ER Ca^{2}+ store, and whilst the mechanism by which NTZ induces Ca^{2+} mobilisation remains unknown, it appears to have a greater effect on the Golgi apparatus.

In conclusion, NTZ inhibits BVDV replication by a post-entry mechanism that is likely to involve the depletion of ATP-sensitive Ca^{2+} stores, as well as the phosphorylation of PKR and eIF2α. Whilst NTZ has no direct effect on IRES-mediated translation, the down-regulation of cap-dependent translation via PKR and eIF2α phosphorylation and reduction in cell proliferation are likely to inhibit viral replication by affecting host factors utilised by the virus. This, together with disruption to the processing and maturation of viral envelope glycoproteins, results in NTZ being potently antiviral against BVDV. Importantly, as well as these anti-proliferative effects, NTZ protects against apoptosis by upregulating BiP and TCTP expression.

Further work is required to elucidate exactly which of the cellular effects of NTZ treatment are responsible for its antiviral attributes, but mobilisation of intracellular Ca^{2+} stores appears to be the primary effect arising from NTZ treatment and might underpin many of the antiviral mechanisms attributed to NTZ to date. With such a myriad of effects arising from a single compound, it perhaps shouldn’t be surprising that NTZ displays antimicrobial activity against such a diverse spectrum of pathogens.

3.5 References

Alonzi DS, Kukushkin NV, Allman SA, Hakki Z, Williams SJ, Pierce L, Dwek RA, Butters TD (2013) Glycoprotein misfolding in the endoplasmic reticulum: identification of released oligosaccharides reveals a second ER-associated degradation pathway for Golgi-retrieved proteins. *Cellular and Molecular Life Sciences* **70:** 2799-2814

Alonzi DS, Neville DC, Lachmann RH, Dwek RA, Butters TD (2008) Glucosylated free oligosaccharides are biomarkers of endoplasmic- reticulum alpha-glucosidase inhibition. *Biochemical Journal* **409:** 571-580

Arnold M, Lang E, Modicano P, Bissinger R, Faggio C, Abed M, Lang F (2014) Effect of Nitazoxanide on Erythrocytes. *Basic & Clinical Pharmacology & Toxicology* **114:** 421-426

Ashiru O, Howe JD, Butters TD (2014) Nitazoxanide, an antiviral thiazolide, depletes ATP-sensitive intracellular Ca(2+) stores. *Virology* **462-463:** 135-148

Bommer UA, Borovjagin AV, Greagg MA, Jeffrey IW, Russell P, Laing KG, Lee M, Clemens MJ (2002) The mRNA of the translationally controlled tumor protein P23/TCTP is a highly structured RNA, which activates the dsRNA-dependent protein kinase PKR. *RNA* **8:** 478-496

Chacon-Cruz E, Oelberg DG, Davis P, Buescher ES (1998) Membrane depolarization and depletion of intracellular calcium stores are associated with delay of apoptosis in human neutrophils. *Journal of Leukocyte Biology* **64:** 759-766

Chen LY, Chiang AS, Hung JJ, Hung HI, Lai YK (2000) Thapsigargin-induced grp78 expression is mediated by the increase of cytosolic free calcium in 9L rat brain tumor cells. *Journal of Cellular Biochemistry* **78:** 404-416

Elazar M, Liu M, McKenna SA, Liu P, Gehrig EA, Puglisi JD, Rossignol JF, Glenn JS (2009) The anti-hepatitis C agent nitazoxanide induces phosphorylation of eukaryotic initiation factor 2alpha via protein kinase activated by double-stranded RNA activation. *Gastroenterology* **137:** 1827-1835

Emanuele S, Calvaruso G, Lauricella M, Giuliano M, Bellavia G, D'Anneo A, Vento R, Tesoriere G (2002) Apoptosis induced in hepatoblastoma HepG2 cells by the proteasome inhibitor MG132 is associated with hydrogen peroxide production, expression of Bcl-XS and activation of caspase-3. *International Journal of Oncology* **21:** 857-865

Garcia MA, Meurs EF, Esteban M (2007) The dsRNA protein kinase PKR: virus and cell control. *Biochimie* **89:** 799-811

Gil LH, van Olphen AL, Mittal SK, Donis RO (2006b) Modulation of PKR activity in cells infected by bovine viral diarrhea virus. *Virus Research* **116:** 69-77

Harding HP, Zhang Y, Zeng H, Novoa I, Lu PD, Calfon M, Sadri N, Yun C, Popko B, Paules R, Stojdl DF, Bell JC, Hettmann T, Leiden JM, Ron D (2003) An integrated stress response regulates amino acid metabolism and resistance to oxidative stress. *Molecular Cell* **11:** 619-633

Jordan R, Nikolaeva OV, Wang L, Conyers B, Mehta A, Dwek RA, Block TM (2002) Inhibition of host ER glucosidase activity prevents Golgi processing of virion-associated bovine viral diarrhea virus E2 glycoproteins and reduces infectivity of secreted virions. *Virology* **295:** 10-19

Korba BE, Montero AB, Farrar K, Gaye K, Mukerjee S, Ayers MS, Rossignol JF (2008b) Nitazoxanide, tizoxanide and other thiazolides are potent inhibitors of hepatitis B virus and hepatitis C virus replication. *Antiviral Research* **77:** 56-63

Lam KK, Zheng X, Forestieri R, Balgi AD, Nodwell M, Vollett S, Anderson HJ, Andersen RJ, Av-Gay Y, Roberge M (2012) Nitazoxanide stimulates autophagy and inhibits mTORC1 signaling and intracellular proliferation of Mycobacterium tuberculosis. *PLoS Pathogens* **8:** e1002691

Lee ES, Yoon CH, Kim YS, Bae YS (2007) The double-strand RNA-dependent protein kinase PKR plays a significant role in a sustained ER stress-induced apoptosis. *FEBS Letters* **581:** 4325-4332

Lee JM, Kusakabe T, Kawaguchi Y, Miyagawa Y, Takahashi M, Mon H, Nho SK, Koga K (2004) Molecular cloning and characterization of the translationally controlled tumor protein gene in Bombyx mori. *Comparative Biochemistry and Physiology Part B: Biochemistry and Molecular Biology* **139:** 35-43

Li WW, Alexandre S, Cao X, Lee AS (1993) Transactivation of the grp78 promoter by Ca2+ depletion. A comparative analysis with A23187 and the endoplasmic reticulum Ca(2+)-ATPase inhibitor thapsigargin. *Journal of Biological Chemistry* **268:** 12003-12009

Micaroni M (2012) Calcium around the Golgi apparatus: implications for intracellular membrane trafficking. *Advances in Experimental Medicine and Biology* **740:** 439-460

Muller J, Sidler D, Nachbur U, Wastling J, Brunner T, Hemphill A (2008) Thiazolides inhibit growth and induce glutathione-S-transferase Pi (GSTP1)-dependent cell death in human colon cancer cells. *International Journal of Cancer* **123:** 1797-1806

Nakagawa M, Sakamoto N, Tanabe Y, Koyama T, Itsui Y, Takeda Y, Chen CH, Kakinuma S, Oooka S, Maekawa S, Enomoto N, Watanabe M (2005) Suppression of hepatitis C virus replication by cyclosporin a is mediated by blockade of cyclophilins. *Gastroenterology* **129:** 1031-1041

Pinton P, Pozzan T, Rizzuto R (1998) The Golgi apparatus is an inositol 1,4,5-trisphosphate-sensitive Ca2+ store, with functional properties distinct from those of the endoplasmic reticulum. *EMBO Journal* **17:** 5298-5308

Porat A, Elazar Z (2000) Regulation of intra-Golgi membrane transport by calcium. *Journal of Biological Chemistry* **275:** 29233-29237

Prostko CR, Dholakia JN, Brostrom MA, Brostrom CO (1995) Activation of the double-stranded RNA-regulated protein kinase by depletion of endoplasmic reticular calcium stores. *Journal of Biological Chemistry* **270:** 6211-6215

Rawlings AJ, Lomas H, Pilling AW, Lee MJ, Alonzi DS, Rountree JS, Jenkinson SF, Fleet GW, Dwek RA, Jones JH, Butters TD (2009) Synthesis and biological characterisation of novel N-alkyl-deoxynojirimycin alpha-glucosidase inhibitors. *ChemBioChem* **10:** 1101-1105

Robert F, Kapp LD, Khan SN, Acker MG, Kolitz S, Kazemi S, Kaufman RJ, Merrick WC, Koromilas AE, Lorsch JR, Pelletier J (2006) Initiation of protein synthesis by hepatitis C virus is refractory to reduced eIF2.GTP.Met-tRNA(i)(Met) ternary complex availability. *Molecular Biology of the Cell* **17:** 4632-4644

Rossignol JF, Abu-Zekry M, Hussein A, Santoro MG (2006) Effect of nitazoxanide for treatment of severe rotavirus diarrhoea: randomised double-blind placebo-controlled trial. *Lancet* **368:** 124-129

Rossignol JF, La Frazia S, Chiappa L, Ciucci A, Santoro MG (2009) Thiazolides, a new class of anti-influenza molecules targeting viral hemagglutinin at the post-translational level. *Journal of Biological Chemistry* **284:** 29798-29808

Rowlands AG, Panniers R, Henshaw EC (1988) The catalytic mechanism of guanine nucleotide exchange factor action and competitive inhibition by phosphorylated eukaryotic initiation factor 2. *Journal of Biological Chemistry* **263:** 5526-5533

Shi Z, Wei J, Deng X, Li S, Qiu Y, Shao D, Li B, Zhang K, Xue F, Wang X, Ma Z (2014) Nitazoxanide inhibits the replication of Japanese encephalitis virus in cultured cells and in a mouse model. *Virology Journal* **11:** 10

Sidler D, Brockmann A, Mueller J, Nachbur U, Corazza N, Renzulli P, Hemphill A, Brunner T (2012) Thiazolide-induced apoptosis in colorectal cancer cells is mediated via the Jun kinase-Bim axis and reveals glutathione-S-transferase P1 as Achilles' heel. *Oncogene* **31:** 4095-4106

Stockis A, De Bruyn S, Gengler C, Rosillon D (2002) Nitazoxanide pharmacokinetics and tolerability in man during 7 days dosing with 0.5 g and 1 g b.i.d. *International Journal of Clinical Pharmacology and Therapeutics* **40:** 221-227

Thastrup O, Cullen PJ, Drobak BK, Hanley MR, Dawson AP (1990) Thapsigargin, a tumor promoter, discharges intracellular Ca2+ stores by specific inhibition of the endoplasmic reticulum Ca2(+)-ATPase. *Proc. Natl. Acad. Sci. USA* **87:** 2466-2470

Wang L, Jeng KS, Lai MM (2011) Poly(C)-binding protein 2 interacts with sequences required for viral replication in the hepatitis C virus (HCV) 5' untranslated region and directs HCV RNA replication through circularizing the viral genome. *Journal of Virology* **85:** 7954-7964

Wei J, Guo M, Ji H, Yan Y, Ouyang Z, Huang X, Hang Y, Qin Q (2012) Grouper translationally controlled tumor protein prevents cell death and inhibits the replication of Singapore grouper iridovirus (SGIV). *Fish and Shellfish Immunology* **33:** 916-925

Xu A, Bellamy AR, Taylor JA (1999) Expression of translationally controlled tumour protein is regulated by calcium at both the transcriptional and post-transcriptional level. *Biochemical Journal* **342:** 683-689

4 Host cell glycoprocessing enzymes as antiviral targets

4.1 Introduction

Almost all enveloped viruses encode glycoproteins that are dependent on host cell machinery to achieve glycosylation, folding and maturation. Oligosaccharides are attached to nascent polypeptides cotranslationally as they are translocated into the lumen of the ER. This glycan, of structure $Glc_3Man_9GlcNAc_2$, is then rapidly processed by α-glucosidases I and II to sequentially remove two glucose monosaccharides, leaving a monoglucosylated glycan, which acts as a substrate for binding the ER resident folding chaperone calnexin, or its soluble homolog calreticulin. Calnexin recruits folding cofactors including the disulphide bond isomerise ERp57 and aids glycoprotein folding. Interaction between calnexin and the nascent glycoprotein is terminated by removal of the final glucose from the glycan, a step again carried out by α-glucosidase II (see Chapter 1, section 1.1.1 for details).

The use of DNJ-based imino sugars to inhibit α-glucosidases is well-established, and such inhibition blocks calnexin-mediated folding of glycoproteins. Inhibition of α-glucosidases retains glycans in a hyperglucosylated state, preventing formation of the monoglucosylated calnexin substrate. These proteins are subsequently redirected into the ER-associated degradation (ERAD) pathway and targeted to the proteasome for degradation. The glycan is released from the protein by PNGase (or a PNGase-like enzyme).

Endo-α-mannosidase, a glycoprocessing enzyme localised to the Golgi apparatus, provides an alternative processing pathway for glucosylated glycans that allows bypass of α-glucosidase action and interaction with calnexin (Lubas & Spiro, 1988;

Moore & Spiro, 1990). Endomannosidase cleaves the α-1,2 glycosidic bond between the glucose-substituted mannose and the remainder of the glycan, removing the glucose cap in one step (Lubas & Spiro, 1987). This allows further processing of the glycan to occur throughout the Golgi, allowing formation of complex glycan structures. In MDBK cells, endomannosidase can only process a restricted subset of substrates – namely monoglucosylated glycans but not bi- or triglucosylated structures (Kukushkin *et al*, 2012).

In this chapter, the antiviral effects of two small molecule inhibitors are investigated, individually and in combination. NAP-DNJ is a glucose-mimicking imino sugar (Figure 4.1) that potently inhibits ER α-glucosidases I and II (Rawlings *et al*, 2009). Here, NAP-DNJ is shown to inhibit α-glucosidases I and II, increasing specific degradation of BVDV envelope glycoprotein E2. In addition, a novel endomannosidase inhibitor, glucose-isofagomine (GlcIFG; Figure 4.1) (Thompson *et al*, 2012), is used. GlcIFG has previously been shown to bind to the active site of endomannosidase, acting as a competitive inhibitor by mimicking the α-1,3-glucose-substituted mannose substrate (Thompson *et al*, 2012). Here, GlcIFG shows *in cellulo* inhibition of endomannosidase and is investigated in combination with NAP-DNJ to investigate whether a two-pronged approach targeting glycoprocessing enzymes would show enhanced antiviral activity against BVDV. Interestingly, solo treatment with GlcIFG exhibited an antiviral effect against BVDV and was capable of inhibiting complex glycan formation, indicating the use of endomannosidase by viral glycoproteins, even in the absence of α-glucosidase inhibition. Finally, the effect of inhibiting complex glycan formation is investigated using the mannosidase inhibitor kifunensine, and shown to be modestly capable of reducing viral infectivity.

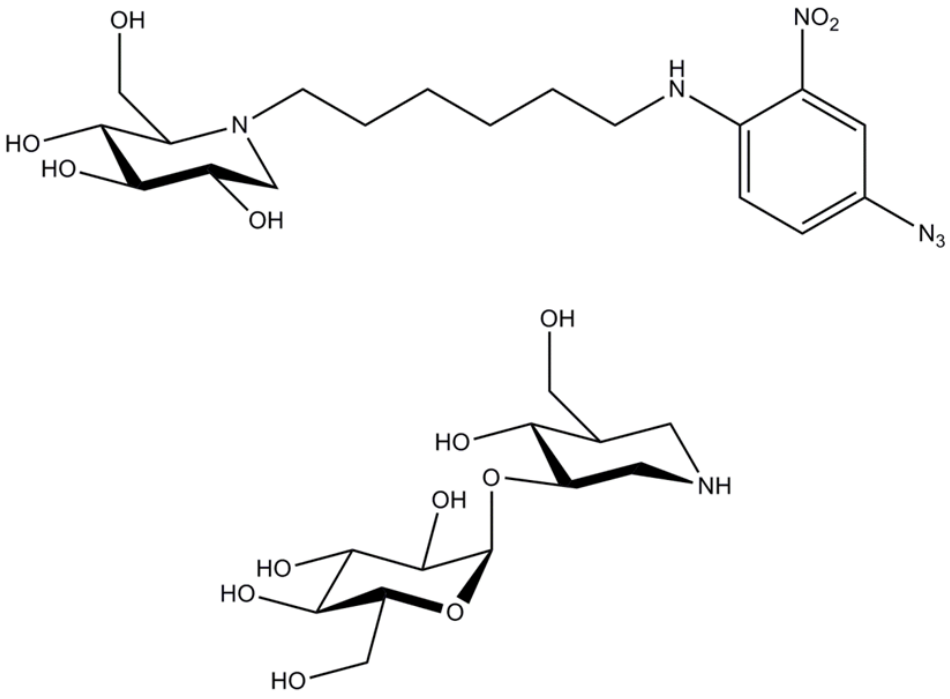

Figure 4.1 - Structures of NAP-DNJ (top) and GlcIFG (bottom).

4.2 Material and Methods

4.2.1 Materials

NAP-DNJ was provided by Dr. Marvin J.-R. Lee (University of Oxford), synthesised according to previously published methods (Rawlings *et al*, 2009). GlcIFG was kindly provided by Dr. Spencer Williams (University of Melbourne). Kifunensine was purchased from Sigma-Aldrich. Compounds were dissolved in DMSO (Sigma-Aldrich) as 1000x stock solutions, resulting in a final concentration of 0.1% DMSO for inhibitor treatment.

4.2.2 Cell culture

MDBK cells were cultured as described in Chapter 2. BVDV-1 (cytopathic NADL strain) was provided by Professor Nicole Zitzmann (Oxford Glycobiology Institute, University of Oxford, UK). MDBK cells were verified to be free from BVDV contamination by RT-PCR.

4.2.3 Cell proliferation assay

Cell proliferation of MDBK cells in the presence of NAP-DNJ, GlcIFG and kifunensine was determined by MTS assay, as described in Chapter 2. Briefly, cells were incubated with compound for 24 h, before a 20:1 mix of MTS:PMS solution was added. After 2 h, formation of formazan product was measured by absorbance at 490 nm. Samples were analysed in triplicate, and CC_{50} values were calculated relative to 0.1% DMSO-treated controls, using non-linear regression analysis.

4.2.4 Carbohydrate analysis

Free oligosaccharide (FOS) analysis of MDBK cells treated with NAP-DNJ and/or GlcIFG for 24 h was performed, with FOS purified, labelled and analysed as described in Chapter 2. Inhibitor treatments were performed in triplicate, with the

amounts of $Man_5GlcNAc_1$, $Glc_1Man_5GlcNAc_1$, $Glc_3Man_5GlcNAc_1$, $Glc_1Man_7GlcNAc_2$ and $Glc_3Man_7GlcNAc_2$ measured, relative to protein concentration or $Man_4GlcNAc_1$ levels, which remained constant for all treatments. Protein concentrations were determined by standard bicinchoninic acid assay, calibrated against a BSA (Sigma-Aldrich) standard curve.

4.2.5 BVDV infection

MDBK cells were infected with BVDV and used for analysis by Western blot, RT-PCR and fluorescence focus-forming assay (FFA). For Western blot analysis of intracellular BVDV proteins, MDBK cells were seeded in 6-well plates and infected with BVDV (MOI = 5 to ensure infection of all cells) for 1 h at 37°C. Viral media was then removed and cells washed with PBS, then incubated for 12 h with NAP-DNJ at different concentrations. After 12 h, cells were harvested, washed with ice-cold PBS and centrifuged for 5 m (1000 x g), before being frozen at -20°C. After thawing and resuspension in 500 µl PBS, cell pellets were lysed by sonication (20 s, 50% duty cycle; Branson Sonifier S500A) and prepared for SDS-PAGE. For Western blot analysis of secreted BVDV proteins, MDBK cells were seeded in 25 cm^2 flasks and infected with BVDV (MOI=1). Cells were washed as above, then incubated for 24 h with NAP-DNJ, GlcIFG or kifunsensine at different concentrations. Cell supernatants were collected, clarified by centrifugation (5 m, 1000 x g), then frozen at -20°C. After thawing, virions were lysed by sonication and prepared for either enzyme digestion or SDS-PAGE.

For RT-PCR and FFA analysis, MDBK cells were seeded in 24-well plates and infected with BVDV (MOI=1) for 1 h. After washing with PBS, cells were incubated with NAP-DNJ, GlcIFG or kifunensine in 500 µl complete media for 24 h. Media was

collected and clarified as above, and 140 µl taken for RT-PCR analysis. The remainder was serially diluted in RPMI media for subsequent infection of naive cells for FFA analysis.

4.2.6 Endoglycosidase treatments

Viral lysates were digested with glycosidases endoglycosidase H (Endo H; New England Biolabs; 500 units/sample) and endomannosidase (1 µg/sample) to identify changes to viral glycoprotein glycosylation. Aliquots were incubated with either water or enzyme for 24 h at 37°C, then separated by SDS-PAGE and analysed by Western blot.

4.2.7 Western blot analysis

Cell lysates and viral lysates were separated by 8% SDS-PAGE. Proteins were then transferred to Immobilon-P membrane (Millipore) by electrophoresis (74 mA, 1 h). Membranes were then blocked overnight at 4°C in 5% milk, 0.1% Tween20 (Sigma-Aldrich) in PBS [blocking solution]. This was followed by incubation with primary antibody diluted in blocking solution for 1 h, washed in 0.1% Tween20 in PBS [washing solution], then incubated with secondary HRP-conjugated antibody for another 1 h. Proteins were visualised by chemiluminescence using ECL Western Blotting Substrate (Pierce Biotechnology) and Amersham Hyperfilm MP (GE Healthcare). Where necessary, membranes were stripped of antibodies by incubation with a low pH solution [15% (w/v) glycine, 0.1% SDS (w/v), 1% Tween 20, pH 2.2] for 2 h, washed with washing solution then blocked overnight in blocking solution. Membranes were then reprobed with antibodies as described above.

Monoclonal antibodies MAb214 and MAb160 (Animal Health Veterinary Laboratories Agency, Weybridge, UK) were used to probe BVDV E2 and NS2/3 respectively (1

µg/ml). Anti-GAPDH polyclonal antibody (Sigma-Aldrich) was used to probe GAPDH. Anti-rabbit and anti-mouse HRP-conjugated secondary antibodies were purchased from Dako UK Ltd, Ely, UK.

4.2.8 Viral titre determination by RT-PCR

Following inhibitor treatment of BVDV-infected MDBK cells, viral RNA was extracted from clarified cell supernatant using a QIAamp viral RNA purification kit (QIAgen, Crawley, UK), according to the manufacturer's instructions, to give 50 µl RNA per sample. Samples were incubated with DNase (37°C for 30 m, then 80°C for 15 m to inactivate) to remove trace DNA. Real-time RT-PCR was carried out using a SYBR green Quantitect RT-PCR kit (QIAgen), with primers that amplified a 334-bp portion of the NS2-coding sequence (forward primer, 5'-AGA AAA CAC AGA AAC CCG ACA GAC-3'; reverse primer, 5'-TTC CAC CAC TAT TGT AGC ATC CG-3'). An Opticon 2 real-time PCR machine (Bio-Rad) was used to carry out the following reactions: 30 m initial incubation at 50°C followed by 15 m at 95°C, then 35 cycles of 15 s at 95°C, 1 m at 50°C, and 1 m at 72°C, before a final extension for 7 m at 72°C. Internal standards prepared from a highly concentrated BVDV stock were used to generate standard curves to titre viral RNA.

4.2.9 Fluorescence focus-forming assay

Following inhibitor treatment of BVDV-infected MDBK cells, clarified cell supernatant was serially diluted (eight 10-fold dilutions) and used to infect naive MDBK cells in 96-well plates. After a 1 h infection period, viral inoculum was removed and replaced with fresh RPMI media. After 16 h overnight incubation to allow virus replication to occur, cells were washed with ice-cold PBS twice and fixed with 4% (v/v) paraformaldehyde (30 m, rt). Cells were washed again with PBS, then blocked with

blocking solution for 2 h. Cells were then permeabilised with 1% Triton-X-100 in PBS (20 m, rt), washed with 1% Tween20 in PBS, and then incubated with primary monoclonal antibody MAb103/105 (2 µg/ml in blocking solution, 1 h, rt; AHVLA). After washing again in Tween20-PBS, cells were incubated with Alexa Fluor® 488 Goat Anti-Mouse IgG (H+L) Antibody (2 µg/ml in blocking solution, 1 h, rt, dark; Life Technologies, Thermo Fisher Scientific, Paisley, UK). Cells were then washed again with Tween20-PBS, nuclei stained with DAPI and viewed using a inverted Nikon Eclipse TE200-U microscope, equipped with a Fluor 10X objective lens, and FITC and UV filter sets. Fluorescent foci were counted, and virus titres (focus forming units (FFU)/ml) calculated.

All assays were carried out on at least three independent occasions and data shown is representative of at least three experiments.

4.3 Results

4.3.1 NAP-DNJ inhibits ER α-glucosidases in MDBK cells

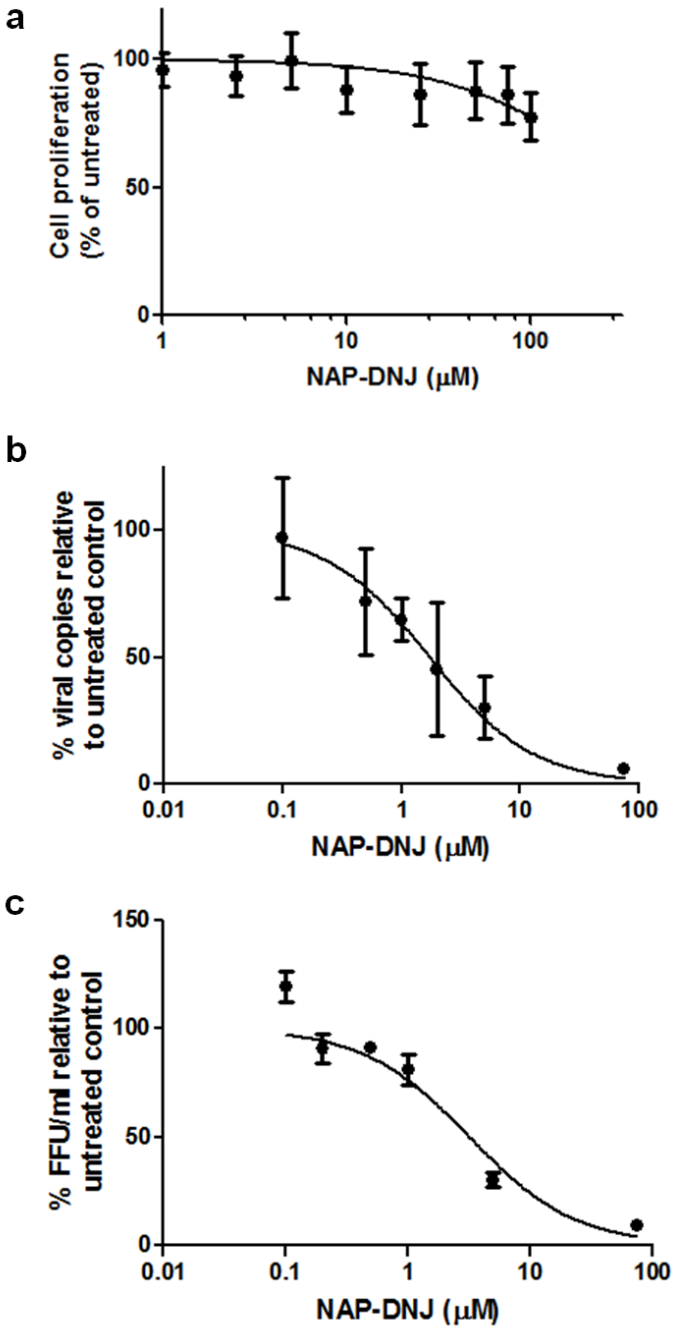

Figure 4.2 – NAP-DNJ inhibits BVDV replication. (a) MTS-based cell proliferation assay. MDBK cells were incubated with NAP-DNJ for 24 h, then incubated with MTS/PMS and absorbance at 490 nm measured, normalised to DMSO-treated control. (b) MDBK cells were infected with BVDV (MOI = 1) and incubated with NAP-DNJ for 24 h. Viral RNA was then extracted from progeny virus and quantified by RT-PCR. Error bars indicate standard deviation of samples ran in triplicate. (c) MDBK cells were infected with BVDV (MOI=1) and incubated with NAP-DNJ for 24 h. Virus progeny was harvested and serially diluted for fluorescence focus-forming assay. Viral infection was detected using anti-BVDV NS2/3 antibody WB103/105.

In vitro inhibition of α-glucosidases I and II by NAP-DNJ has been demonstrated previously, together with *in cellulo* inhibition in HL60 cells (Rawlings *et al*, 2009). In order to study the effects of NAP-DNJ on BVDV, first the effects on cell proliferation and *in cellulo* inhibition of α-glucosidases in MDBK cells were assessed. MDBK cells were incubated with up to 100 μM NAP-DNJ for 24 h. The effect of NAP-DNJ on cell proliferation was then determined by addition of MTS/PMS solution, measuring absorbance at 490 nm after 2 h incubation. No significant effect of NAP-DNJ was observed on cell proliferation up to 75 μM treatment (CC_{50} >> 100 μM; Figure 4.2a).

Imino sugars that inhibit α-glucosidases have previously been shown to be antiviral against BVDV (Branza-Nichita *et al*, 2001). The antiviral effect of NAP-DNJ against BVDV was investigated by quantifying virus secreted from BVDV-infected MDBK cells incubated with NAP-DNJ (Figure 4.2b). NAP-DNJ reduced BVDV secretion in a concentration-dependent manner, with an IC_{50} of 1.75 ± 0.47 μM. A similar reduction was observed in infectivity (Figure 4.2c).

MDBK cells were then incubated with up to 75 μM NAP-DNJ for 24 h and harvested for FOS analysis. FOS were purified, labelled with 2-AA and analysed by NP-HPLC. Treatment with low concentrations of NAP-DNJ (up to 1 μM) exclusively produced monoglucosylated FOS species, such as $Glc_1Man_5GlcNAc_1$, due to α-glucosidase II inhibition only (Figure 4.3). At higher concentrations, inhibition of α-glucosidase I was also observed, with the accumulation of triglucosylated species such as $Glc_3Man_5GlcNAc_1$ and $Glc_3Man_7GlcNAc_2$.

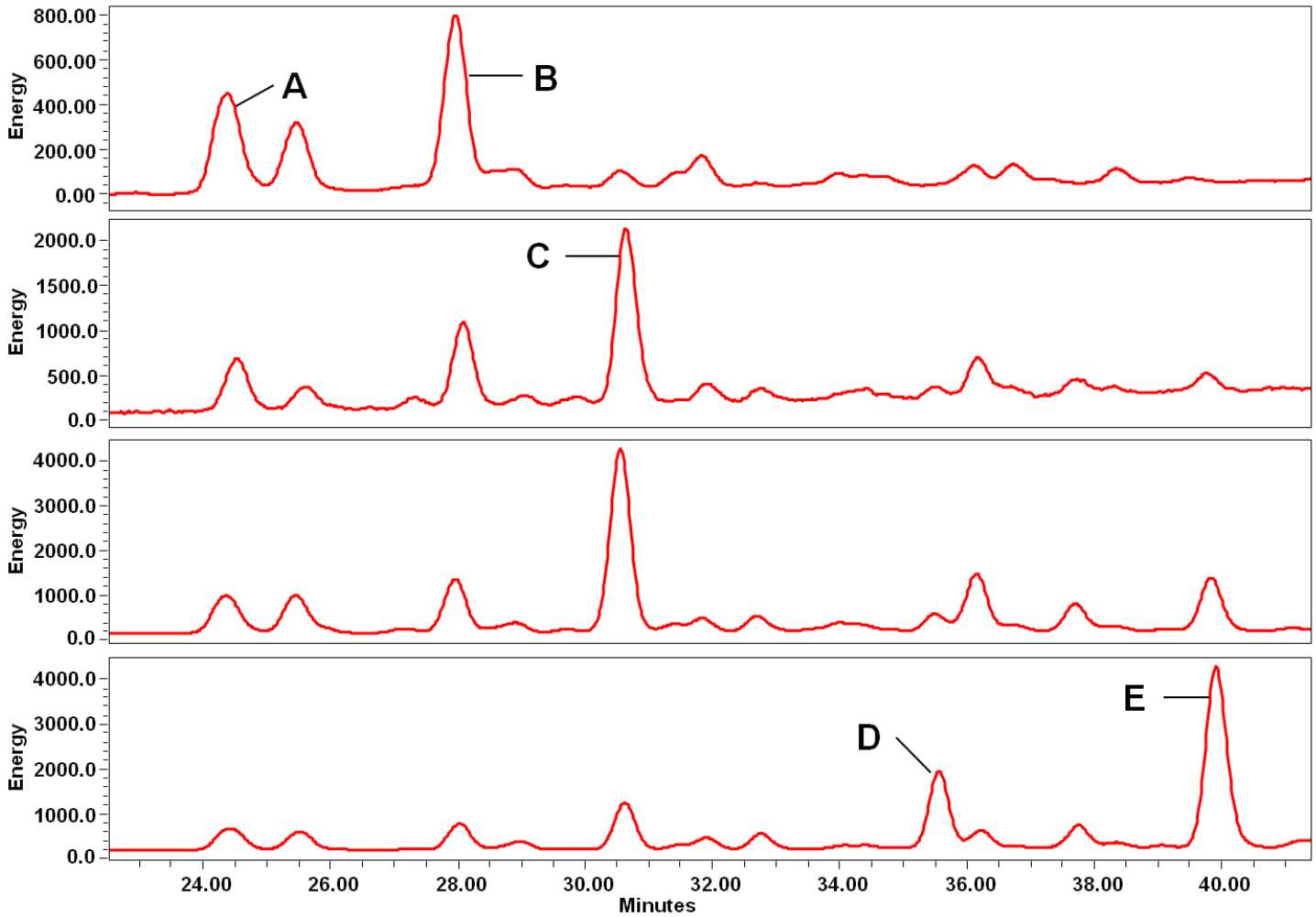

Figure 4.3 – Representative HPLC profiles of FOS analysis of MDBK cells treated with NAP-DNJ. MDBK cells were incubated with (from top) either DMSO, 1 μM, 5 μM or 75 μM NAP-DNJ for 24 h. FOS were then purified from lysed cells, labelled with 2-anthranilic acid and analysed by NP-HPLC. A – $Man_4GlcNAc_1$. B – $Man_5GlcNAc_1$. C – $Glc_1Man_5GlcNAc_1$. D – $Glc_3Man_5GlcNAc_1$. E – $Glc_3Man_7GlcNAc_2$.

4.3.2 Inhibition of α-glucosidases by NAP-DNJ results in specific degradation of BVDV glycoproteins

To further characterise the effect of α-glucosidase inhibition on BVDV, the level and glycosylation of the envelope protein E2 were analysed by Western blotting (Figure 4.4a). Following infection of MDBK cells with BVDV and incubation with up to 75 μM NAP-DNJ for 24 h, an increase in apparent molecular weight of E2 and the heterodimer E1E2 was detected by Western blotting, indicating increased glucosylation of intracellular viral glycans due to α-glucosidase inhibition. In addition to this, the band intensity of E2 and E1E2 were measured by densitometry, normalised to GAPDH intensity, and compared to NS2/3 (Figure 4.4b). With increasing concentration of NAP-DNJ up to 20 μM, specific degradation of the glycoprotein heterodimer E1E2 is observed, whilst amount of NS2/3 remains constant. Treatment with 20 μM NAP-DNJ resulted in a greater than 50% reduction in amount of E1E2, whilst NS2/3 levels remained unaffected. At higher concentrations, a reduction in amount of NS2/3 was also observed.

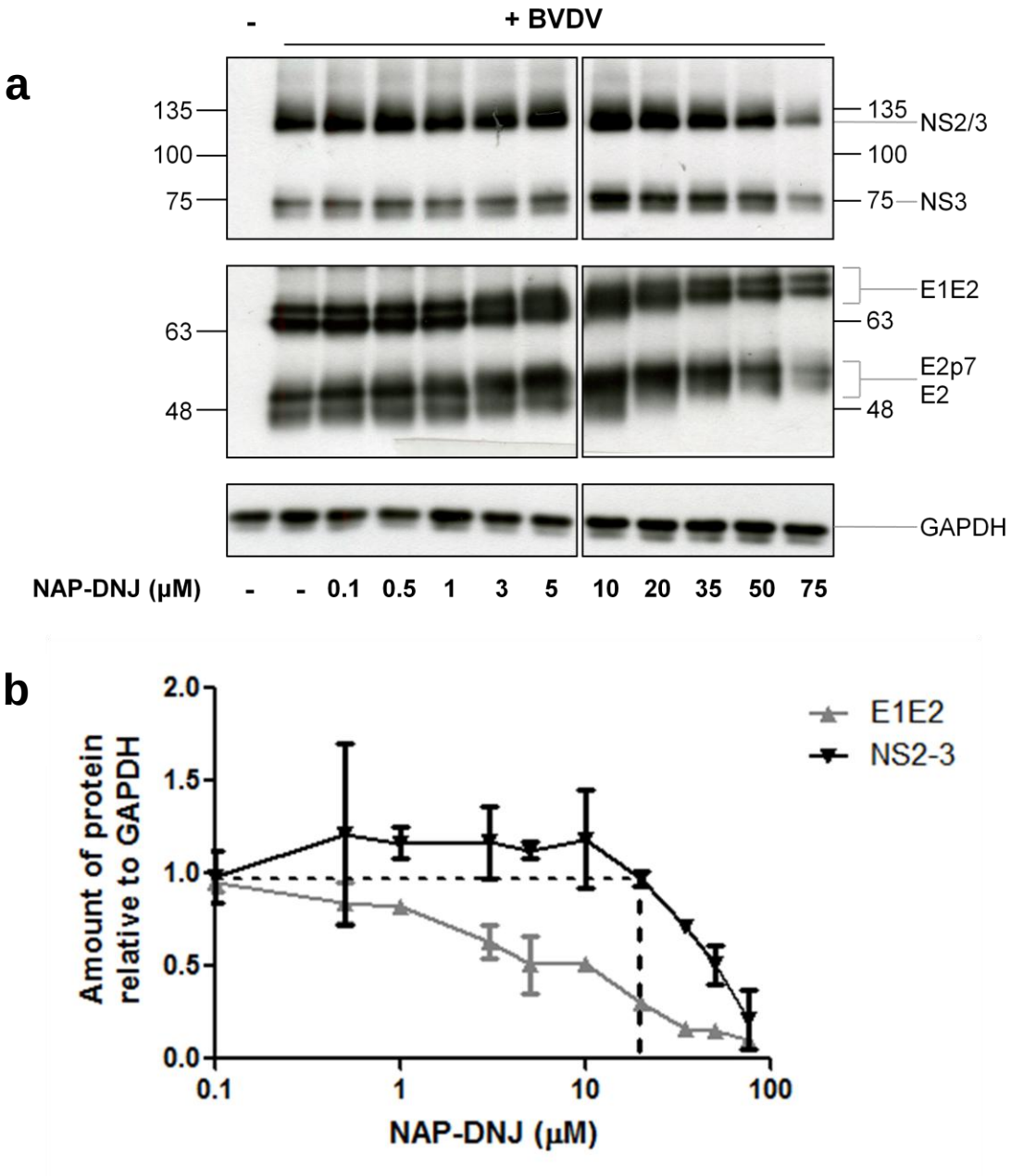

Figure 4.4 – NAP-DNJ prevents deglucosylation of BVDV E2, targeting it for degradation. MDBK cells were infected with BVDV and incubated with up to 75 µM NAP-DNJ for 24 h. Cells were lysed and proteins separated by SDS-PAGE. Proteins were analysed by Western blotting using antibodies against BVDV E2 (MAb214), NS2/3 (MAb160) and GAPDH. Band intensities were measured by scanning blots and measuring by densitometry using ImageJ (NIH). Error bars show standard deviation of three independent samples.

4.3.3 NAP-DNJ prevents complex glycan formation in secreted virions

Virion-associated E2 protein displays partial resistance to Endo H digestion, indicating glycoprocessing in the Golgi apparatus and formation of complex glycans (Jordan *et al*, 2002), whilst treatment with imino sugars has been shown to inhibit complex glycan formation in BVDV (Jordan *et al*, 2002). The effect of NAP-DNJ on glycosylation in virion-associated E2 was investigated by Western blot analysis of viral lysates using a monoclonal antibody, WB214, specific for BVDV E2. NAP-DNJ treatment reduced secretion of virion-associated E2 (Figure 4.5a). A decrease in electrophoretic mobility was also observed. To further investigate this apparent change in mobility, viral lysates were digested with endoglycosidase H (Endo H; Figure 4.5b) and recombinant endomannosidase (Figure 4.5c). High mannose and hybrid glycans are removed by Endo H, but complex glycans are insensitive to digestion. As expected, E2 protein is partially digested by Endo H, indicating a mixed population of complex and non-complex glycans. Treatment with the mannosidase inhibitor kifunensine, which prevents complex glycan formation, results in complete digestion by Endo H. Endo H sensitivity increases in a concentration-dependent manner following NAP-DNJ treatment. With 1 μM NAP-DNJ, where exclusive α-glucosidase II inhibition is observed, no change to Endo H sensitivity is detected. At higher concentrations, where α-glucosidase I inhibition also occurs, sensitivity increases and at 75 μM, E2 appears completely sensitive to Endo H digestion.

To determine whether virion-associated E2 glycans display a glucose cap, viral lysates were digested with recombinant endomannosidase, which cleaves glycans internally between glucose-substituted mannose and the remainder of the oligosaccharide. At higher concentrations of NAP-DNJ, removal of the glucose cap by endomannosidase can be seen by Western blot (Figure 4.5c).

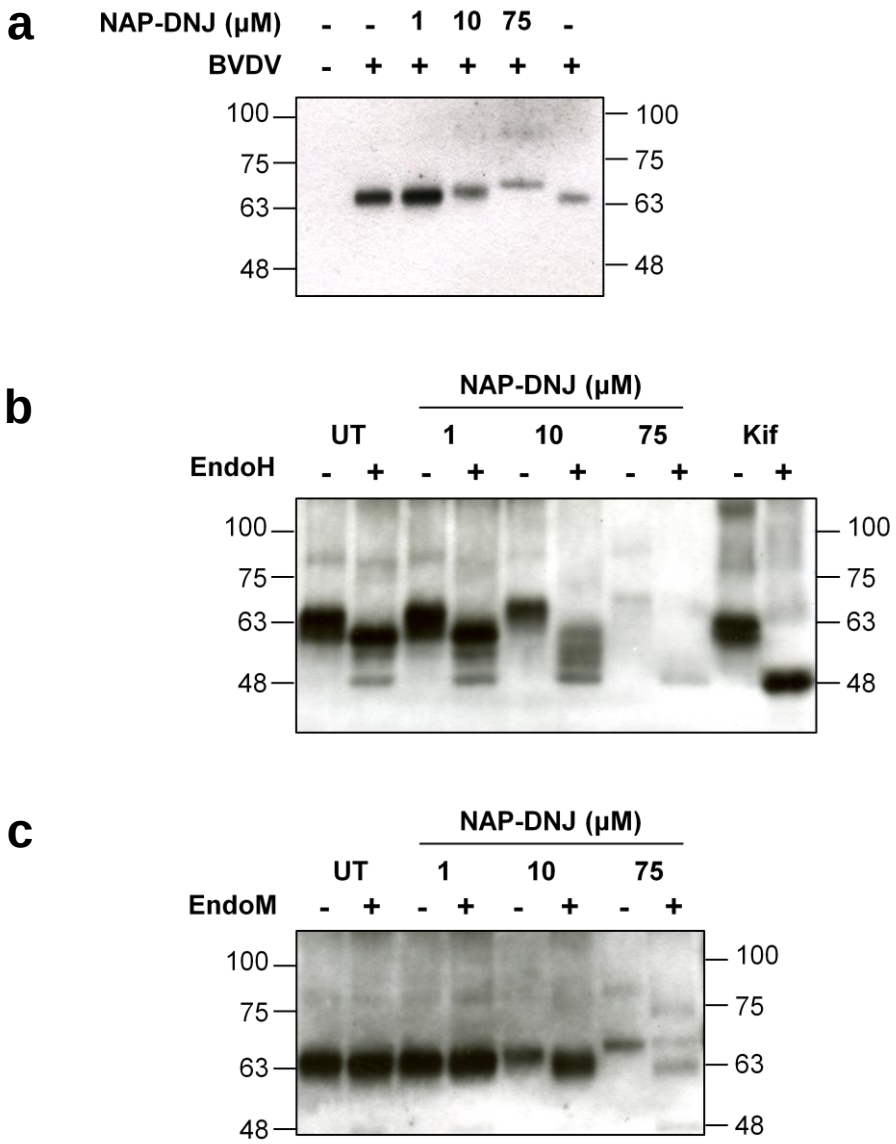

Figure 4.5 – NAP-DNJ alters BVDV E2 glycosylation in secreted virions. MDBK cells were infected with BVDV and treated with NAP-DNJ or 10 μM kifunensine (Kif) for 24 h. Virus progeny was concentrated and lysed, then analysed by Western blot (a). Viral lysates were also digested for 24 h with either Endo H (b) or endomannosidase (Endo M; c), then analysed by Western Blot. Anti-BVDV E2 antibody MAb214 was used following SDS-PAGE under non-reducing conditions.

4.3.4 GlcIFG inhibits endomannosidase in MDBK cells

Golgi endo-α-mannosidase provides an alternative processing pathway for achieving complex glycan formation distinct from ER α-glucosidase action. Endomannosidase cleaves internally between the glucose-substituted mannose and the remainder of the glycan to remove the glucose cap, negating the need for processing by α-glucosidases and allowing the glycan to progress through further processing steps to a complex form.

Inhibition of α-glucosidase II alone with low concentrations of NAP-DNJ was insufficient to prevent complex glycan formation, suggesting the possible involvement of endomannosidase in overcoming this blockage to the glycan processing pathway. As such, the effect of inhibiting endomannosidase, both alone and in combination with low concentrations of NAP-DNJ was investigated.

First, the effect of the endomannosidase inhibitor GlcIFG on cell proliferation was determined (Figure 4.6). GlcIFG had no significant effect on proliferation up to 1 mM in concentration.

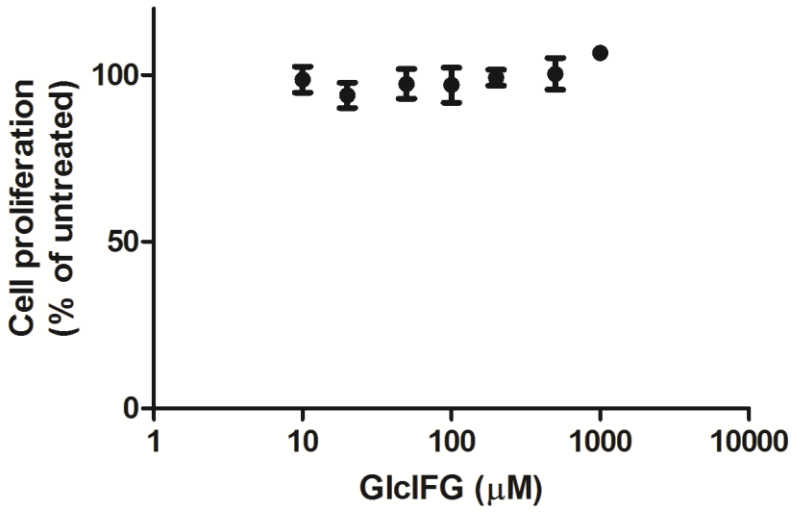

Figure 4.6 - Effect of GlcIFG on MDBK cell proliferation. MDBK cells were incubated with GlcIFG (up to 1 mM) for 24 h, then incubated with MTS/PMS and absorbance at 490 nm measured, normalised to DMSO-treated control. Error bars indicate standard deviation of three independent samples.

Inhibition of endomannosidase with GlcIFG was investigated *in cellulo* by FOS analysis of MDBK cells following treatment with GlcIFG and/or NAP-DNJ for 24 h. FOS were purified from cell lysates, labelled with 2-AA and separated by NP-HPLC (Figure 4.7). Two distinct pools of FOS can be identified. The first possess a single GlcNAc residue at the reducing terminus of the oligosaccharide and are derived from the cytosol, having been processed by cytosolic ENGase. The second possess a dual GlcNAc core and are localised to the ER and not subjected to ENGase activity. As previously discussed, inhibition of α-glucosidase II causes an accumulation of both cytosolic and ER-localised monoglucosylated FOS. Cotreatment of MDBK cells with NAP-DNJ and GlcIFG resulted in a specific increase in ER-localised FOS $Glc_1Man_7GlcNAc_2$, relative to $Man_4GlcNAc_1$ and $Glc_1Man_5GlcNAc_1$ (Figure 4.8). This increase in monoglucosylated FOS accumulating in the ER compartment, that result from misfolded glycoproteins being retrotrafficked from the Golgi, indicates inhibition of endomannosidase. In the absence of α-glucosidase inhibition, GlcIFG treatment

results in a small yet significant increase in $Glc_1Man_7GlcNAc_2$, suggesting that endomannosidase processing in MDBK cells is a relatively minor, yet active route for deglucosylation of glycans when α-glucosidase processing is uninterrupted.

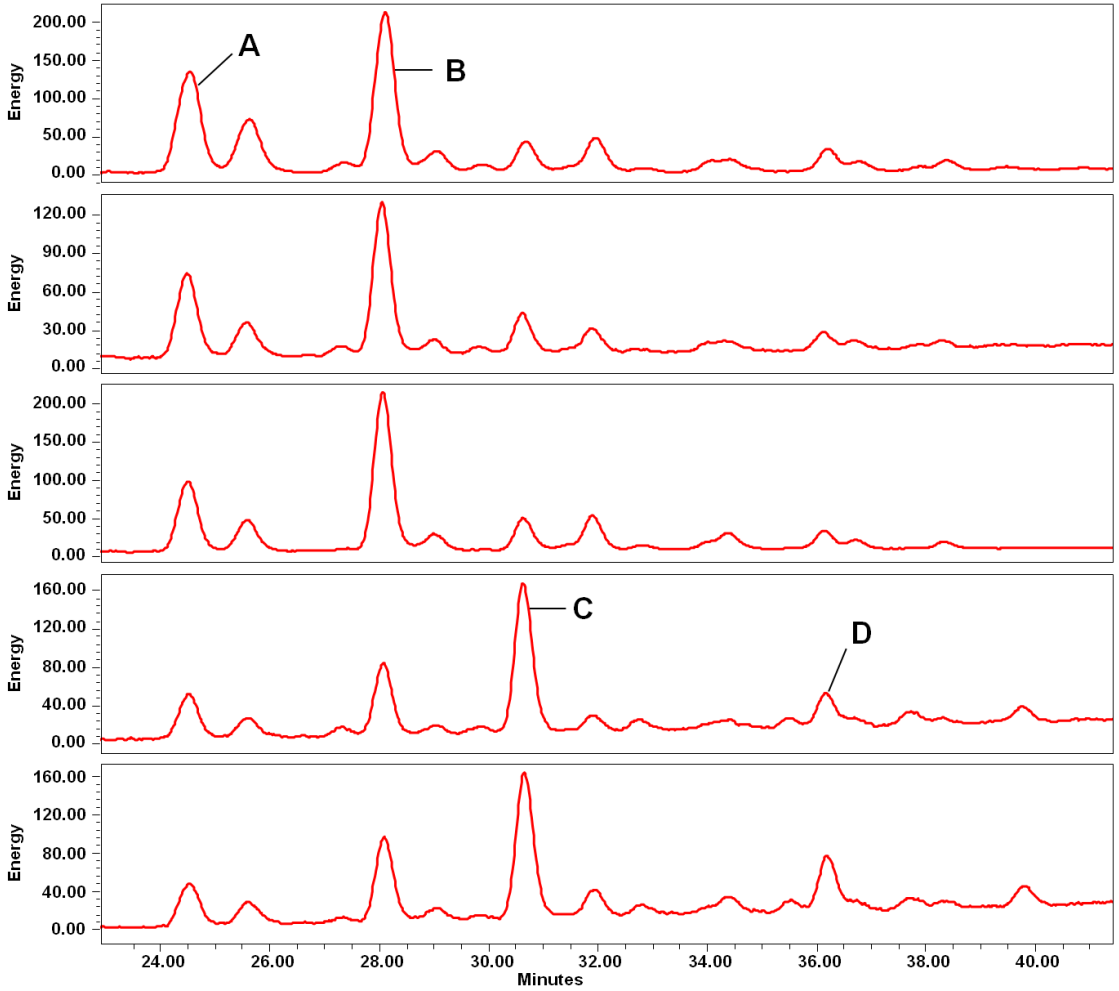

Figure 4.7 - Representative HPLC profiles of FOS analysis of MDBK cells treated with GlcIFG and NAP-DNJ. MDBK cells were either mock-infected (row 1) or infected with BVDV (MOI = 1; rows 2-5), and treated with DMSO (rows 1 and 2), 1 mM GlcIFG (row 3), 1 μM NAP-DNJ (row 4) or both 1 mM GlcIFG and 1 μM NAP-DNJ (row 5) for 24 h. FOS were purified from lysed cells, labelled with 2-AA and analysed by NP-HPLC.
A – $Man_4GlcNAc_1$. B – $Man_5GlcNAc_1$. C – $Glc_1Man_5GlcNAc_1$. D – $Glc_3Man_5GlcNAc_1$.

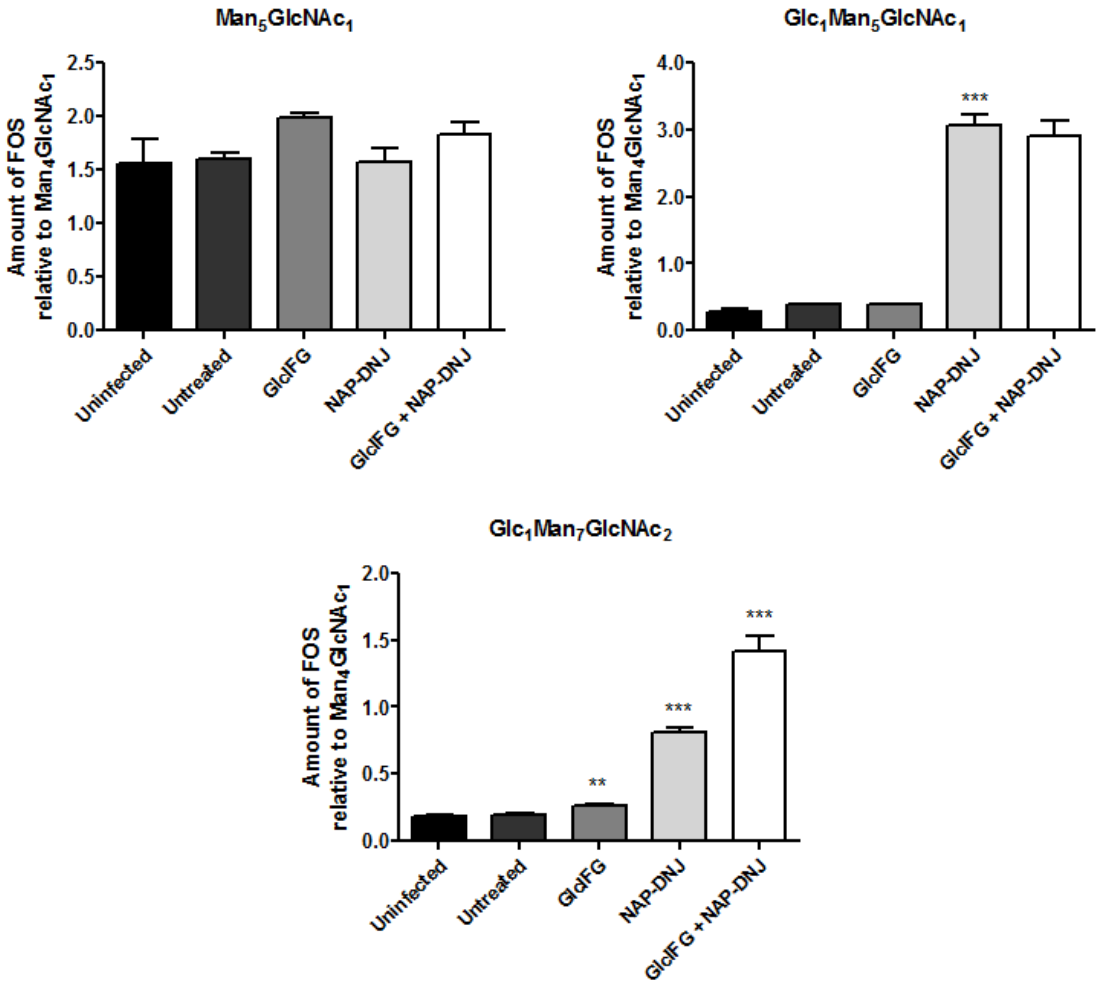

Figure 4.8 – Free oligosaccharide (FOS) analysis of MDBK cells. MDBK cells infected with BVDV and incubated with DMSO, 1 mM GlcIFG and/or 1 μM NAP-DNJ for 24 h. FOS were then purified from cells and separated by NP-HPLC. Amounts of each FOS species were normalised to levels of $Man_4GlcNAc_1$, which remained constant for all treatments. Error bars indicate standard deviation. ** $p<0.01$; *** $p<0.001$, student's t-test.

4.3.5 Inhibition of endomannosidase prevents complex glycan formation

The effect of endomannosidase inhibition on the glycosylation of virion-associated E2 protein was examined by Western blot analysis of E2 following digestion of viral lysates with Endo H and endomannosidase (Figure 4.9). GlcIFG treatment, both alone and in combination with NAP-DNJ treatment, caused a slight increase in electrophoretic mobility of E1E2 heterodimer (Figure 4.9a). This difference is further clarified by Endo H digestion of viral lysates. Endomannosidase inhibition by GlcIFG resulted in a marked increase in sensitivity to Endo H digestion, indicating a reduction in complex glycan formation, even in the absence of α-glucosidase inhibition (Figure 4.9b). Virion-associated E2 from cells incubated with GlcIFG were confirmed to contain monoglucosylated glycans by endomannosidase digestion, which caused a small decrease in apparent molecular weight of E1E2 heterodimer, corresponding to the release of glucose-substituted mannose residues from the glycoprotein (Figure 4.9c).

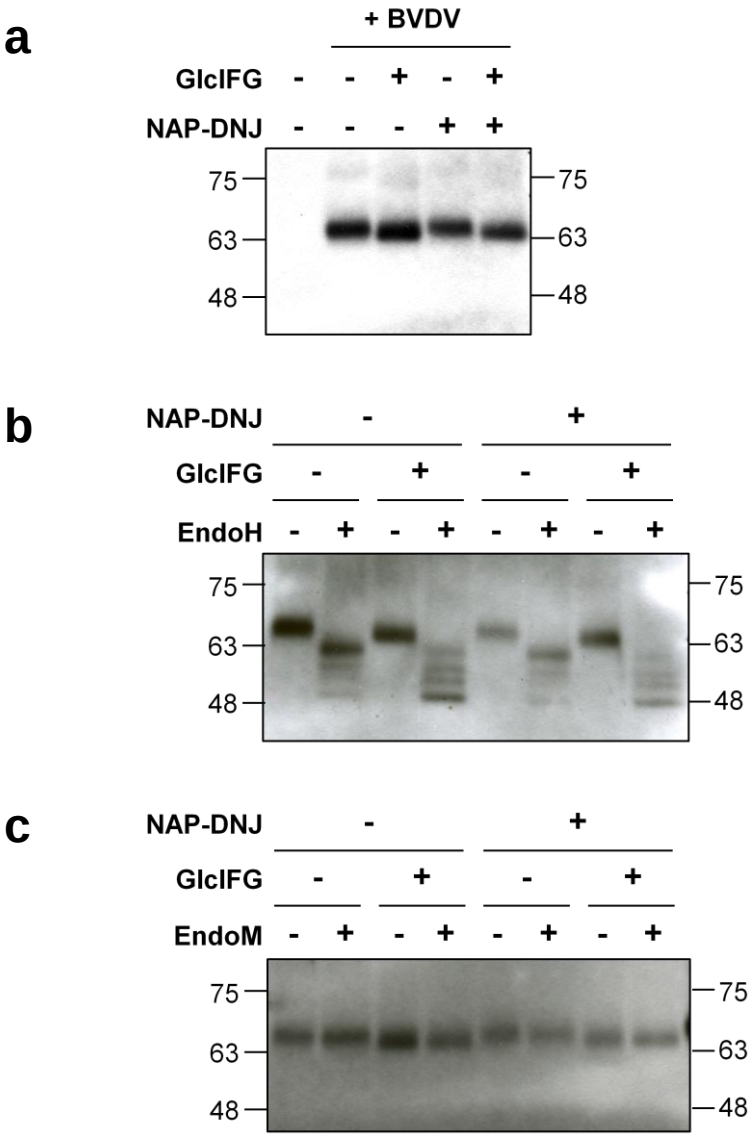

Figure 4.9 - Glycan analysis of BVDV E2 following endomannosidase inhibition. MDBK cells were infected with BVDV and incubated with 1 mM GlcIFG and/or 1 μM NAP-DNJ for 24 h. Secreted virions were concentrated and lysed, and subjected to enzyme digestion and Western blotting analysis. (a) Virion-associated E2 following GlcIFG and/or NAP-DNJ treatment. (b) Viral lysates digested with Endo H for 24 h, then probed for E2. (c) Viral lysates digested with endomannosidase (Endo M), then probed for E2. Monoclonal anti-E2 WB214 antibody was used.

4.3.6 Antiviral activity of GlcIFG

To determine whether endomannosidase inhibition in combination with glucosidase inhibition would have an antiviral effect on BVDV, virus progeny was collected from BVDV-infected MDBK cells incubated with GlcIFG and/or NAP-DNJ and used for fluorescence focus-forming assay (FFA) (Figure 4.10). GlcIFG treatment alone showed an antiviral effect (IC_{50} = 531.3 ± 74.5 µM), and enhanced the antiviral effect observed from α-glucosidase II inhibition (1 µM NAP-DNJ vs. 1 µM NAP-DNJ with 1 mM GlcIFG; two-tailed student's t-test, p=0.0038).

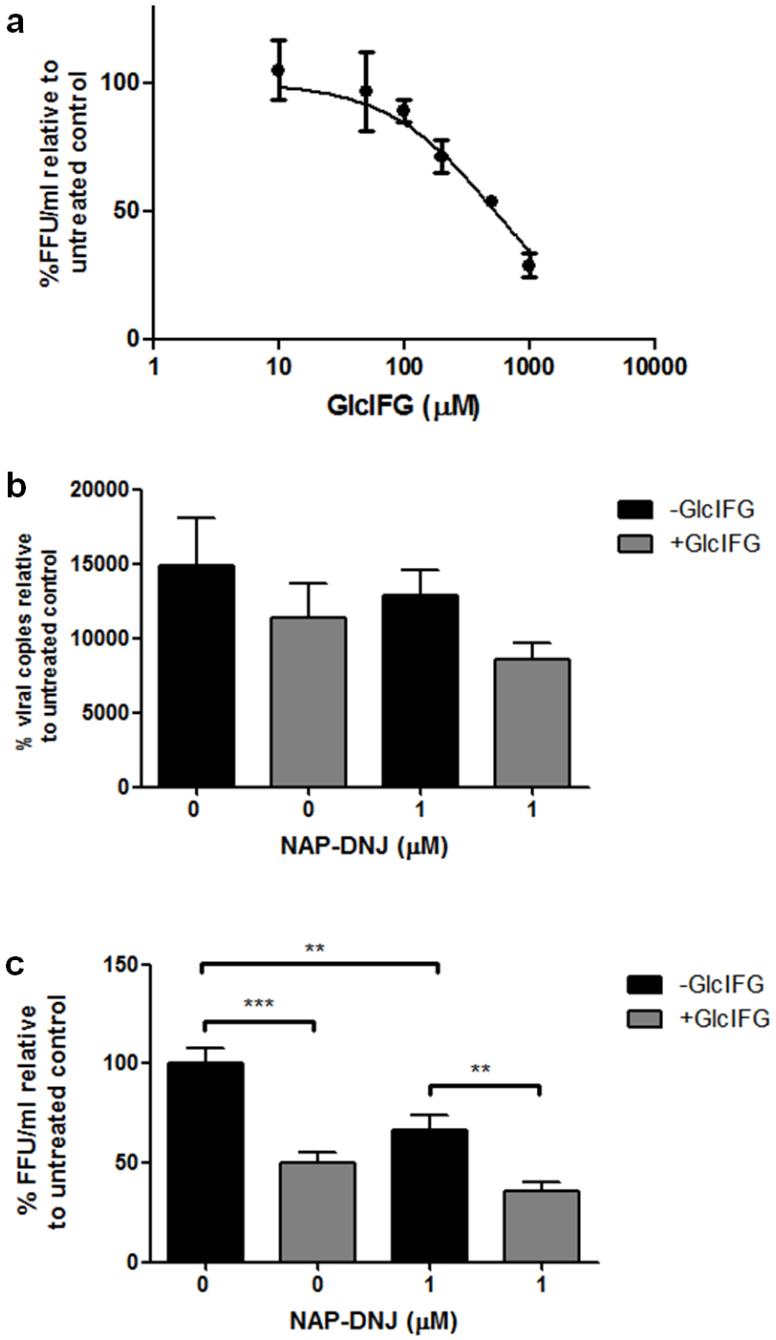

Figure 4.10 – Antiviral activity of GlcIFG. (a) MDBK cells were infected with BVDV (MOI=1) and incubated with GlcIFG for 24 h. Virus progeny was harvested and serially diluted for fluorescence focus-forming assay. Viral infection was detected using anti-BVDV NS2/3 antibody WB103/105. (b) MDBK cells were infected with BVDV (MOI = 1) and incubated with 1 mM GlcIFG and/or 1 μM NAP-DNJ for 24 h. Viral RNA was then extracted from progeny virus and quantified by RT-PCR. Error bars indicate standard deviation of samples ran in triplicate. (c) Fluorescence focus-forming assay following treatment with GlcIFG and/or NAP-DNJ. Focus-forming units (FFU) were normalised to virus from DMSO-treated controls. Error bars indicate standard deviation of three replicates. ** $p<0.01$, *** $p<0.001$, two-tailed student's t-test.

4.3.7 Kifunensine treatment reduces BVDV infectivity

With the antiviral effect of GlcIFG correlating with the loss of complex glycans on viral glycoproteins, it was subsequently investigated whether inhibition of complex glycan formation alone, by kifunensine treatment, would be sufficient to induce an antiviral effect. The effect of kifunensine on cell proliferation was first investigated, as well as the effect of kifunensine treatment on BVDV E2 glycans across a range of concentrations (Figure 4.11). No effect on cell proliferation was observed up to 100 μM (CC_{50} >> 200 μM). Treatment of BVDV-infected MDBK cells for 24 h with 1 μM kifunensine was sufficient to fully sensitise BVDV E2 glycans to Endo H digestion (Figure 4.11b). At 0.1 μM, a marginal increase in Endo H sensitivity was observed. Subsequently, the effect of kifunensine treatment on BVDV infectivity was investigated across these concentrations (Figure 4.12). Treatment with 1 μM kifunensine was sufficient to reduce BVDV infectivity, assayed by focus-forming assay, by approximately 50% (Figure 4.12a). Increasing kifunensine up to 50 μM did not result in any further enhancement of antiviral activity. Treatment with 0.1 μM kifunensine, which induces only a minor glycan alteration to BVDV E2, had no significant antiviral effect compared to untreated control. The effect on viral production and secretion was determined by RT-PCR quantification of viral RNA copies (Figure 4.12b). No reduction in viral secretion was observed up to 10 μM kifunensine, indicating the antiviral effects observed are a result of decreased infectivity of progeny virus.

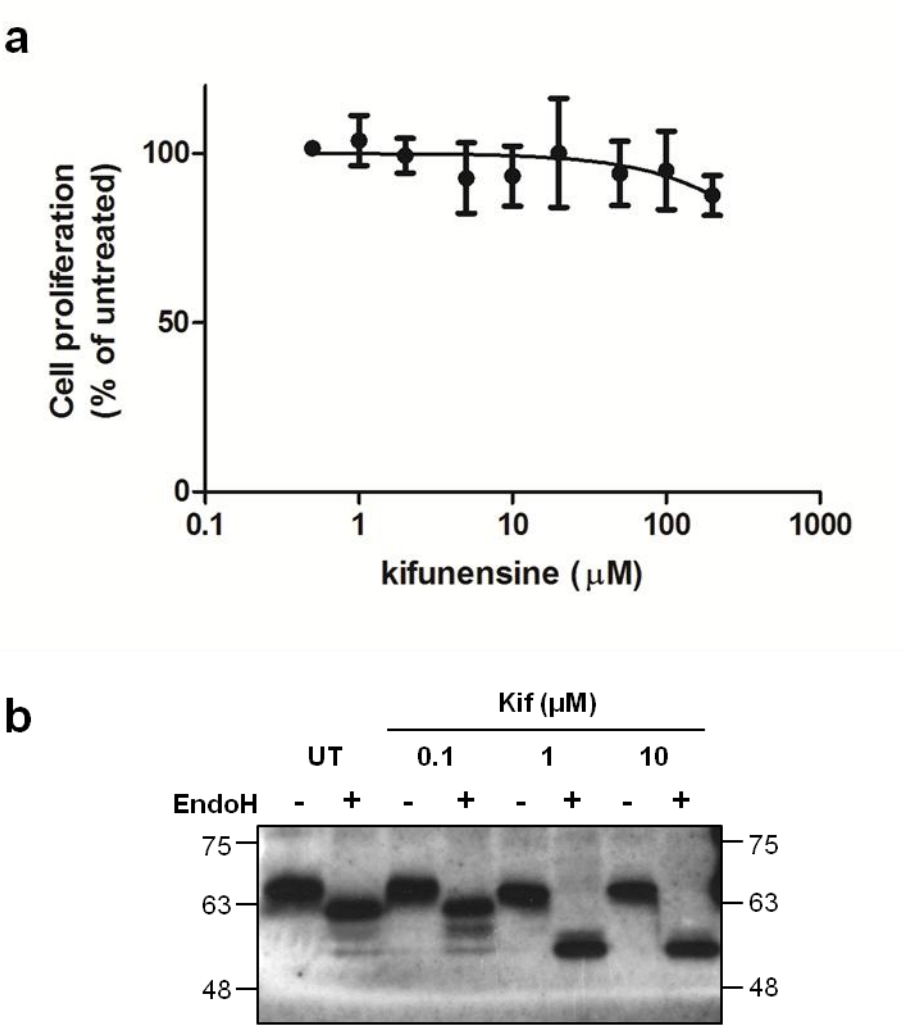

Figure 4.11 – (a) Effect of kifunensine on cell proliferation. MDBK cells were incubated with kif at different concentrations for 24 h, then assayed for effects on cell proliferation using MTS. Error bars indicate standard deviation. (b) Effect of kifunensine (Kif) on BVDV E2 glycoprotein. MDBK cells were infected with BVDV (MOI = 1) and incubated with kifunensine for 24 h. Viral progeny were collected, lysed and incubated with water or Endo H for 24 h to digest non-complex glycans. Digests were separated by SDS-PAGE under non-reducing conditions and then probed by Western blot for BVDV E2, using monoclonal antibody MAb214.

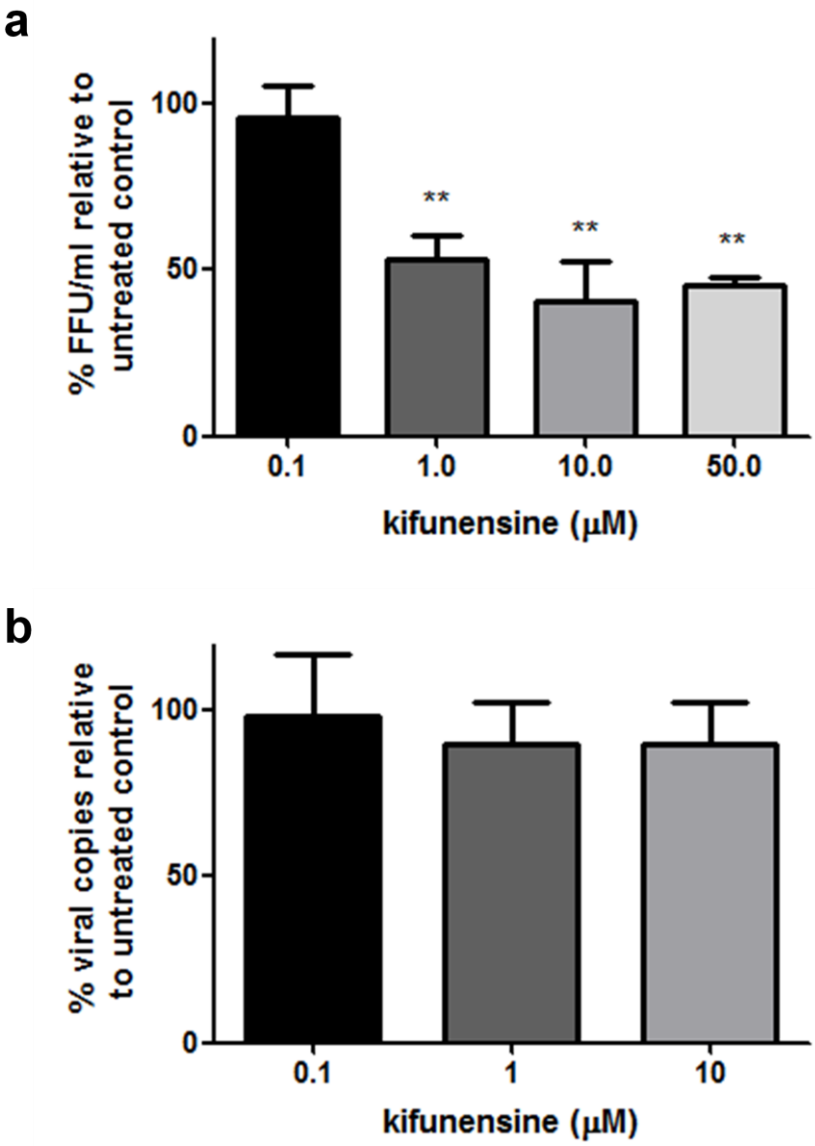

Figure 4.12 – Antiviral effects of kifunensine treatment. MDBK cells were infected with BVDV and incubated with kifunensine for 24 h. Viral progeny was then collected and assayed by focus-forming assay (a) and RT-PCR (b). Error bars indicate standard deviation. ** $p<0.01$, student's t-test.

4.4 Discussion

The secretory pathway plays a crucial role in the life cycle of many viruses, providing host cell machinery utilised by viral proteins to undergo folding and glycosylation, as well as a site for virion assembly and a pathway for cellular exit. As such, the host cell glycoprocessing enzymes provide a target by which viral glycosylation can be altered or prevented, affecting viral protein folding, virion assembly, secretion and infectivity.

4.4.1 ER α-glucosidases as antiviral targets

The antiviral potential of α-glucosidase inhibitors has been appreciated for some time, with antiviral activity previously demonstrated against a range of viruses, including HIV (Ratner *et al*, 1991), BVDV (Zitzmann *et al*, 1999), dengue virus (Courageot *et al*, 2000), Ebola virus (Chang *et al*, 2013), as well as reducing HCV pseudoparticle infectivity (Chapel *et al*, 2007).

NAP-DNJ is a highly potent inhibitor of ER α-glucosidases, with an *in vitro* IC_{50} against rat liver α-glucosidase I of 0.017 μM, approximately 40-fold more potent than NB-DNJ (IC_{50} = 0.68 μM) (Rawlings *et al*, 2009). The inhibition of NAP-DNJ against α-glucosidases *in cellulo* has also been demonstrated, with 50 μM treatment of HL60 cells producing 25-fold more triglucosylated FOS than cells treated with 50 μM NB-DNJ (Rawlings *et al*, 2009).

Here, the activity of NAP-DNJ as an α-glucosidase inhibitor and as a potential antiviral compound against BVDV has been investigated. As has previously been shown in HL60 cells (Rawlings *et al*, 2009), NAP-DNJ is a potent inhibitor of both ER α-glucosidases, causing accumulation of monoglucosylated and triglucosylated FOS, indicating α-glucosidase II and I inhibition respectively. NAP-DNJ reduced BVDV

secretion in a concentration-dependent manner, with an IC_{50} of 1.75 ± 0.47 μM. Interestingly, this value is approximately 40-fold greater than the IC_{50} of 0.04 ± 0.01 μM observed for NAP-DNJ against dengue virus in monocytes (Miller *et al*, 2012).

At low concentrations of NAP-DNJ (up to 1 μM), inhibition of glucosidase II alone is observed, and is sufficient for a small yet significant antiviral effect against BVDV to be observed. With increasing concentration of NAP-DNJ, inhibition of α-glucosidase I rises, and the reduction in viral secretion increases further. The effect of NAP-DNJ on BVDV glycoproteins directly can be observed by Western blot analysis of the envelope glycoprotein E2. As has previously been demonstrated with other DNJ-based imino sugars (Jordan *et al*, 2002), treatment with NAP-DNJ results in a change in apparent molecular weight of both intracellular and secreted E1E2 heterodimer. As NAP-DNJ concentration increases, the apparent molecular weight increases due to increased glucosylation of the glycoprotein glycans.

In MDBK cells, in the absence of an endomannosidase enzyme that can remove triglucosylated caps from glycans, inhibition of α-glucosidases prevents further processing of glycans to complex structures. As such, viral-associated E2 protein from NAP-DNJ treated cells displays non-complex glycans that are sensitive to Endo H digestion. The presence of a glucose cap on these glycoproteins was confirmed by digestion with recombinant human endomannosidase.

NAP-DNJ-mediated inhibition of α-glucosidases results in the specific degradation of BVDV envelope glycoproteins, as shown in Figure 4.4. Whilst concentrations of over 35 μM are required before a reduction in the amount of non-glycosylated BVDV non-structural protein NS2/3 is observed, concentration as low as 1 μM is sufficient to reduce the intracellular amount of E1E2 heterodimer. This intracellular reduction in

envelope glycoprotein is mirrored in the amount secreted, as well as the drop in viral RNA copies.

4.4.2 Golgi endomannosidase as an antiviral target

In MDBK cells, Golgi endomannosidase is capable only of processing a restricted subset of glucosylated glycan species. Whilst human endomannosidase from Hep G2 cells has been shown to digest a broad variety of glycans *in vitro*, MDBK endomannosidase has been found to only display activity on monoglucosylated species (Kukushkin *et al*, 2012). As such, it was hypothesised that a combined approach of treating BVDV-infected MDBK cells with both an α-glucosidase inhibitor, NAP-DNJ, and an endomannosidase inhibitor, GlcIFG, may, even with just low concentration of NAP-DNJ where only α-glucosidase II inhibition is observed, be sufficient to block complex glycan formation entirely.

The *in cellulo* effect of GlcIFG was assessed by FOS analysis, in both the presence and absence of NAP-DNJ. In the absence of α-glucosidase inhibition, GlcIFG treatment resulted in a minor increase in $Glc_1Man_7GlcNAc_2$ compared with $Glc_1Man_5GlcNAc_1$. As FOS species possessing a $GlcNAc_2$ chitobiose core represent a Golgi-retrieved population, this is expected. In the presence of α-glucosidase II inhibition, this increase in $Glc_1Man_7GlcNAc_2$ is greatly enhanced. With α-glucosidase II activity inhibited by a low concentration (1 μM) of NAP-DNJ, nascent glycoproteins remain in a monoglucosylated state. A portion of these can be trafficked to the Golgi and processed by endomannosidase, whereby they can subsequently undergo further processing to give rise to complex glycan structures. However, co-treatment with GlcIFG successfully inhibits endomannosidase, resulting in an increase in Golgi-retrieved FOS possessing a monoglucosylated cap, such as $Glc_1Man_7GlcNAc_2$.

Subsequently, the effect of GlcIFG on BVDV E2 protein was examined by Western blot analysis and glycosidase digestion. Surprisingly, treatment with GlcIFG alone, in the absence of α-glucosidase inhibition, was sufficient to induce a marked change in glycosylation of E1E2 heterodimers in secreted virions. GlcIFG treatment, like NAP-DNJ treatment, increased sensitivity of E1E2 to Endo H digestion, indicating a loss of complex glycan structures. This effect strongly implies that BVDV glycoproteins are processed by and at least in part dependent on the activity of endomannosidase to achieve complex glycans, even in the absence of any blockage to the α-glucosidase mediated processing pathway.

GlcIFG shows antiviral activity against BVDV, reducing infectivity with an IC_{50} of 531 ± 74.5 μM. Only a small reduction is observed on viral secretion, suggesting that inhibition of endomannosidase results in the production of less infectious particles. In combination with NAP-DNJ, the antiviral effect of GlcIFG is enhanced further. This promising result suggests that a two-pronged approach of targeting both α-glucosidases and endomannosidase should be investigated further.

4.4.3 Antiviral activity of kifunensine against BVDV

With inhibition of endomannosidase alone proving to be antiviral against BVDV, it was subsequently investigated whether blocking of complex glycan formation on viral proteins would be sufficient to elicit an antiviral effect. As such, BVDV-infected MDBK cells were incubated with the mannosidase inhibitor kifunensine. Treatment with 1 μM kifunensine for 24 h blocked complex glycan formation completely, and reduced viral infectivity by approximately 50%. Interestingly, the antiviral effect of kifunensine was found to not be dose-dependent, with higher concentrations failing to result in any further reduction in viral infectivity. At lower concentrations, such as

0.1 μM, where little effect on complex glycan formation was observed, no antiviral effect was detected. No effect on viral secretion, as determined by quantitative RT-PCR, was observed, indicating that the antiviral effect of kifunensine was solely a result of reduced infectivity.

The intriguing antiviral effects observed from both GlcIFG and kifunensine raise further questions regarding the role of the envelope glycoproteins in BVDV secretion and infectivity. The reduction in infectivity following kifunensine treatment suggests that complex glycans play an important, yet evidently not essential role in infection. Further experiments are clearly required to elucidate the mechanism of this. It is possible that inhibition of complex glycan formation results in a distortion or rearrangement of packing in the viral envelope, which in turn could reduce binding affinity of virions to naïve cells. Alternatively, complex glycans may play a more direct role in cell binding and entry. The significant antiviral effect observed following inhibition of endomannosidase suggests a large proportion of viral envelope glycoproteins are dependent on endomannosidase for glycoprocessing. Additionally, whilst kifunensine-mediated inhibition of complex glycan formation results in an approximate 50% reduction in viral infectivity, a larger antiviral effect is obtainable through GlcIFG treatment, without complete loss of complex glycans. This suggests that inhibition of endomannosidase is having an additional antiviral effect distinct from complex glycan formation, and may play a role in viral assembly and secretion.

Targeting enzymes of the host cell glycoprocessing pathway with small molecule inhibitors offers a number of opportunities to affect and distort viral biogenesis, leading to a reduction in overall viral infection. Whilst blocking the formation of complex glycans alone on viral envelope glycoproteins produces a modest antiviral effect, the glycoprocessing pathway can also be manipulated to enhance

degradation of viral glycoproteins, resulting in greatly reduced viral output. In addition, the use of small molecule inhibitors targeting specific glycoprocessing enzymes enhances our understanding of the glycoprocessing pathway itself and how viral proteins interact with it.

4.5 References

Branza-Nichita N, Durantel D, Carrouee-Durantel S, Dwek RA, Zitzmann N (2001) Antiviral effect of N-butyldeoxynojirimycin against bovine viral diarrhea virus correlates with misfolding of E2 envelope proteins and impairment of their association into E1-E2 heterodimers. *Journal of Virology* **75:** 3527-3536

Chang J, Warren TK, Zhao X, Gill T, Guo F, Wang L, Comunale MA, Du Y, Alonzi DS, Yu W, Ye H, Liu F, Guo JT, Mehta A, Cuconati A, Butters TD, Bavari S, Xu X, Block TM (2013) Small molecule inhibitors of ER alpha-glucosidases are active against multiple hemorrhagic fever viruses. *Antiviral Research* **98:** 432-440

Chapel C, Garcia C, Bartosch B, Roingeard P, Zitzmann N, Cosset FL, Dubuisson J, Dwek RA, Trepo C, Zoulim F, Durantel D (2007) Reduction of the infectivity of hepatitis C virus pseudoparticles by incorporation of misfolded glycoproteins induced by glucosidase inhibitors. *Journal of General Virology* **88:** 1133-1143

Courageot MP, Frenkiel MP, Dos Santos CD, Deubel V, Despres P (2000) Alpha-glucosidase inhibitors reduce dengue virus production by affecting the initial steps of virion morphogenesis in the endoplasmic reticulum. *Journal of Virology* **74:** 564-572

Jordan R, Nikolaeva OV, Wang L, Conyers B, Mehta A, Dwek RA, Block TM (2002) Inhibition of host ER glucosidase activity prevents Golgi processing of virion-associated bovine viral diarrhea virus E2 glycoproteins and reduces infectivity of secreted virions. *Virology* **295:** 10-19

Kukushkin NV, Easthope IS, Alonzi DS, Butters TD (2012) Restricted processing of glycans by endomannosidase in mammalian cells. *Glycobiology* **22:** 1282-1288

Lubas WA, Spiro RG (1987) Golgi endo-alpha-D-mannosidase from rat liver, a novel N-linked carbohydrate unit processing enzyme. *Journal of Biological Chemistry* **262:** 3775-3781

Lubas WA, Spiro RG (1988) Evaluation of the role of rat liver Golgi endo-alpha-D-mannosidase in processing N-linked oligosaccharides. *Journal of Biological Chemistry* **263:** 3990-3998

Miller JL, Lachica R, Sayce AC, Williams JP, Bapat M, Dwek R, Beatty PR, Harris E, Zitzmann N (2012) Liposome-mediated delivery of iminosugars enhances efficacy against dengue virus in vivo. *Antimicrobial Agents and Chemotherapy* **56:** 6379-6386

Moore SE, Spiro RG (1990) Demonstration that Golgi endo-alpha-D-mannosidase provides a glucosidase-independent pathway for the formation of complex N-linked oligosaccharides of glycoproteins. *Journal of Biological Chemistry* **265:** 13104-13112

Ratner L, vander Heyden N, Dedera D (1991) Inhibition of HIV and SIV infectivity by blockade of alpha-glucosidase activity. *Virology* **181:** 180-192

Rawlings AJ, Lomas H, Pilling AW, Lee MJ, Alonzi DS, Rountree JS, Jenkinson SF, Fleet GW, Dwek RA, Jones JH, Butters TD (2009) Synthesis and biological characterisation of novel N-alkyl-deoxynojirimycin alpha-glucosidase inhibitors. *ChemBioChem* **10:** 1101-1105

Thompson AJ, Williams RJ, Hakki Z, Alonzi DS, Wennekes T, Gloster TM, Songsrirote K, Thomas-Oates JE, Wrodnigg TM, Spreitz J, Stutz AE, Butters TD, Williams SJ, Davies GJ (2012) Structural and mechanistic insight into N-glycan processing by endo-alpha-mannosidase. *Proc. Natl. Acad. Sci. USA* **109:** 781-786

Zitzmann N, Mehta AS, Carrouee S, Butters TD, Platt FM, McCauley J, Blumberg BS, Dwek RA, Block TM (1999) Imino sugars inhibit the formation and secretion of bovine viral diarrhea virus, a pestivirus model of hepatitis C virus: implications for the development of broad spectrum anti-hepatitis virus agents. *Proc. Natl. Acad. Sci. USA* **96:** 11878-11882

5 General Discussion

5.1 Discussion

Many enveloped viruses are critically reliant on host cell glycoprocessing machinery to achieve correct glycosylation, folding and maturation of envelope glycoproteins. BVDV expresses three glycoproteins E^{rns}, E1 and E2, with E1 and E2 having been shown to associate with and depend on calnexin, allowing correct folding of each protein and the subsequent formation of E1E2 heterodimers (Branza-Nichita *et al*, 2001), which is essential for viral entry (Ronecker *et al*, 2008). Association with calnexin, following glycosylation by OST and subsequent trimming by α-glucosidases, has been demonstrated for glycoproteins from a range of viruses as well as BVDV, including influenza virus (Peterson *et al*, 1995), rotavirus (Mirazimi *et al*, 1998), dengue virus (Limjindaporn *et al*, 2009) and HCV (Choukhi *et al*, 1998). Through inhibition of ER α-glucosidases, association with calnexin can be prevented by blocking the deglucosylation of glycans to the monoglucosylated calnexin substrate. Antiviral activity of various α-glucosidase inhibitors have previously been demonstrated against a number of glycoprotein-encoding viruses.

The antiviral potential of targeting other glycoprocessing enzymes has been less fully characterised. Host cell mannosidases are utilised by viral glycoproteins as they progress through the secretory pathway and undergo complex glycan formation. Inhibition of mannosidases with DMJ has no effect on infectivity of influenza or Rous sarcoma virus (Elbein *et al*, 1984; Bosch *et al*, 1985), yet conversely, DMJ has been shown to enhance the antiviral effect of mannose-binding lectins against HIV in cell culture (Balzarini, 2007). Endomannosidase has also been shown to be used by viral

glycoproteins (Karaivanova *et al*, 1998), but to date inhibition of endomannosidase has not been demonstrated as a potential antiviral target.

The range of small molecules discussed in this thesis demonstrate a number of mechanisms for altering viral glycosylation and inhibiting viral replication and infectivity, and highlight the potential of targeting host cell machinery as an antiviral mechanism that is less likely to give rise to resistant mutants.

The antiviral effect of α-glucosidases I and II inhibition has been demonstrated previously for many different imino sugars, as discussed in Chapter 1 (section 1.3.2). NB-DNJ and CAST alone have been shown to possess antiviral activity against HBV (Block *et al*, 1994), HIV (Fischer *et al*, 1995), BVDV (Zitzmann *et al*, 1999), cytomegalovirus (Taylor *et al*, 1988), dengue virus (Whitby *et al*, 2005) and influenza A virus (Saito & Yamaguchi, 2000), amongst others.

The work in this thesis investigates the antiviral mechanisms of different small molecules that share the glycoprotein processing pathway as a common target but differ greatly in their respective mechanisms of action. The DNJ-based imino sugars discussed in Chapter 2 and NAP-DNJ discussed in Chapter 4 display their antiviral activity principally through α-glucosidase inhibition, resulting in a significant reduction in virion production due to inhibition of calnexin-mediated viral glycoprotein folding and subsequent E1E2 heterodimerisation. Inhibition of endomannosidase by GlcIFG, discussed in Chapter 4, is also shown to reduce virion production, both alone and in combination with α-glucosidase inhibition. Kifunensine-mediated mannosidase inhibition reduces viral infectivity without affecting secretion, highlighting the importance of complex glycan formation in viral infection. Whilst these small molecules exert their antiviral capacity through direct enzyme inhibition, the

thiazolide NTZ, discussed in Chapter 3, appears to induce less specific cellular alterations in order to inhibit viral replication, but nevertheless targets the ER and Golgi compartments. Together these molecules demonstrate some of the numerous mechanisms available for targeting host cell enzymes and compartments in order to exert an antiviral effect on BVDV.

Inhibition of α-glucosidases by DNJ-based imino sugars such as NAP-DNJ results in inhibition of complex glycan formation, as is also observed with other glycoprocessing inhibitors GlcIFG and kifunensine. However, α-glucosidase inhibitors differ greatly from those that target glycoprocessing enzymes further downstream (ie. post-interaction with the calnexin cycle), as by inhibiting glucosidase activity, they are able to prevent subsequent association with ER folding chaperones calnexin and calreticulin. In doing so, chaperone-mediated folding of viral glycoproteins can be prevented, enhancing their specific degradation through ERAD, as is observed following NAP-DNJ mediated inhibition of α-glucosidase I. Processing by endomannosidase or mannosidase I, the cellular targets of GlcIFG and kifunensine respectively, occurs distinct from or downstream of calnexin-mediated folding, and as such, inhibition of these glycoprocessing enzymes is less likely to directly result in viral glycoprotein degradation. This is likely the explanation as to why α-glucosidase inhibitors, such as *N*B-DNJ and CAST, are well-characterised as antiviral compounds and antiviral activity of α-glucosidase inhibitors has been demonstrated against a broad range of viruses, whereas the antiviral potential of targeting other glycoprocessing enzymes has been less thoroughly explored.

Nevertheless, inhibition of both endomannosidase and mannosidase I by GlcIFG and kifunensine respectively results in a reduction in infectivity in BVDV. Whilst endomannosidase is not part of the central calnexin-mediated quality control cycle, it

is known that processing by endomannosidase in the Golgi can occur upstream of ERAD (Kukushkin *et al*, 2011). Further experiments are required to elucidate whether endomannosidase plays any role in glycoprotein folding or quality control, but it is apparent that it is readily utilised by BVDV envelope glycoproteins, even in the absence of α-glucosidase inhibition. This may simply be a result of oversaturation of the calnexin-mediated processing pathway during viral infection, resulting in an overflow of hyperglucosylated viral glycoproteins into the Golgi before glucosidase processing can occur. Nonetheless, inhibition of endomannosidase processing by GlcIFG results in a significant antiviral effect that should be investigated further. In addition, the potential of endomannosidase as an antiviral target needs to be investigated in other cell lines with different viruses, where the enzyme is capable of processing a wider range of substrates. It may be that the effects observed with GlcIFG here are specific to BVDV due to the increased substrate specificity of MDBK endomannosidase.

Kifunensine, on the other hand, appears to have a more modest antiviral effect on BVDV, with a maximal reduction in infectivity of approximately 50% where complete inhibition of mannosidase I is observed. Unlike α-glucosidase inhibitors, which increase ERAD degradation of viral glycoproteins, kifunensine has previously been shown to inhibit ERAD through mannosidase I inhibition (Tokunaga *et al*, 2000). As such, it would not be expected that kifunensine treatment would exert an antiviral effect on BVDV by increasing degradation of envelope glycoproteins. Instead, kifunensine appears to reduce infectivity of BVDV virions by inhibiting complex glycan formation alone, with no reduction in viral secretion observed, suggesting a role of the glycan in BVDV infection. It is clear that complex glycans are not essential for the infection process, as complete inhibition of complex glycan formation, as

determined by Western blot analysis following kifunensine treatment, results in only a 50% reduction in infectivity. Further work is required to establish what role E1 and E2 glycans play in BVDV binding and entry. BVDV is known to bind bovine CD46 prior to entry (Maurer *et al*, 2004), a cell surface protein that has no known carbohydrate recognition domains. It is plausible however that disruption of E1 and E2 glycosylation disrupts or alters packing in the viral envelope, which could in turn lead to a weaker interaction with host cell binding factors.

With both NAP-DNJ and GlcIFG also inhibiting complex glycan formation, it is likely that this will affect BVDV infectivity, in addition to increasing the degradation of viral glycoproteins, although the resultant glycan state following inhibitor treatment is clearly distinct from that observed with kifunensine. Kifunensine treatment results in a homogenous array of high-mannose glycans with no glucose cap, whilst NAP-DNJ and GlcIFG treatment produces viral glycans with glucose caps intact, but which may have undergone some mannosidase processing on the B and C arms of the glycan (Figure 1.1).

Full characterisation and glycan analysis of BVDV glycoproteins following different treatments would provide great detail into the exact effects of these small molecules, and may elucidate further any role the glycans play in infection, but to date sufficient purification of E1 and E2 for subsequent glycan analysis has not been achieved.

As detailed in Chapter 3, the mechanism by which NTZ inhibits BVDV replication appears not to be a direct result of disrupting viral glycosylation. Instead, NTZ has a more global effect on the cell, depleting ER and Golgi Ca^{2+} stores and reducing cell proliferation and division. A precise, direct target of NTZ is still to be identified, but it appears likely that many of the observed effects are a result of Ca^{2+} mobilisation.

Like with the other small molecules discussed, NTZ treatment impairs glycoprotein processing and prevents complex glycan formation. However, whilst NAP-DNJ, GlcIFG and kifunensine have specific well-characterised enzymatic targets that they competitively inhibit, NTZ instead appears to disrupt viral glycosylation as a side-effect of depletion of ER and Golgi Ca^{2+} stores. Many glycoprocessing enzymes possess Ca^{2+}-binding sites, including α-glucosidase II (Trombetta *et al*, 1996) and α-1,2-mannosidase (Schutzbach & Forsee, 1990), as well as calnexin and calreticulin. Such Ca^{2+}-binding sites are thought to be important for ER lumenal retention (Sonnichsen *et al*, 1994). In addition, elevation of cytosolic [Ca^{2+}] is known to disrupt Golgi trafficking (Porat & Elazar, 2000), which is likely to impede viral secretion as well as impairing complex glycan formation. It remains to be established what contribution to the antiviral effect of NTZ results from the disruption to glycoprocessing.

Regardless of this, it is clear that the secretory pathway and the host cell glycoprotein processing pathway that is heavily utilised by many enveloped viruses is an effective target for a range of antiviral compounds. Targeting host cell machinery can be a complementary approach to direct-acting antiviral therapy. By targeting the host cell rather than the virus directly, indirect-acting antiviral compounds are likely to affect a broader range of viruses and genotypes, and less likely to give rise to resistant escape mutants. With the host cell glycoprotein processing pathway being utilised by many pathogens, it remains a promising and inviting antiviral target.

5.2 References

Balzarini J (2007) The alpha(1,2)-mannosidase I inhibitor 1-deoxymannojirimycin potentiates the antiviral activity of carbohydrate-binding agents against wild-type and mutant HIV-1 strains containing glycan deletions in gp120. *FEBS Letters* **581:** 2060-2064

Block TM, Lu X, Platt FM, Foster GR, Gerlich WH, Blumberg BS, Dwek RA (1994) Secretion of human hepatitis B virus is inhibited by the imino sugar N-butyldeoxynojirimycin. *Proc. Natl. Acad. Sci. USA* **91:** 2235-2239

Bosch JV, Tlusty A, McDowell W, Legler G, Schwarz RT (1985) The mannosidase inhibitors 1-deoxymannojirimycin and swainsonine have no effect on the biosynthesis and infectivity of Rous sarcoma virus. *Virology* **143:** 342-346

Branza-Nichita N, Durantel D, Carrouee-Durantel S, Dwek RA, Zitzmann N (2001) Antiviral effect of N-butyldeoxynojirimycin against bovine viral diarrhea virus correlates with misfolding of E2 envelope proteins and impairment of their association into E1-E2 heterodimers. *Journal of Virology* **75:** 3527-3536

Choukhi A, Ung S, Wychowski C, Dubuisson J (1998) Involvement of endoplasmic reticulum chaperones in the folding of hepatitis C virus glycoproteins. *Journal of Virology* **72:** 3851-3858

Elbein AD, Legler G, Tlusty A, McDowell W, Schwarz R (1984) The effect of deoxymannojirimycin on the processing of the influenza viral glycoproteins. *Archives of Biochemistry and Biophysics* **235:** 579-588

Fischer PB, Collin M, Karlsson GB, James W, Butters TD, Davis SJ, Gordon S, Dwek RA, Platt FM (1995) The alpha-glucosidase inhibitor N-butyldeoxynojirimycin inhibits human immunodeficiency virus entry at the level of post-CD4 binding. *Journal of Virology* **69:** 5791-5797

Karaivanova VK, Luan P, Spiro RG (1998) Processing of viral envelope glycoprotein by the endomannosidase pathway: evaluation of host cell specificity. *Glycobiology* **8:** 725-730

Kukushkin NV, Alonzi DS, Dwek RA, Butters TD (2011) Demonstration that endoplasmic reticulum-associated degradation of glycoproteins can occur downstream of processing by endomannosidase. *Biochemical Journal* **438:** 133-142

Limjindaporn T, Wongwiwat W, Noisakran S, Srisawat C, Netsawang J, Puttikhunt C, Kasinrerk W, Avirutnan P, Thiemmeca S, Sriburi R, Sittisombut N, Malasit P, Yenchitsomanus PT (2009) Interaction of dengue virus envelope protein with

endoplasmic reticulum-resident chaperones facilitates dengue virus production. *Biochemical and Biophysical Research Communications* **379:** 196-200

Maurer K, Krey T, Moennig V, Thiel HJ, Rumenapf T (2004) CD46 is a cellular receptor for bovine viral diarrhea virus. *Journal of Virology* **78:** 1792-1799

Mirazimi A, Nilsson M, Svensson L (1998) The molecular chaperone calnexin interacts with the NSP4 enterotoxin of rotavirus in vivo and in vitro. *Journal of Virology* **72:** 8705-8709

Peterson JR, Ora A, Van PN, Helenius A (1995) Transient, lectin-like association of calreticulin with folding intermediates of cellular and viral glycoproteins. *Molecular Biology of the Cell* **6:** 1173-1184

Porat A, Elazar Z (2000) Regulation of intra-Golgi membrane transport by calcium. *Journal of Biological Chemistry* **275:** 29233-29237

Ronecker S, Zimmer G, Herrler G, Greiser-Wilke I, Grummer B (2008) Formation of bovine viral diarrhea virus E1-E2 heterodimers is essential for virus entry and depends on charged residues in the transmembrane domains. *Journal of General Virology* **89:** 2114-2121

Saito T, Yamaguchi I (2000) Effect of glycosylation and glucose trimming inhibitors on the influenza A virus glycoproteins. *Journal of Veterinary Medical Science* **62:** 575-581

Schutzbach JS, Forsee WT (1990) Calcium ion activation of rabbit liver alpha 1,2-mannosidase. *Journal of Biological Chemistry* **265:** 2546-2549

Sonnichsen B, Fullekrug J, Nguyen Van P, Diekmann W, Robinson DG, Mieskes G (1994) Retention and retrieval: both mechanisms cooperate to maintain calreticulin in the endoplasmic reticulum. *Journal of Cell Science* **107:** 2705-2717

Taylor DL, Fellows LE, Farrar GH, Nash RJ, Taylor-Robinson D, Mobberley MA, Ryder TA, Jeffries DJ, Tyms AS (1988) Loss of cytomegalovirus infectivity after treatment with castanospermine or related plant alkaloids correlates with aberrant glycoprotein synthesis. *Antiviral Research* **10:** 11-26

Tokunaga F, Brostrom C, Koide T, Arvan P (2000) Endoplasmic reticulum (ER)-associated degradation of misfolded N-linked glycoproteins is suppressed upon inhibition of ER mannosidase I. *Journal of Biological Chemistry* **275:** 40757-40764

Trombetta ES, Simons JF, Helenius A (1996) Endoplasmic reticulum glucosidase II is composed of a catalytic subunit, conserved from yeast to mammals, and a tightly bound noncatalytic HDEL-containing subunit. *Journal of Biological Chemistry* **271:** 27509-27516

Whitby K, Pierson TC, Geiss B, Lane K, Engle M, Zhou Y, Doms RW, Diamond MS (2005) Castanospermine, a potent inhibitor of dengue virus infection in vitro and in vivo. *Journal of Virology* **79:** 8698-8706

Zitzmann N, Mehta AS, Carrouee S, Butters TD, Platt FM, McCauley J, Blumberg BS, Dwek RA, Block TM (1999) Imino sugars inhibit the formation and secretion of bovine viral diarrhea virus, a pestivirus model of hepatitis C virus: implications for the development of broad spectrum anti-hepatitis virus agents. *Proc. Natl. Acad. Sci. USA* **96:** 11878-11882